



YAŞAR UNIVERSITY  
GRADUATE SCHOOL OF NATURAL AND APPLIED SCIENCES

MASTER THESIS

**A PREDICTIVE CONTROL STRATEGY FOR  
OPTIMAL POWER SHARING AND BATTERY  
THERMAL MANAGEMENT IN HYBRID ELECTRIC  
VEHICLES**

AHMET KAAAN ŞANAL

THESIS ADVISOR: DR. EMRAH BIYIK

ELECTRICAL AND ELECTRONICS ENGINEERING

PRESENTATION DATE: 15.01.2019

BORNOVA / İZMİR  
JANUARY 2019



We certify that, as the jury, we have read this thesis and that in our opinion it is fully adequate, in scope and in quality, as a thesis for the degree of Master of Science

**Jury Members:**

Asst. Prof. Dr. Emrah BIYIK  
Yaşar University

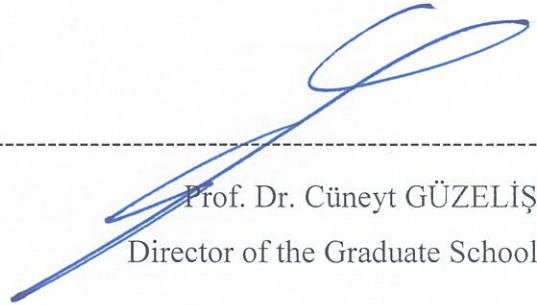
**Signature:**



Asst. Prof. Dr. Hacer ŞEKERCİ  
Yaşar University



Assoc. Prof. Dr. Mutlu BOZTEPE  
Ege University



Prof. Dr. Cüneyt GÜZELİŞ  
Director of the Graduate School



## ABSTRACT


# A PREDICTIVE CONTROL STRATEGY FOR OPTIMAL POWER SHARING AND BATTERY THERMAL MANAGEMENT IN HYBRID ELECTRIC VEHICLES

Şanal, Ahmet Kaan

Msc, Electrical Electronics Engineering

Advisor: Dr. Emrah Bıyık

January 2019



The rapid depletion of fossil fuels and their adverse environmental impact became a serious problem that must be considered immediately. It is anticipated that we will run out crude oil reserves in the near future. For this reason, fuel economy concept for automobiles has become more significant in the past decades. Hybrid electric vehicles (HEVs), is one of the best solution to overcome with these mentioned problems. HEVs contains both internal combustion engine (ICE) and electric motor (EM). In most cases, electric motors can be charged by only battery. However, in this case, the life of battery becomes an important problem. Thus, supercapacitors are also used to charge EM as an alternative component. Although, batteries have higher energy density than supercapacitors, the ability of releasing energy (power density) is lower. Also, cycling the battery at high depth of discharge (DOD) rate, high C-rate, reduces the life of it. Because of the importance of battery's life and advantages of supercapacitor, total power demand that is needed for car will be split into ICE, battery and supercapacitor.

In this thesis, the aims are to reduce the fuel consumption rate of the car and increase the life of the battery. The key points to achieve these aims are improving energy management strategy (EMS) for sharing the total power between ICE, battery and supercapacitor in an optimum way and designing thermal management strategy (TMS) to control battery temperature. For these purposes, optimization-based model predictive control (MPC) is designed. Model predictive control is an advance method that is used to control a process while tracking the references and satisfying

constraints. MPC solves an optimization problem at each time step in order to adjust the control action by predicting the plant output. In this project, a closed-loop model is developed in order to get closer to the desired reference signal as much as possible. Because of the complication of the plant, better solution can be evaluated by examining the plant block by block. For this purpose, MATLAB/Simulink is one of the most promising simulation program to take on the challenging steps.

The first step of realizing this thesis is to derive the mathematical model of each block. The ICE, supercapacitor, battery, vehicle dynamic of HEVs and battery thermal blocks are modeled independently. The outputs of these five blocks are fuel consumption, supercapacitor state of charge (SOC), battery state of charge (SOC) speed of vehicle and battery temperature respectively.

After deriving the mathematical models of each component, MPC is constructed into the system and at the end, the results are investigated. In this step, we have applied six different cases. In each case, we have achieved to track output references with only small errors. In first two cases, the positive effects of supercapacitor on C-rate and fuel consumption rate are demonstrated. By using supercapacitor, C-rate and fuel consumption rate are improved 24.49% and 5.221% respectively. In another case, speed control of fan is carried out to decrease the temperature of battery. When this battery temperature control is included in the MPC, the speed and battery temperature references are tracked by 0.03 m/s and 0.12 °C average error respectively.

**Keywords:** Hybrid Electric Vehicles, Power Sharing, Battery Thermal Management, Model Predictive Control, C-rate

## ÖZ

# HİBRİT ELEKTRİKLİ ARAÇLARDA EN İYİ GÜÇ PAYLAŞIMI VE BATARYA ISIL YÖNETİMİ İÇİN BİR ÖNGÖRÜLÜ KONTROL STRATEJİSİ

Şanal, Ahmet Kaan

Yüksek Lisans, Elektrik Elektronik Mühendisliği

Danışman: Dr. Emrah Bıyık

Ocak 2019

Fosil yakıtların hızla tükenmekte olması, insanlar için dikkate alınması gereken ciddi bir problem haline gelmiştir. İşlenmemiş yakıt rezervlerinin yakın bir tarihte tükeneceği tahmin edilmektedir. Bu sebeple, son yıllarda otomobiller için yakıt ekonomisi kavramı daha önemli hale gelmiştir. Hibrit araçlar, söz konusu sorunların üstesinden gelmek için en iyi çözümlerden birisidir. Hibrit araçlar hem içten yanmalı motor hem de elektrik motorunu birlikte taşımaktadır. Çoğu durumda elektrik motoru sadece batarya ile şarj edilmektedir. Ancak bu durumda da bataryanın ömrü önemli bir problem olmaktadır. Bu yüzden süper kapasitörler elektrik motorunu şarj etmek için alternatif eleman olarak kullanılmaktadır. Bataryalar süper kapasitörlerden daha yüksek enerji yoğunluğuna sahip olmalarına rağmen, enerjiyi aktarma konusunda daha düşük yeteneğe sahiptirler. Ayrıca desarj derinliği döngüsünün hızlı olması, yüksek C parametresi, bataryanın ömrünü kısaltmaktadır. Batarya ömrünün önemi ve süper kapasitör kullanımının avantajlarından dolayı, aracın ihtiyaç duyduğu toplam güç, içten yanmalı motor, batarya ve süper kapasitör arasında bölünmektedir.

Bu tezde amaçlar, aracın yakıt tüketimini düşürmek ve bataryanın ömrünü uzatmaktır. Bu amaçları gerçekleştirmek için kilit noktalar, toplam gücü içten yanmalı motor, batarya ve süper kapasitör arasında optimum olarak paylaştıran bir enerji yönetim stratejisi geliştirmek ve batarya sıcaklığını kontrol edecek bir ısı yönetim stratejisi geliştirmektir. Bu amaçlar için optimizasyon tabanlı modele dayalı öngörülü kontrol (MPC) sistemi tasarlanmıştır. MPC, süreç kontrolü yaparken referansı takip eden ve kısıtlamalara uyan gelişmiş bir kontrol yöntemidir. MPC, kontrol eylemini ayarlamak için sistem çıktısını tahmin eder ve bunu gerçekleştirmek

için her zaman adımında bir optimizasyon problemi çözer. Bu projede, istenilen referans sinyaline olabildiğince yaklaşabilmek için kapalı çevrim kontrol modeli geliştirilmiştir. Sistemin karmaşık yapısından dolayı, sistemi bloklar halinde incelemek daha iyi bir sonuç vermektedir. Bu karmaşık yapıyı çözmek amacıyla, MATLAB/Simulink programı en iyi çözümlerden bir tanesini sunmaktadır.

Tezi gerçekleştirirken ilk adım, her bir bloğun matematiksel modelini çıkartmaktır. İçten yanmalı motor, süper kapasitör, batarya, hibrit aracın dinamik yapısı ve batarya ısıl blokları ayrı ayrı modellenmiştir. Bu beş bloğun çıktıları sırasıyla, yakıt tüketimi, süper kapasitörün şarj durumu, bataryanın şarj durumu, aracın hızı ve batarya sıcaklığı şeklindedir.

Her bir bileşenin matematiksel modeli elde edildikten sonra, MPC sisteme uyarlanmış ve son olarak sonuçlar incelenmiştir. Bu adımda, altı farklı çalışma yaptık. Her adımda çıkış referanslarını küçük hata payları ile takip etmeyi başardık. İlk iki çalışmada, süper kapasitörün C parametresi ve yakıt tasarrufuna olan pozitif etkileri gösterilmiştir. Süper kapasitör kullanılarak C parametresi ve yakıt tüketimi sırası ile 24.49% ve 5.221% iyileştirilmiştir. Bir başka durumda, batarya sıcaklığını düşürebilmek için fan hız kontrol sistemi uygulanmıştır. MPC batarya sıcaklık kontrolünü kapsadığı zaman, hız ve batarya sıcaklığı 0.03 m/s ve 0.12 °C ortalama hata ile takip edilmiştir.

**Anahtar Kelimeler:** Hibrit Elektrikli Araçlar, Güç Paylaşımı, Batarya Isıl Yönetimi, Model Öngörülü Kontrol, C-Parametresi



## **ACKNOWLEDGEMENTS**

First of all, I would like to thank my supervisor Dr. Emrah Bıyık for his guidance and patience during this study. I also would like to thank my jury members for their valuable comments on the presented work.

I would like to express my enduring love to my parents, who are always supportive, loving and caring to me in every possible way in my life.

I would like to express my gratitude to my boss Bülent Eraslan for encouraging support during this study.

Ahmet Kaan ŞANAL

İzmir, 2019

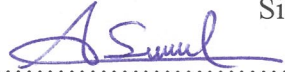


## TEXT OF OATH

I declare and honestly confirm that my study, titled “A PREDICTIVE CONTROL STRATEGY FOR OPTIMAL POWER SHARING AND BATTERY THERMAL MANAGEMENT IN HYBRID ELECTRIC VEHICLES” and presented as a Master’s Thesis, has been written without applying to any assistance inconsistent with scientific ethics and traditions. I declare, to the best of my knowledge and belief, that all content and ideas drawn directly or indirectly from external sources are indicated in the text and listed in the list of references.

Ahmet Kaan Şanal

Signature



January 16, 2019



# TABLE OF CONTENTS

ABSTRACT .....	v
ÖZ.....	vii
ACKNOWLEDGEMENTS.....	ix
TEXT OF OATH.....	xi
TABLE OF CONTENTS.....	xiii
LIST OF FIGURES .....	xvii
LIST OF TABLES.....	xxi
SYMBOLS AND ABBREVIATIONS.....	xxii
CHAPTER 1 INTRODUCTION .....	1
1.1. Motivation.....	1
1.2. Literature Review.....	2
1.2.1. History of MPC.....	5
1.2.2. MPC Applications in Automotive Industry .....	6
1.3. Aim of Study .....	7
1.4. Outline of Thesis.....	8
CHAPTER 2 OVERVIEW OF HYBRID VEHICLES .....	9
2.1. Background and Types of Hybrid Vehicles .....	9
2.1.1. Parallel Hybrid Vehicles .....	9
2.1.2. Series Hybrid Vehicles.....	10
2.1.3. Power Split Hybrid Vehicles.....	11
2.2. Battery Technology .....	11
2.2.1. Lead Acid Batteries.....	11
2.2.2. Nickel-Metal Hydride (NIMH) Batteries.....	12
2.2.3. Lithium-ion Batteries .....	12
2.3. Supercapacitor Technology.....	12
CHAPTER 3 OVERVIEW OF MODEL PREDICTIVE CONTROL.....	14
3.1. What is Model Predictive Control?.....	14

3.2. MPC Design Parameters and Related Terms .....	15
3.2.1. Sample Time .....	16
3.2.2. Prediction Horizon .....	16
3.2.3. Control Horizon .....	17
3.2.4. Constraints .....	17
3.2.5. Weights .....	17
3.3. Structure and Elements of MPC .....	17
3.3.1. Prediction Model .....	18
3.3.2. Objective Function .....	18
3.3.3. Optimization Algorithm to Compute the Control Law .....	19
3.4. Advantages and Disadvantages of MPC .....	19
<b>CHAPTER 4 MATHEMATICAL MODEL OF HYBRID VEHICLE COMPONENTS .....</b>	<b>21</b>
4.1. Mathematical Model of Hybrid Vehicle .....	21
4.1.1. Vehicle Dynamic Model .....	22
4.1.2. Internal Combustion Engine (ICE) Model .....	24
4.1.3. Battery Model .....	24
4.1.4. Supercapacitor Model .....	25
4.1.5. Thermal Model of Battery .....	26
4.1.5.1. Air Density .....	27
4.1.5.2. Specific Heat .....	27
4.1.5.3. Dynamic Viscosity .....	27
4.1.5.4. Kinematic Viscosity .....	28
4.1.5.5. Thermal Conductivity .....	28
4.1.5.6. Prandtl Number .....	28
4.1.5.7. Reynolds Number .....	29
4.1.5.8. Nusselt Number .....	30
4.1.5.9. Heat Transfer Rate .....	31
4.1.5.10. Temperature Change .....	33
4.2. Simulink Model of Hybrid Vehicle .....	34
4.2.1. Simulink Model of Vehicle Dynamic .....	34
4.2.2. Simulink Model of Internal Combustion Engine (ICE) .....	35
4.2.3. Simulink Model of Battery .....	36
4.2.4. Simulink Model of Supercapacitor .....	37
4.2.5. Simulink Model of Battery Temperature .....	39

4.3. Mathematical Model of MPC.....	40
CHAPTER 5 MODELLING ENERGY AND THERMAL MANAGEMENT STRATEGIES AND SIMULATION RESULTS.....	42
5.1. Energy Management Strategy .....	43
5.1.1. Power Split for ICE, Battery and Supercapacitor .....	44
5.1.1.1. Controller Synthesis for First Case.....	45
5.1.1.2. Simulation Results for First Case .....	47
5.1.2. Power Split for ICE and Battery .....	52
5.1.2.1. Controller Synthesis for Second Case.....	52
5.1.2.2. Simulation Results for Second Case.....	53
5.1.3. Power Split for Battery and SC.....	56
5.1.3.1. Controller Synthesis for Third Case .....	56
5.1.3.2. Simulation Results for Third Case.....	57
5.1.4. Power Split for only ICE.....	59
5.1.4.1. Controller Synthesis for Fourth Case.....	59
5.1.4.2. Simulation Results for Fourth Case .....	60
5.2. Battery Thermal Management Strategy .....	62
5.2.1. Controller Synthesis for Thermal Management Strategy.....	62
5.2.2. Simulation Results for Thermal Management Strategy.....	63
5.3. Combined Energy Management and Thermal Management Strategies .....	66
5.3.1. Controller Synthesis for Combined Strategies .....	68
5.3.2. Simulation Results for Combined EMS and TMS.....	69
5.4. Discussion of Results .....	72
CHAPTER 6 CONCLUSIONS AND FUTURE RESEARCH .....	74
6.1. Conclusion.....	74
6.2. Future Work .....	75
REFERENCES .....	76
APPENDIX 1 – Battery Temperature Code .....	81
APPENDIX 2 – A Sample MATLAB/Simulink MPC Toolbox Interface for Only Test Case 6 .....	86





## LIST OF FIGURES

<b>Figure 2.1.</b> Parallel Structure of Hybrid Vehicles.....	10
<b>Figure 2.2.</b> Series Structure of Hybrid Vehicles .....	10
<b>Figure 2.3.</b> Power Split Structure of Hybrid Vehicles .....	11
<b>Figure 2.4.</b> Comparison of Battery and Supercapacitor in terms of Energy and Power Density Features.....	13
<b>Figure 3.1.</b> The Control Strategy of Model Predictive Control .....	15
<b>Figure 3.2.</b> Basic structure of MPC.....	18
<b>Figure 4.1.</b> Longitudinal Forces on Vehicle .....	22
<b>Figure 4.2.</b> All Types of Heat Transfer Methods.....	27
<b>Figure 4.3.</b> Properties of Air at 1atm Pressure .....	29
<b>Figure 4.4.</b> The Behavior of Fluid in Laminar and Turbulent Flow .....	29
<b>Figure 4.5.</b> The Geometric Arrangement of Tube Bank in Cross Flow.....	31
<b>Figure 4.6.</b> Flow Condition in Staggered Tube.....	32
<b>Figure 4.7.</b> Simulink Model of Vehicle Dynamic.....	35
<b>Figure 4.8.</b> Simulink Model of ICE .....	36
<b>Figure 4.9.</b> The Simulink Model of Battery .....	37
<b>Figure 4.10.</b> Summary of Supercapacitor Device Characteristics .....	38
<b>Figure 4.11.</b> Simulink Model of Supercapacitor.....	39
<b>Figure 4.12.</b> Simulink Model of Battery Temperature.....	40
<b>Figure 4.13.</b> Structure of MPC with Mathematical Formulation .....	41
<b>Figure 5.1.</b> Block Diagram of Overall System.....	42
<b>Figure 5.2.</b> HWFET Driving Cycle Tracking .....	47
<b>Figure 5.3.</b> UDDS Driving Cycle Tracking .....	47
<b>Figure 5.4.</b> Battery Temperature Reference Tracking .....	48
<b>Figure 5.5.</b> Power Split Analysis for Three Power Sources.....	49
<b>Figure 5.6.</b> Fuel Consumption of Hybrid Vehicle in HWFET.....	50

<b>Figure 5.7.</b> Battery Power and State of Charge Level .....	51
<b>Figure 5.8.</b> Supercapacitor Power and State of Charge Level .....	51
<b>Figure 5.9.</b> Power Split Analysis for ICE and Battery.....	53
<b>Figure 5.10.</b> Fuel Consumption Rate of Hybrid Vehicle without Supercapacitor .....	54
<b>Figure 5.11.</b> Battery C-rate Comparison for Two Scenarios: i) with Supercapacitor and ii) without Supercapacitor .....	55
<b>Figure 5.12.</b> Battery Power and SOC Level without Supercapacitor .....	56
<b>Figure 5.13.</b> Power Split Analysis for Battery and SC .....	58
<b>Figure 5.14.</b> C-rate Graph without ICE .....	58
<b>Figure 5.15.</b> Power and SOC Values for Both Battery and SC .....	59
<b>Figure 5.16.</b> Power Split Analysis for Only ICE .....	61
<b>Figure 5.17.</b> Fuel Consumption Analysis for Only ICE .....	61
<b>Figure 5.18.</b> Block Diagram of Nonlinear Model.....	63
<b>Figure 5.19.</b> Speed of Fan and Temperature Change of Nonlinear Model.....	64
<b>Figure 5.20.</b> Comparison of Linear and Nonlinear Model .....	65
<b>Figure 5.21.</b> Block Diagram of State-Space Model.....	65
<b>Figure 5.22.</b> Speed of Fan and Temperature Change of State-Space Model.....	66
<b>Figure 5.23.</b> Simulink Block Diagram of Combined EMS and TMS.....	67
<b>Figure 5.24.</b> Speed Tracking for Combined EMS and Nonlinear TMS .....	69
<b>Figure 5.25.</b> Speed Tracking and Power Split for Combined EMS and Linear TMS .....	70
<b>Figure 5.25.</b> Fuel Consumption Rate for Combined EMS and TMS .....	70
<b>Figure 5.26.</b> Comparison of Fan Control and Temperature Change for State-Space and Nonlinear Model .....	71
<b>Figure A2.1.</b> Adjustment of MPC default conditions .....	86
<b>Figure A2.2.</b> Input and output configuration of MPC.....	87
<b>Figure A2.3.</b> Sample time, prediction horizon, control horizon and constraints adjustment interface .....	87
<b>Figure A2.4.</b> Weights adjustment interface .....	88





## LIST OF TABLES

<b>Table 4.1.</b> Constants of equation 4.23 for Staggered Flow .....	30
<b>Table 4.2.</b> Vehicle Coefficients.....	34
<b>Table 4.3.</b> ICE Coefficients.....	35
<b>Table 4.4.</b> Battery Coefficients (Toyota Prius Technical Specifications Including Battery Details, 2012).....	36
<b>Table 4.5.</b> Specifications of Different Types of Supercapacitors.....	38
<b>Table 4.6</b> Coefficients of Battery Thermal Model .....	39
<b>Table 5.1.</b> Features of Different Control Cases.....	43
<b>Table 5.2.</b> Different Estimated C-rate Values for Case 1, Case 2 and Case 3 .....	72
<b>Table 5.3</b> Different estimated fuel consumption rate values for Case 1, Case 2, Case 4 and Case 6.....	73

## SYMBOLS AND ABBREVIATIONS

### ABBREVIATIONS:

HEVs	Hybrid Electric Vehicles
ICE	Internal Combustion Engine
EM	Electric Motor
DOD	Depth of Discharge
MPC	Model Predictive Control
EMS	Energy Management Strategy
TMS	Thermal Management Strategy
SOC	State of Charge
ESS	Energy Storage System
ECMC	Equivalent Consumption Minimization Strategy
MAC	Model Algorithmic Control
DMC	Dynamic Matrix Control
GPC	Generalized Predictive Control

### SYMBOLS:

$F_{net}$	Net forces on vehicle
$a$	Acceleration
$F_{air}, F_{roll}, F_{gravity}$	Resistive forces.
$v$	Vehicle velocity
$C_d$	Drag coefficient of vehicle
$A$	Effective cross sectional area of vehicle
$C_{roll}$	Rolling resistance coefficient
$m$	Vehicle mass
$g$	Gravitational acceleration

$\theta$	Angle of slope
$\rho$	Gravitational acceleration
$\theta$	Angle of slope
$\rho$	Density of air
$z$	Vehicle elevation
$T$	Air temperature
$P_{ICE}$	ICE power
$P_{Brake}$	Brake power of vehicle
$C_f$	Calorific value
$F_c$	Fuel consumption
$Q_k$	Latest charge level
$Q_{k-1}$	Previous charge level
$\Delta t$	Elapsed time
$\dot{\eta}_{char}, \dot{\eta}_{dis}$	Charging and discharging efficiencies
$V_{OC}$	Open circuit voltage of battery
$C_{battery}$	Battery cells capacity
$\mu$	Dynamic viscosity
$\tau$	Shearing stress on fluid
$\lambda$	Thermal conductivity
$Re$	Reynold number
$Pr$	Prandtl number
$Nu$	Nusselt number





# CHAPTER 1

## INTRODUCTION

### 1.1. Motivation

The deterioration of environmental conditions is one of the biggest problems of mankind. Since the crude oil reserves reduce and energy problems occur, subjects of energy efficiency and saving the energy are getting more important day by day. Especially, the decline of oil reserves and adversely effects of CO<sub>2</sub> on atmosphere heads scientist for alternative energy sources.

The reduction of oil reserves has especially affected the automotive industry and it directs automotive firms to design more efficient engines which consume less fuel and to find different modes of energy in the last 20 years period. This seeking leads the idea of integrating the electric motors into the car. Thus, the combination of electric motor and internal combustion engine is used. The technology of the combination of these two motor types is called as “hybrid technology”. In this technology, the propulsion power which is demanded by car can be powered by either power sources (motors) or both sources at the same time. Another alternative technology, electric-only usage has not provided enough range for automobiles yet. Also electric vehicles need some time to charge. Because of these disadvantages, hybrid electric vehicles seem better solution for people.

Hybrid electric vehicles (HEVs) have been increasing in automotive market rapidly. The improvement in hybrid car technology can offer considerably reduced fuel consumption, compared to a conventional engine-only vehicle (Karabasoglu et al., 2018; Poramapojana and Chen, 2012). Also HEVs offer some specific features such as extended battery life, engine downsizing and regenerative braking. However, the HEVs must be supported by some control strategies to improve performance and achieve the aim of reducing fuel consumption. It means that, the overall performance of HEVs is attached to the energy management strategy. The purpose of energy

management systems, which is developed by optimal control strategies, is to make lower fuel consumption with a high performance of the vehicle.

The methods of reduced fuel consumption can be listed as:

In hybrid vehicles, power of internal combustion engine and electric motor can be split by controller which allows the vehicle follow the optimum speed-torque points.

In most hybrid vehicles, the engine and the electric motor can give the power for wheels at the same time. In most cases, the power can be derived by motor, so that the engine size becomes smaller. This allows usage of lower power engines.

In hybrid cars, the usage of motor as a generator technology is valid. This technology is called as “Regenerative Braking”. Regenerative braking is the recovery of kinetic energy during braking. In a conventional vehicle, a majority of the kinetic energy is converted during friction braking into heat and emitted unused into the environment. Hybrid cars can use the electric motor to recuperate at least a portion of the kinetic energy for reuse. This enables lowering fuel consumption and balancing CO<sub>2</sub> emission.

The fuel economy is also dependent on the energy storage systems. The batteries represent a big part of vehicle cost so that the life of the battery is another factor that must be considered. The capacity and life of the battery can be adversely affected by temperature, high or low state of charge and fast depth of discharge (Choi and Lim, 2002). Lowering the stress on battery and holding the battery temperature in a specific interval, are the main purposes of energy management strategy. Thanks to good energy management strategy, it is possible to reduce the cost of the battery and increase the life of it.

## **1.2. Literature Review**

Literature review can be examined into two groups, including modelling and control strategies. Modelling is quite important for all types of vehicle design and control strategies. When the whole process is thought, the modelling in some simulators reduce the cost and time wasting. Simulators allow modify the models in a favor of user. It is much easier to develop than prototypes. For this purpose, many commercial simulation software programs are developed. In most cases, MATLAB<sup>®</sup> Software is used because of the lower prices and high speed performance.

Modelling part is not that much vary from each other. In most cases, vehicle dynamic, battery, ICE and transmission system are designed individually (Poramapojana and Chen, 2012; Wang et al., 2014). When only the modelling part examined, the difference appears when supercapacitor and thermal model are added to the system. The benefits of using a supercapacitor with battery in the energy storage system are discussed many times by some researchers. The researchers proposed the usage of supercapacitor in HEVs reduces cycling the battery at high peak powers. In this examination, the fuel consumption is also improved (Borhan and Vahidi, 2010). Another research indicates that implementation of supercapacitor reduces stress on battery and it helps reduce the size of the battery by adjusting high and short peaks of power (Sadoun et al., 2011). Another approach is to add supercapacitors to the city busses and to compare the results with only battery systems for different driving cycles. In this research, it is reached up that the busses are better capable of storing energy and recovering energy in braking mode. In addition, they have showed that supercapacitors prolong the electric range of the busses (Lajunen, 2010). The implementation of supercapacitor enables increasing the vehicle performances in different ways. In different experiment, thanks to the ability of fast charge and discharge of supercapacitor, the acceleration performance of the vehicle, working condition of battery and fuel economy performance are improved (Jinrui et al., 2006).

The thermal aspect of the battery is also quite important for the life of the battery. The temperature of the battery can be affected by various impacts. The examinations proved that, the temperature of battery could be influenced by driving behavior, battery initial temperatures and ambient temperatures. They also indicated that, initial condition parameters for battery temperature are significant for fuel consumption of vehicle (Li and Zhu, 2014). In most cases, the single cell model is used to make better aspect for thermal model of battery. Then, it could be generalized for total cells in battery module (Ismail et al., 2013). In thermal modelling part, these parameters are thought individually in this thesis.

The control strategy is the key point of this thesis. After modelling all required data, the controller should be developed to manage whole systems in a favor of user desires. In literature, researchers investigated different control strategies for different purposes. In some cases, they focus on fuel consumption and battery life, whereas in some, they focus on energy management strategy for energy storage systems (ESS)

by taking the temperature of battery as a reference. Dynamic programming is one of the best solutions that is used to find the most appropriate controller for these purposes. In one paper, they have reduced the current demands to the battery by an average of 62% over real world driving cycles. They have achieved prolonging the battery life and performance (Karabasoglu et al., 2018). Another strategy for optimizing the fuel consumption is equivalent consumption minimization strategy (ECMS). Researchers have demonstrated that ECMS is also good option for these purposes (Sciarretta and Guzzella, 2007). When the control parameters of the system have increased, the model predictive control (MPC) gives the best solution to solve these optimization problems. MPC is widely used for automotive applications in literature. By using MPC controller algorithm, fuel consumption and cycling rate of battery (C-rate) is reduced (Borhan and Vahidi, 2010). Another research demonstrated that by maintaining desired battery state of charge (SOC) and speed, the controller can minimize fuel consumption and improve the vehicle performance. In this paper, they have achieved their target by considering torque split for different types of engines (Poramapojana and Chen, 2012). In another paper, they presents a novel MPC control strategy by taking different parameters into account like required velocity, SOC, fuel consumption and torques for different sources. They have proposed that MPC contribute the fuel economy by looking for fuel consumption and engine efficiency (Lu et al., 2013).

In every energy storage system devices, there is an optimal temperature that these devices should operate. If the battery temperature increases and exceeds the optimal temperatures, because of the internal structure of the battery, the life of it will be adversely affected. In one experiment, research workers focus on the terminal voltage of the battery. They want to hold this voltage in a specific interval by focusing on the temperature of the battery. They aim to keep the temperature between 15 and 40 °C and they succeed to get desired terminal voltage (Altaf et al., 2017). Another approach for thermal management strategy is to take several parameters into account such as fuel consumption, SOC etc. and to add cooling system for battery as an assistant. It could be achieved either adjusting the mentioned parameters or the cooling times (Hasselby, 2013). Also, another strategy is applied in literature that the fan speed can be controlled by MPC controller to track desired parameters. By

speeding up the velocity of fan, the temperature of battery is kept below 40 °C (Masoudi and Azad, 2017).

### **1.2.1. History of MPC**

The first studies on MPC traced back to the late 1970s. Richalet et al. (1978) found a new method which is called Model Predictive Heuristic Control. This method simplifies the way of tuning the parameters of the systems that are hard to be controlled by PID controllers. Calculating the constraints and finding the optimal controller was not in this controller's concern. Later, name of Model Algorithmic Control (MAC) was given to this control strategy.

Engineers Cutler and Ramaker (1979) described a new MPC strategy which is called Dynamic Matrix Control (DMC). The proposed optimization method for constrained systems was based on the fact that the control action is solved by linear programming in each time step.

Peterka (1984) found a new method which is called Predictor-Based Self-Tuning Control. This method is developed to better overcome the measurable disturbances of systems. This method is appropriate for real time computation since the algorithm of this method is numerically robust.

Clarke et al. (1987) offered a method of Generalized Predictive Control (GPC). This method is based on generalized minimum variance and pole placement. This method can be used to handle either simple plants or a complex plant like nonminimum phase and unstable open loop systems.

Clarke and Scattolini (1991) intended Constraint Receiving Horizon Predictive Control (CRHPC) for handling the optimization problems where the conventional controllers can fail. This method has beneficial stabilization features for small horizons. It has robust capability of dealing with complex plants.

After researchers found new methods, they focus on improving the performance of MPC. Kouvaritakis et al. (1992) proposed new algorithm for GPC to get more robust stability theory. They improved stability margin of the system by changing the transfer function operators with some polynomial operators. Bemporad and Morari (1999) demonstrated new method that has strong ability to deal with constraints and instability. Grimm et al. (2005) presented stability results for unconstrained discrete

time nonlinear systems. Grüne et al. (2010) expressed a formula that satisfies all controller criteria and stabilization conditions without stabilizing constraints. Prabhu and George (2014) described easy way to choose the best prediction horizon and they demonstrated the stability and high performance of overall system.

### **1.2.2. MPC Applications in Automotive Industry**

MPC has several advantages that will be mentioned in Section 3.4. In recent years, the development in MPC algorithms and computational speed of microprocessors encourage scientist to be interested in MPC in automotive industry.

In automotive industry, there are many MPC applications, including diesel engine, fuel consumption, traction, steering, speed and thermal control. In addition MPC controller technology is supported by several automotive companies such as Ford, BMW, Honda, Toyota, etc. (Hrovat et al., 2012). Garcia et al. (1989) shows the superior futures of MPC in different industries. One approach of using MPC in automotive industry is to focus on diesel engine air path. The researchers indicated that MPC can improve the dynamic of air path and reduce the CO<sub>2</sub> emission of the car (Ortner and Del Re, 2007). Another approach is to carry out some experiments to find optimal traction of car. The main purpose of this research is to minimize required torque. Researchers achieved 20% reduction of peak amplitude and they increase the performance of the car (Borrelli et al., 2006). In another experiment, Cairano et al. (2010) improved MPC strategy to control steering of a vehicle by actuating active front steering (AFS). They have tested their design with different steering positions and they verified stabilization.

In many researches, including this thesis, the cornerstone of designing high performance MPC is tracking vehicle speed. Cairano et al. (2012) focused on improving idle speed performance and robustness by considering minimizing the time and effort. They proved that the better performances can be obtained by improving idle speed control and it directly affects other parameters of vehicle, including fuel consumption. In another paper, researchers demonstrated the importance of thermal management strategy for vehicle engine performance. They improved model predictive control allocation (MPCA) for two actuators with different constraints intervals (Vermillion et al., 2011).

Almost all types of MPC controllers for different purposes that are mentioned above, are used by Ford Motor Company (Hrovat et al., 2012). By improving performance of MPC controller, this control strategy can be embedded into Electronic Control Unit (ECU) of all types of vehicles.

### **1.3. Aim of Study**

Nowadays, studies mostly focus on reducing CO<sub>2</sub> emission in cars, because of catastrophic effects of it. It is proved that, carbon emission adversely affects human health and environment. One of the main reasons of this emission is that the burning of fossil fuels releases carbon dioxide. Hence, there is a direct proportion between fuel consumption and CO<sub>2</sub> emission. It could be inferred that if fuel consumption is achieved to decrease, the catastrophic effects of CO<sub>2</sub> will also be decreased. For this reason, scientists concentrate on developing energy management strategies to decrease fuel consumption of car.

In this thesis, one of the top priorities is to make optimum power split and to decrease hybrid vehicle's fuel consumption because of mentioned reasons. To achieve this, energy management strategy (EMS) should be developed. This strategy should split power in most economic way between main power sources of vehicle, including ICE, supercapacitor and battery, by considering minimization of fuel consumption. Cornerstone of developing EMS is to design controller. In this thesis, model predictive control (MPC) is determined to improve EMS.

Another purpose of EMS is to reduce stress on battery for prolonging life of it. Key point of achieving this task is not to use battery frequently. Instead of using only battery for electric part of vehicle, another alternative energy storage system (ESS) which is supercapacitor is used. Since supercapacitor can be charged much more times than battery, it is good alternative to help battery.

For the last purpose of this thesis, thermal management strategy (TMS) is developed. The aim of this strategy is to adjust speed of fan, located next to the battery, to keep the battery temperature in a specific interval. Temperature is the other negative effects for battery life.

As a summary of aim of study is to develop EMS and TMS by using MPC to achieve these three mentioned purposes. When overall system is thought, MPC will

determine the power of all three sources and speed of fan. While MPC is determining these, it also considers some parameters, including state of charge (SOC) of battery and supercapacitor. To get better results from this strategy, MPC should also keep SOC values in specific interval. The reliability of MPC can be observed by looking at whether MPC holds desired parameters in these intervals or not.

#### **1.4. Outline of Thesis**

Chapter 1 includes literature review related to this thesis. It also mentions about the aim of this thesis.

Chapter 2 gives brief information about hybrid vehicles and its components. This chapter describes the types of hybrid vehicles, battery and supercapacitor technologies.

Chapter 3 describes basic information about MPC controller. This chapter conveys the history, working principle and advantages and disadvantages of MPC.

Chapter 4 includes first step of designing energy and thermal management strategies. It includes mathematical models of all process and Simulink block diagrams.

In Chapter 5, the design of MPC controller by considering EMS, TMS and combined these two strategies are discussed. After that, the results of control process are demonstrated.

In Chapter 6, the conclusion and contribution of thesis have been discussed. Then, the future works was shaped according to obtained results.



## **CHAPTER 2**

### **OVERVIEW OF HYBRID VEHICLES**

#### **2.1. Background and Types of Hybrid Vehicles**

The history of hybrid cars almost stretches back as long as conventional automobiles. The first hybrid car was built by Ferdinand Porsche in 1899. It was using the gasoline engine to deliver the power to the electric motor that has the link to the wheels. In the categorization of hybrid vehicles, this system is considered as parallel system.

Hybrid vehicles are divided into three main groups, depending on the operation of the motors in the vehicle, either interdependent or independent of each other.

##### **2.1.1. Parallel Hybrid Vehicles**

In parallel hybrid vehicles, two engines can operate together or at the different times independently. Generally, on such vehicles, the electric motor is in operation during start-stop operations, when the vehicle consumes the most fuel, and when the vehicle rises above a certain speed, it leaves its place to internal combustion engine. The battery is mostly charged during regenerative braking. It can be charged by electric motor when the power demand of vehicle is low, by using electric motor as a generator. Honda Civic and Honda Accord are used parallel hybrid technology (Wikipedia, the free encyclopedia, “Honda Civic Hybrid”, 2015). Parallel hybrid structure is shown in Figure 2.1.

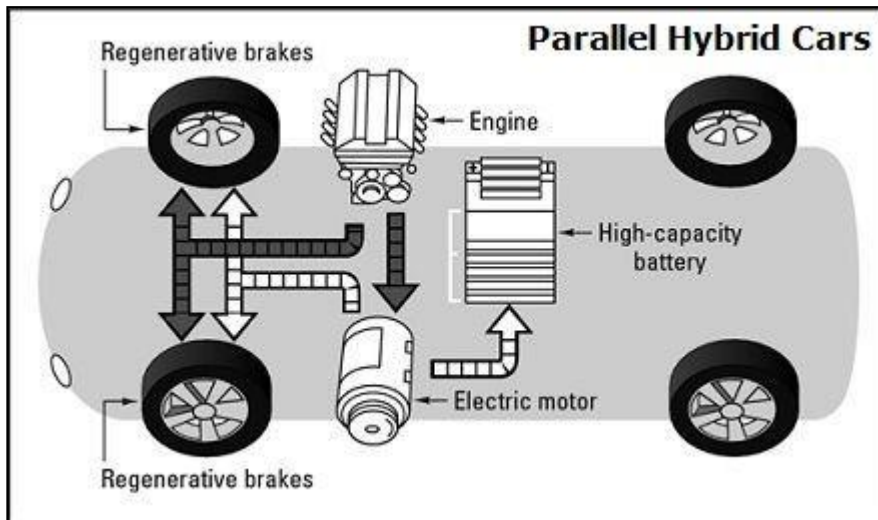


**Figure 2.1.** Parallel Structure of Hybrid Vehicles

### 2.1.2. Series Hybrid Vehicles

Unlike parallel hybrid, this system requires generator. In series hybrid vehicles, two engines operate interdependently. Internal combustion engine is used to charge batteries via generator. The voltage in the charged batteries is transferred to the electric motor via the powertrain. Electric motors provide the power to drive the wheels. Series hybrid technology is generally used by buses and other urban vehicles that must do a lot of start-stop action (Brahma et al., 2000). Series hybrid structure is shown in Figure 2.2.

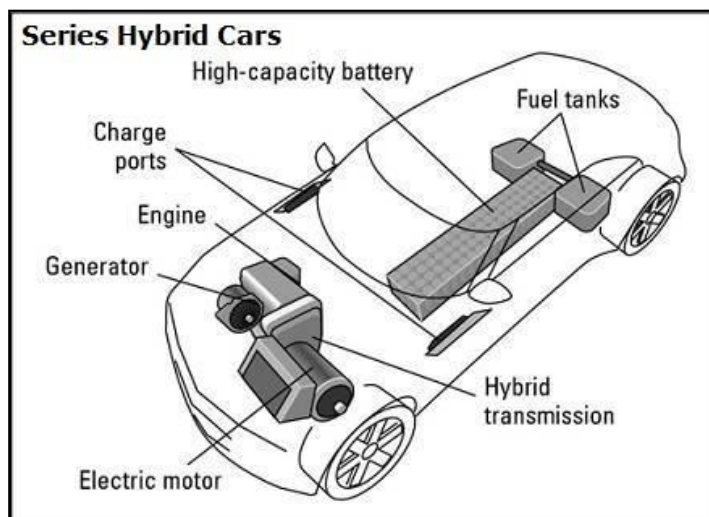


**Figure 2.2.** Series Structure of Hybrid Vehicles

### 2.1.3. Power Split Hybrid Vehicles

These types of hybrid vehicles can be summarized as the combination of parallel and series hybrid vehicles. By using this combination, the ICE can be used to drive the wheel directly like parallel hybrid vehicles and it can be disconnected from the wheels so that only the electric motor can deliver the power to the wheels like series hybrid vehicles. Toyota Prius is one of the example which uses this technology. Figure 2.3 shows the structure of power split hybrid vehicle.

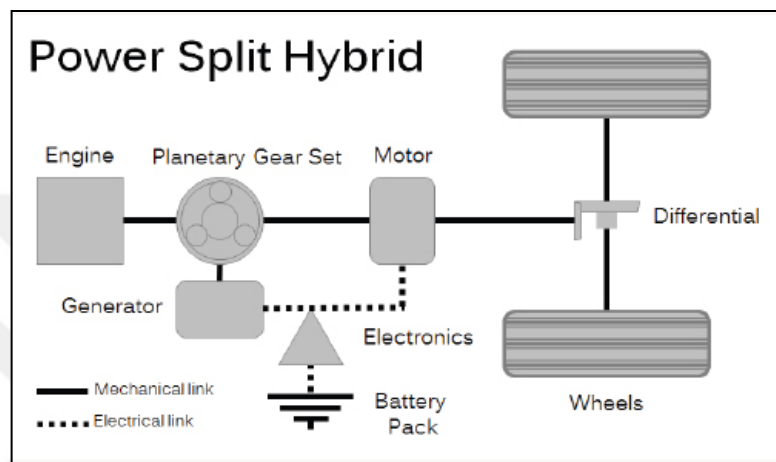


**Figure 2.3.** Power Split Structure of Hybrid Vehicles

## 2.2. Battery Technology

In HEVs, one of the most essential components is battery. Batteries are capable of storing the high amount of energy in a small volume. Batteries provide the demanded power to the electric motor. In addition, it recovers the vehicle kinetic energy in the regenerative braking mode without using any plug-in device. The batteries use chemical reactions while charging and discharging and produce a voltage between their output terminals. The fundamental element is electromechanical cell which is contained by batteries. Voltages generated by these cells are called electromotive force.

Basically, there are three types of batteries that are used in HEVs.

### 2.2.1. Lead Acid Batteries

Lead acid batteries are safe and they have good proven performance to use in HEVs. However, when it is compared with other types of batteries, the life of it is considerably lower. Also, the energy capacity of lead acid batteries is lower.

Furthermore, this type of battery is considered the most toxic one. Because of these disadvantages, lead acid batteries are not being used in HEVs anymore.

### **2.2.2. Nickel-Metal Hydride (NIMH) Batteries**

Hybrid vehicles mostly use NIMH batteries to power the engine. The most important feature of this battery is that it can be easily rechargeable. It produces more energy and it is more “green” than lead acid battery. However, these batteries store less energy than lithium-ion batteries.

### **2.2.3. Lithium-ion Batteries**

Lithium-ion batteries keep the largest amounts of energy when they are compared with other two. It gives the car enough range until it is needed to be charged again. It can be easily rechargeable like NIMH batteries. It is the most “green” battery type in these three. Because of these advantages, Lithium-ion batteries seems to be best option, however it is more expensive than others. Li-ion batteries contain cobalt in their formula and this element tends to explode. Thus, scientists are working on it to use alternative source instead of using cobalt.

## **2.3. Supercapacitor Technology**

The supercapacitors are energy storage devices that can store much more energy than typical electrolytic capacitors. The internal structure of supercapacitor contains two conducting metal plates and dielectric material between them. In standard supercapacitors, the conducting metal part is consisting of carbon/carbon layers. In most supercapacitors, one layer of conducting metal consist of carbon, whereas other layer being of metal oxides such as lead, nickel oxide and lithium-ion.

They typically store less energy than batteries, but in contrast, they have much more energy density and cycling life. Because of these reasons, supercapacitors are used in applications that require fast charge and discharge issues. Also, they have more compact size, lighter and less harmful than batteries.

In this thesis, the well known supercapacitor Maxwell is selected. The specifications of this supercapacitor are mentioned in section 4.2.4. Figure 2.4 shows the comparison of supercapacitor and different types of batteries in terms of energy and power densities.

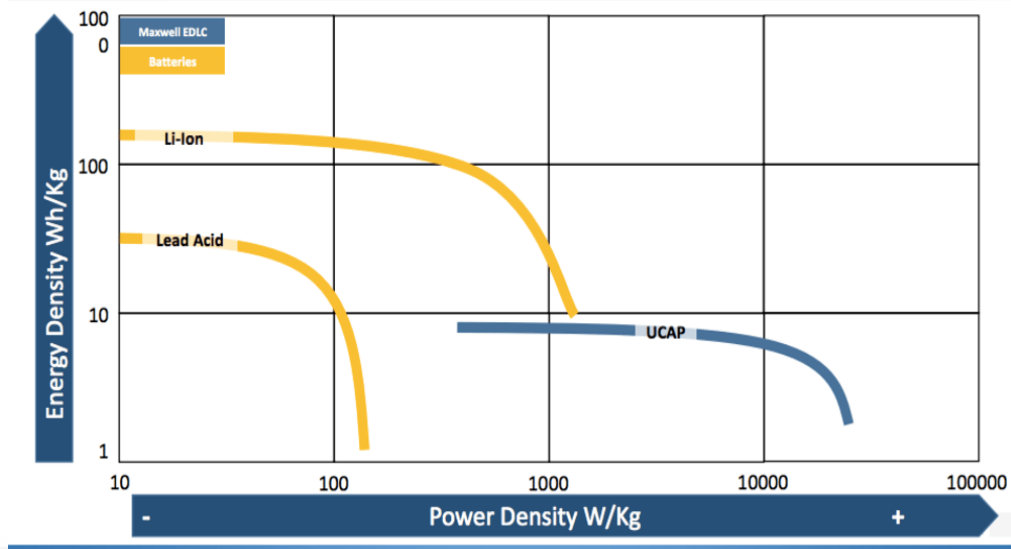


**Figure 2.4.** Comparison of Battery and Supercapacitor in terms of Energy and Power Density Features

This figure is the summary of comparison of batteries and supercapacitor. As it can be seen from the figure, supercapacitors have less energy density and more power density than batteries. Therefore, supercapacitors can supply required power in a short period of time.

## **CHAPTER 3**

### **OVERVIEW OF MODEL PREDICTIVE CONTROL**

#### **3.1. What is Model Predictive Control?**

Model Predictive Control (MPC) is a feedback control system that uses a model to make prediction about future outputs of a system. The goal of the controllers is to calculate the input to the plant while the output of the plant follows desired outputs. The MPC strategy of computing this input is predicting future.

MPC uses model of the plant and optimizer inside the controller. Optimizer is used to be ensured that the system output tracks the desired reference. The aim of MPC is to minimize the determined cost function by predicting the process behavior in specific horizon. MPC also uses dynamic equations by shifting forward the horizon by one time step. For this reason, MPC is also known as Receding Horizon Control (RHC).

In MPC, the signals, computed by controller and send to the plant, are called manipulated variables whereas plant outputs are called output variables.

There are three main ideas behind Model Predictive Control (Rossiter, 2003):

- Predicting future process behavior using a dynamic equation of the process over a prediction horizon
- Calculating control signal sequence that minimize the cost function
- After each optimization step, the first value of the calculated control sequence is sent to the system while the horizon is shifting forward

The strategy of MPC is illustrated in Figure 3.1.

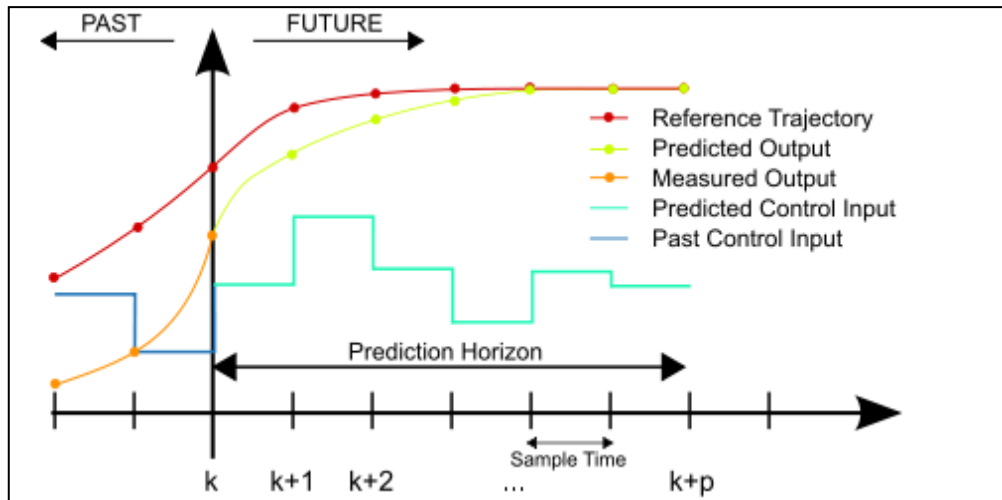


**Figure 3.1.** The Control Strategy of Model Predictive Control

The strategy can be explained as:

- The state of a process is calculated at each time instant by considering the known values such that past inputs and outputs and current output. The estimated control states of the process can be represented as  $x(k)$ . This state will be the initial point of the optimization in the next step. The value of 'k' is between 1 and p. In this figure, p is the prediction horizon that shows the number of predicted future time steps. It shows how far the controller predicts into the future.
- In next step, the plant model is used to anticipate the future sequence of the measured outputs by considering future control signals. The controller computes these future control signals in a specific horizon. This horizon is called control horizon. In this horizon, the optimizer finds the best future control signals by taking into account the action of keeping the outputs as close as possible to the reference.
- At the last step, the controller takes the first instance move and ignores the rest of the trajectory. After that, controller repeats all sequences for the next time step.

### 3.2. MPC Design Parameters and Related Terms

There are several parameters that are used in MPC design process. Understanding these parameters is also the essential point for learning the logic of MPC. The basic

idea for designing controller will be mentioned in the next section. In this section, the important parameters, that should be considered while designing, are indicated.

First of all, the general terms are explained. The inputs of the controller, which directly affect the output of system, are called manipulated variables. In addition, the plant output, which can be calculated, is called measured output. In all types of controllers, including MPC, the general system is called plant. All plants are influenced by some environmental factors. The environmental factors that affect the controller performance are called disturbances.

Next step is to mention about design parameters. These parameters are:

- Sample time
- Prediction horizon
- Control horizon
- Constraints
- Weights

All these parameters are briefly examined.

### **3.2.1. Sample Time**

The sample time is the parameter that is used to determine the rate at which the controller computes the control algorithm. It should be carefully adjusted because when it becomes too big, the controller cannot give fast reactions to the disturbances. On the other hand, when the sample time is too small, the controller can overreact to disturbances, however this situation causes an excessive computational load. Because of these reasons, finding right value for sampling time is quite important.

### **3.2.2. Prediction Horizon**

At each time step, the MPC controller predicts the measured output and the optimizer seeks the optimal sequence of manipulated variables that drives the measured output as close to the set point as possible. The number of predicted future time steps is called prediction horizon. If this time is too short, by the time the controller makes the next movement, it could be too late to come up with disturbances. In a



contradiction, If prediction horizon is too long, then unexpected situations, that controller is not able to detect, can occur.

### **3.2.3. Control Horizon**

If the set of future control actions leading to predicted plant output, the number of control moves to time step are called control horizon. Each control move in the control horizon is needed to be computed by optimizer. Thus, the value of control horizon is important for duration of controller's computations.

### **3.2.4. Constraints**

Constraints are really important parameter that is used to prevent some damages for system components. In MPC language, constraints are upper and lower limits of desired zone that controller should operate. There are two types of constraints. One of them is hard constraints which cannot be violated. Other one is soft constraints that could be violated.

### **3.2.5. Weights**

MPC can deal with different optimization problems at the same time. For a designer, some problem can be more important than others. The designer can adjust the weights of inputs and outputs according to significance criteria. Adjusting weight coefficient in balanced, gives the smooth control action.

Another parameter is rate weight, which is used to penalize aggressive control moves.

## **3.3. Structure and Elements of MPC**

All types Model Predictive Controller (MPC) have three basic elements (Camacho and Alba, 2013). These are:

- Prediction Model
- Objective Function
- Optimization Algorithm to Compute the Control Law

Before talking about the components of MPC, the basic structure of MPC is illustrated in Figure 3.2.

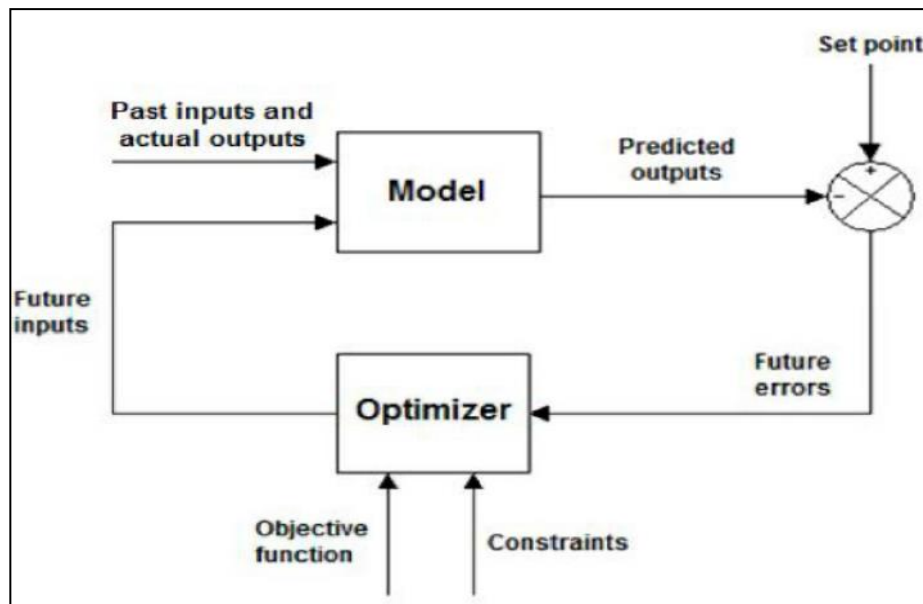


**Figure 3.2.** Basic structure of MPC

### 3.3.1. Prediction Model

Modelling is the key point of MPC. As it is mentioned before, a model is used to predict the future plant output and it is used to find optimal control actions, by considering past and current values.

Modelling part can be examined into two groups that are the process model and disturbances model. For the process model, the relationship between inputs and outputs of the model can be constructed with different methods such that, impulse response, step response, transfer function and state space. Constructing the model of disturbances is also really important. It can be expressed by the difference between the measured output and the real model output. The effects of disturbances cannot be ignored.

### 3.3.2. Objective Function

When the whole system is thought, the optimizer is taking also quite important part in controller design. The aim of the optimizer is to minimize objective function of the system. Another purpose of the optimizer is setting the future output to follow reference signal while the error is penalized.

### **3.3.3. Optimization Algorithm to Compute the Control Law**

Obtaining the control action values is the last component of MPC and this part is also really crucial. To get the values of this control action, the cost function should be minimized. To do this, the values of predicted outputs are calculating with respect to past values of inputs, outputs and future control signals by taking advantage of model. At the last part, iterative method of optimization is used to obtain an expression that is achieved to minimize objective function.

### **3.4. Advantages and Disadvantages of MPC**

Model Predictive Control has several advantages. These are:

- MPC can handle multi-input multi-output (MIMO) systems as well as single-input single-output (SISO) systems.
- MPC can handle constraints.
- MPC has preview capability.
- MPC can deal with interactions between system inputs and outputs.
- It is beneficial for both linear and nonlinear process models.
- It is able to cope with the complex processes.
- MPC also allows feed forward control to compensate for disturbances.
- It is capable of satisfying constraints and tracking the reference point in systems that has complex dynamic, non minimum phase, long delay times and unstable ones.
- The MPC technology can be adapted for many sectors and it is an open technology for future extensions.

MPC has the following disadvantages:

- MPC requires a powerful, fast processor with a large memory. Thus, it is more expensive than most controllers which are used in industry.
- It requires the mathematical model. For this reason, it could be challenging to get the model of process.

- The derivation of control law can be harder when the number of constraints of the system increases.



## **CHAPTER 4**

### **MATHEMATICAL MODEL OF HYBRID VEHICLE COMPONENTS**

Designing both energy management and thermal management strategies in hybrid vehicle by using MPC requires following steps:

- First step is to derive the mathematical model of each component in hybrid vehicle individually.
- Then, the formulations should be embedded into the blocks that are created in MATLAB/Simulink.
- The connection of system inputs and outputs for each block should be made.
- After all connections are carried out, the whole system is thought as one that has multi input multi output (MIMO). This part is called plant of a system.
- Next step is constructing MPC. In this step, Model Predictive Control Toolbox is used to design controller.
- Closed loop system is designed by making the connection between MPC and plant of the system.
- Tuning all design parameters of model predictive controller is crucial point.
- After tuning, the controller is exported into the MPC block.
- The last step is observing the performance of controller by simulating overall system in MATLAB®.

All these steps are examined in this thesis respectively. In this chapter, mathematical model and Simulink model of vehicle components are investigated. Then the mathematical model of MPC is briefly mentioned.

#### **4.1. Mathematical Model of Hybrid Vehicle**

Modelling of the vehicle is one of the most important part in this thesis. Since the internal structure of hybrid vehicle's components is so complex, the model can be

represented by relatively simple. In hybrid vehicles, there are several components, which should be considered, including vehicle dynamic, internal combustion engine, battery, supercapacitor, and temperature of battery. Controller will share the power between ICE, battery and supercapacitor optimally. Before designing MPC, the mathematical models of these parameters are derived. The accuracy and stability of controller depends on these mathematical models. In this section, plant model is examined profoundly.

#### 4.1.1. Vehicle Dynamic Model

In this section, the mathematical formulation of vehicle dynamic is derived by using longitudinal motion of the vehicle. The total forces acting about the vehicle are evaluated by taking Newton's laws of motion into account. For better understanding of this law, total forces acting on vehicle is shown in Figure 4.1.

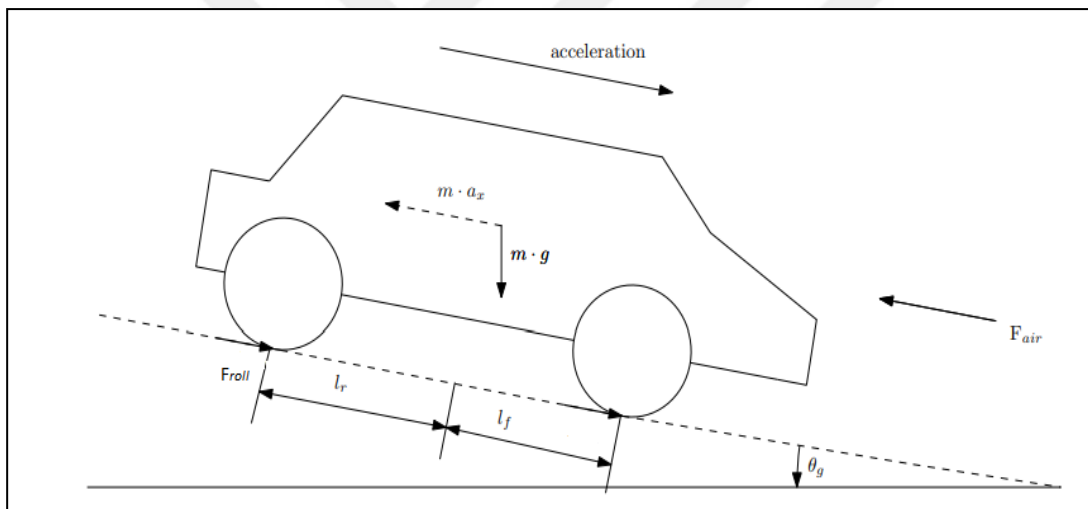


**Figure 4.1.** Longitudinal Forces on Vehicle

Using Newton's law of motion, the force output by motors can be calculated from following equation:

$$F_{\text{motor}} = F_{\text{net}} + F_{\text{resistive}} \quad (4.1)$$

$$F_{\text{resistive}} = F_{\text{air}} + F_{\text{roll}} + F_{\text{gravity}} \quad (4.2)$$

While the net force in equation (4.1) is calculated from well known Newton's law, the net force can be written as the multiplication of vehicle mass and acceleration. In equation (4.2), the total forces that resist the motion of the vehicle are formulated. In this equation,  $F_{\text{air}}$  is a force which is acting opposite to the motion of vehicle with

respect to surrounding air.  $F_{roll}$  stands for rolling resistance which occurs when wheel rolls on a surface. This force causes dissipation of energy.  $F_{gravity}$ , can be simply explained as attraction between two masses or the force that exists while one mass pulled by another. The formulations of these forces can be expressed from following equations (Karabasoglu et al., 2018):

$$F_{air} = \frac{1}{2} \rho v^2 C_d A \quad (4.3)$$

$$F_{roll} = C_{roll} mg \cos \theta \quad (4.4)$$

$$F_{gravity} = mg \sin \theta \quad (4.5)$$

$$F_{net} = ma \quad (4.6)$$

$$\rho = \frac{0.0289}{8.314 * T} * 101.325 * \left(1 - \frac{0.0065 * z}{T}\right)^{\frac{0.0289 * g}{8.314 * 0.0065}} \quad (4.7)$$

where

$F_{net}$	Net forces on vehicle [Newton]
$a$	Acceleration [ $m/s^2$ ]
$F_{air}, F_{roll}, F_{gravity}$	Resistive forces [Newton]
$v$	Vehicle velocity [m/s]
$C_d$	Drag coefficient of vehicle
$A$	Effective cross sectional area of vehicle [ $m^2$ ]
$C_{roll}$	Rolling resistance coefficient
$m$	Vehicle mass [kg]
$g$	Gravitational acceleration [ $m/s^2$ ]
$\theta$	Angle of slope [radians]
$\rho$	Density of air [ $kg/m^3$ ]
$z$	Vehicle elevation [m]
$T$	Air temperature [K]

After finding total force on vehicle, it can be converted into total power loss of the vehicle. The expression of total loss of vehicle can be concluded:

$$P_{\text{loss}} = \frac{F_{\text{resistive}} * v}{\eta} \quad (4.8)$$

where  $P_{\text{loss}}$  is the total loss of vehicle in watt,  $\eta$  is total drivetrain efficiency, including mechanical and electrical efficiency.

#### 4.1.2. Internal Combustion Engine (ICE) Model

In this thesis, for control purposes, we are interested in the power and corresponding fuel consumption, and we assume constant gear ratio and ignore torque dynamics. ICE is only used to observe fuel consumption of the vehicle. To get the fuel consumption, the value of calorific value should be noticed. Calorific value is the energy term which is contained by any types of fuel. It is the heat produced by combustion of a specified quantity of fuel. Relationship between power and fuel consumption can be simply expressed from following equation:

$$P_{\text{brake}} = \frac{P_{\text{ICE}}}{\eta} \quad (4.9)$$

$$F_c = \frac{P_{\text{brake}}}{C_f} * 0.72 \quad (4.10)$$

where

$P_{\text{ICE}}$	ICE power determined by MPC [W]
$P_{\text{brake}}$	Brake power of vehicle [W]
$C_f$	Calorific value [J/kg]
$F_c$	Fuel consumption [lt/h]

#### 4.1.3. Battery Model

Battery is the main electric source of hybrid vehicles. In battery model, there are three significant terms, including regenerative braking, state of charge (SOC) and C-rate. In section 1.1, regenerative braking was already briefly mentioned.

SOC is defined as available capacity of battery which is able to provide required power of vehicle. In other words, amount of energy left in a battery. In literature, the formulation of SOC is more complex (Poramapojana and Chen, 2012). In this thesis, the expression for charge level of battery is given by (Karabasoglu et al., 2018):



$$Q_k = Q_{k-1} + \frac{P_{Battery} * \Delta t}{\eta_{char}}, \quad P_{Battery} < 0 \quad (4.11)$$

$$Q_k = Q_{k-1} + \eta_{dis} * P_{Battery} * \Delta t, \quad P_{Battery} > 0 \quad (4.12)$$

where

$Q_k$  Latest charge level [kWh]

$Q_{k-1}$  Previous charge level [kWh]

$P_{Battery}$  Power consumption determined by MPC [kW]

$\Delta t$  Elapsed time [hours]

$\eta_{char}, \eta_{dis}$  Charging and discharging efficiencies of battery respectively

Another important term in battery model is C-rate. C-rate is described as the discharge intensity of battery (Miller et al., 2005). In general cases, discharging the battery at high C-rate adversely affects the battery life and it is proved by using the combination of supercapacitor and battery (Miller, 2007). For example, a C-rate of 1C is known as one hour discharge and it shows discharge current will discharge whole battery in 1 hour. The formulation of C-rate is expressed by (Borhan and Vahidi, 2010):

$$C_{rate} = \frac{P_{battery}}{0.69 * V_{OC} * C_{battery}} \quad (4.13)$$

where

$V_{OC}$  Open circuit voltage of battery [V]

$C_{battery}$  Battery cells capacity [Ah]

#### 4.1.4. Supercapacitor Model

Supercapacitor is the assistant source of energy storage system in our designed hybrid vehicle. The reason of using supercapacitor is to keep C-rate of battery in optimal interval and to prolong the life of the battery. The mathematical model of supercapacitor is exactly same as battery model. The mathematical formulation of supercapacitor is given by:

$$Q_k = Q_{k-1} + \frac{P_{supercapacitor} * \Delta t}{\eta_{char}}, \quad P_{supercapacitor} < 0 \quad (4.14)$$

$$Q_k = Q_{k-1} + \eta_{dis} * P_{supercapacitor} * \Delta t, \quad P_{supercapacitor} > 0 \quad (4.15)$$

where

$Q_k$	Latest charge level [kWh]
$Q_{k-1}$	Previous charge level [kWh]
$P_{supercapacitor}$	Power consumption determined by MPC [kW]
$\Delta t$	Elapsed time [hours]
$\dot{\eta}_{dis}, \dot{\eta}_{char}$	Charging and discharging efficiencies of supercapacitor

#### 4.1.5. Thermal Model of Battery

The temperature of battery is one of the main issues in this thesis. Since the temperature adversely affects life of the battery, it is needed to be investigated. The aim of thermal model is to keep the battery surface temperature in specific interval. For this reason, the fan is used to cool down the temperature. Determining the rate of cooling is attached to the term of heat transfer rate. In this part, some of the terms related with heat transfer rate is also indicated with thermal model of battery for better understanding.

There are three types of heat transfer terms, including conduction, convection and radiation. Conduction is the heat transfer concept, transmitted through the material from more energetic side to lower side. Convection is the heat transfer type, which is occurred by the temperature difference between fluid and substance. In other words, the energy transfer happens due to the molecular interaction of these two materials. Radiation is the last type of heat transfer and it is defined as the heat transmission as electromagnetic waves. In this case, there are conduction and convective heat transfer types due to the interaction between battery and air flow. Figure 4.2 illustrates all types of heat transfer.

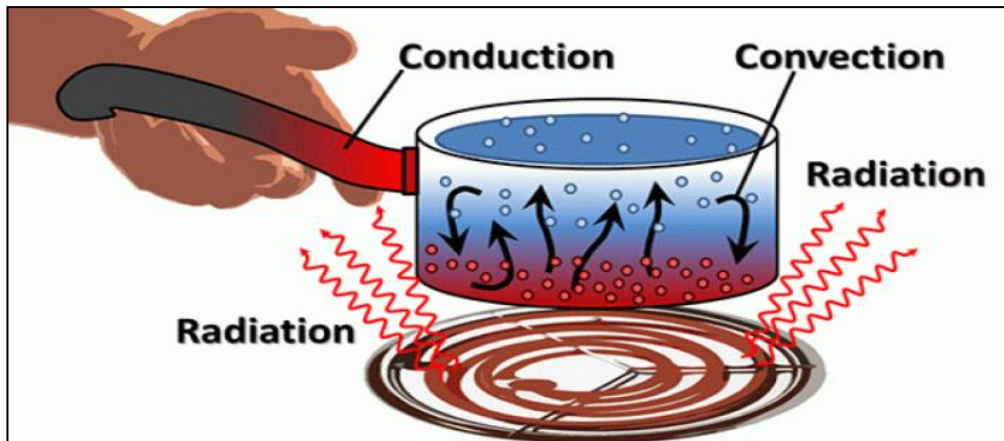


**Figure 4.2.** All Types of Heat Transfer Methods

There are several terms which should be known to get the mathematical model of convective heat transfer. These parameters are briefly examined.

#### 4.1.5.1. Air Density

Air density is defined as the specific weight of an air divided by its volume. This parameter varies with temperature and pressure. The formulation of air density is given by:

$$\rho = \frac{m}{V} \quad (4.16)$$

where,  $\rho$  is air density in  $\text{kg/m}^3$ ,  $m$  is mass of an air in kg,  $V$  is volume of air in  $\text{m}^3$ .

#### 4.1.5.2. Specific Heat

It is the amount of heat required to raise the temperature  $1^\circ\text{C}$ . In other saying, specific heat is the derivative of material's heat with respect to the temperature.

$$C = \frac{dQ}{dT} \quad (4.17)$$

where,  $C$  is specific heat in Joule/Kelvin,  $Q$  is material heat in Joule,  $T$  is material temperature in Kelvin.

#### 4.1.5.3. Dynamic Viscosity

This is the measurement of required force to deal with internal friction in a fluid.

$$\mu = \tau * \frac{dy}{dc} \quad (4.18)$$

where,  $\mu$  is dynamic viscosity in  $\text{Ns/m}^2$ ,  $\tau$  is shearing stress on fluid in  $\text{N/m}^2$ ,  $dy$  is unit distance between layers in meter,  $dc$  is unit velocity in  $\text{m/s}$ .

#### 4.1.5.4. Kinematic Viscosity

This term is defined as the dynamic viscosity divided by air density.

$$v = \frac{\mu}{\rho} \quad (4.19)$$

where,  $v$  is kinematic viscosity in  $\text{m}^2/\text{s}$ ,  $\mu$  is dynamic viscosity in  $\text{Ns/m}^2$ ,  $\rho$  is fluid density in  $\text{kg/m}^3$ .

#### 4.1.5.5. Thermal Conductivity

Thermal conductivity shows the heat conduction capacity of materials.

$$\lambda = \frac{P \cdot t}{A \cdot \Delta t} \quad (4.20)$$

where,  $\lambda$  is thermal conductivity in  $\text{W/K.m}$ ,  $P$  is power in watt,  $A$  is transmitted surface area in  $\text{m}^2$ ,  $\Delta t$  is temperature difference causes heat transfer in Kelvin,  $t$  is thickness of material in  $\text{m}$ .

#### 4.1.5.6. Prandtl Number

Prandtl Number is one of the dimensionless numbers which is defined as the ratio of momentum diffusivity to the thermal diffusivity. This number shows that how fast the thermal diffusion takes place in its direction when it is compared with momentum diffusion.

$$Pr = \frac{\mu \cdot C}{\lambda} \quad (4.21)$$

where,  $Pr$  is Prandtl Number which has no unit,  $\mu$  is dynamic viscosity in  $\text{kg/m.s}$ ,  $C$  is specific heat in  $\text{J/kg.K}$ ,  $\lambda$  is thermal conductivity in  $\text{W/K.m}$ .

The values of parameters which are mentioned so far are illustrated in Figure 4.3.

Temp. $T, ^\circ\text{C}$	Density $\rho, \text{kg/m}^3$	Specific Heat $c_p$ $\text{J/kg}\cdot\text{K}$	Thermal Conductivity $k, \text{W/m}\cdot\text{K}$	Thermal Diffusivity $\alpha, \text{m}^2/\text{s}$	Dynamic Viscosity $\mu, \text{kg/m}\cdot\text{s}$	Kinematic Viscosity $\nu, \text{m}^2/\text{s}$	Prandtl Number Pr
-150	2.866	983	0.01171	$4.158 \times 10^{-6}$	$8.636 \times 10^{-6}$	$3.013 \times 10^{-6}$	0.7246
-100	2.038	966	0.01582	$8.036 \times 10^{-6}$	$1.189 \times 10^{-6}$	$5.837 \times 10^{-6}$	0.7263
-50	1.582	999	0.01979	$1.252 \times 10^{-5}$	$1.474 \times 10^{-5}$	$9.319 \times 10^{-6}$	0.7440
-40	1.514	1002	0.02057	$1.356 \times 10^{-5}$	$1.527 \times 10^{-5}$	$1.008 \times 10^{-5}$	0.7436
-30	1.451	1004	0.02134	$1.465 \times 10^{-5}$	$1.579 \times 10^{-5}$	$1.087 \times 10^{-5}$	0.7425
-20	1.394	1005	0.02211	$1.578 \times 10^{-5}$	$1.630 \times 10^{-5}$	$1.169 \times 10^{-5}$	0.7408
-10	1.341	1006	0.02288	$1.696 \times 10^{-5}$	$1.680 \times 10^{-5}$	$1.252 \times 10^{-5}$	0.7387
0	1.292	1006	0.02364	$1.818 \times 10^{-5}$	$1.729 \times 10^{-5}$	$1.338 \times 10^{-5}$	0.7362
5	1.269	1006	0.02401	$1.880 \times 10^{-5}$	$1.754 \times 10^{-5}$	$1.382 \times 10^{-5}$	0.7350
10	1.246	1006	0.02439	$1.944 \times 10^{-5}$	$1.778 \times 10^{-5}$	$1.426 \times 10^{-5}$	0.7336
15	1.225	1007	0.02476	$2.009 \times 10^{-5}$	$1.802 \times 10^{-5}$	$1.470 \times 10^{-5}$	0.7323
20	1.204	1007	0.02514	$2.074 \times 10^{-5}$	$1.825 \times 10^{-5}$	$1.516 \times 10^{-5}$	0.7309
25	1.184	1007	0.02551	$2.141 \times 10^{-5}$	$1.849 \times 10^{-5}$	$1.562 \times 10^{-5}$	0.7296
30	1.164	1007	0.02588	$2.208 \times 10^{-5}$	$1.872 \times 10^{-5}$	$1.608 \times 10^{-5}$	0.7282
35	1.145	1007	0.02625	$2.277 \times 10^{-5}$	$1.895 \times 10^{-5}$	$1.655 \times 10^{-5}$	0.7268
40	1.127	1007	0.02662	$2.346 \times 10^{-5}$	$1.918 \times 10^{-5}$	$1.702 \times 10^{-5}$	0.7255
45	1.109	1007	0.02699	$2.416 \times 10^{-5}$	$1.941 \times 10^{-5}$	$1.750 \times 10^{-5}$	0.7241
50	1.092	1007	0.02735	$2.487 \times 10^{-5}$	$1.963 \times 10^{-5}$	$1.798 \times 10^{-5}$	0.7228
60	1.059	1007	0.02808	$2.632 \times 10^{-5}$	$2.008 \times 10^{-5}$	$1.896 \times 10^{-5}$	0.7202
70	1.028	1007	0.02881	$2.780 \times 10^{-5}$	$2.052 \times 10^{-5}$	$1.995 \times 10^{-5}$	0.7177
80	0.9994	1008	0.02953	$2.931 \times 10^{-5}$	$2.096 \times 10^{-5}$	$2.097 \times 10^{-5}$	0.7154
90	0.9718	1008	0.03024	$3.086 \times 10^{-5}$	$2.139 \times 10^{-5}$	$2.201 \times 10^{-5}$	0.7132
100	0.9458	1009	0.03095	$3.243 \times 10^{-5}$	$2.181 \times 10^{-5}$	$2.306 \times 10^{-5}$	0.7111

**Figure 4.3.** Properties of Air at 1atm Pressure

#### 4.1.5.7. Reynolds Number

Reynolds Number is one of dimensionless numbers which is defined by the ratio of inertial forces to viscous forces. This number tells us whether the flow of fluid is laminar or turbulent. Figure 4.4 shows the difference between laminar and turbulent flow.

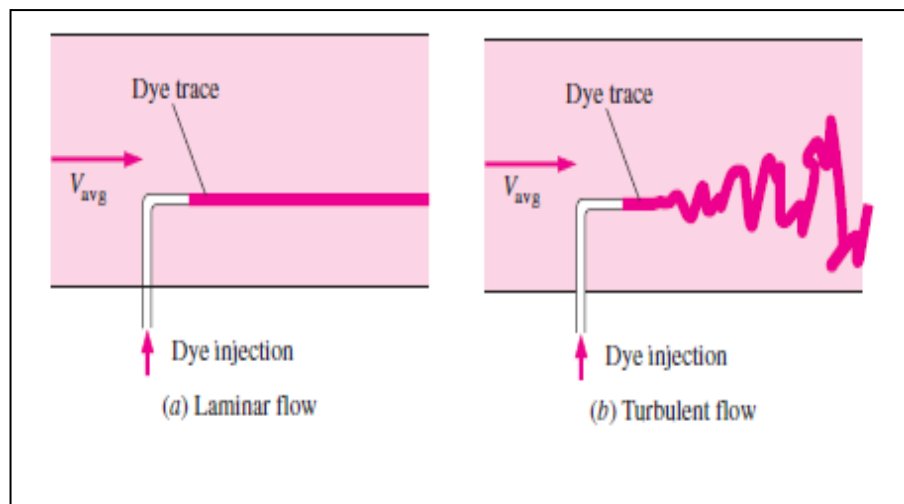


**Figure 4.4.** The Behavior of Fluid in Laminar and Turbulent Flow

If the Reynolds Number is low, the flow characteristic is laminar because the viscous forces are dominant and the motion of fluid is smooth. In contrast, if the Reynolds

Number is high, the inertial forces become dominant and it causes eddy current and vortices. These additional forces cause turbulent flow.

$$Re = \frac{\rho * v * L}{\mu} \quad (4.22)$$

where, Re is Reynolds Number which is dimensionless,  $\rho$  is the fluid density in kg/m<sup>3</sup>,  $v$  is velocity of the fluid m/s, L is a linear dimension in m,  $\mu$  is dynamic viscosity in kg/m.s.

#### 4.1.5.8. Nusselt Number

This dimensionless number is quite important to determine convective heat transfer. It is expressed by the ratio between convective and conductive heat transfers. There are several formulations of Nusselt Number, but in this thesis, Nusselt Number is determined as a function of Reynolds and Prandtl Numbers. Since the cells of battery are assumed to be set of staggered tubes (Masoudi and Azad, 2017), the formulation will be expressed with respect to this assumption.

$$Nu = C * Re^m * Pr_i^{0.36} * \left(\frac{Pr_i}{Pr_s}\right)^{1/4} \quad (4.23)$$

where,  $Nu$  is dimensionless Nusselt Number, Re is dimensionless Reynold Number,  $Pr_i$  is dimensionless Prandtl Number for ambient air,  $Pr_s$  is dimensionless Prandtl Number for battery surface temperature. C and m constants are determined with respect to Reynold Number. Table 4.1 shows how to determine the values of these constant numbers.

**Table 4.1.** Constants of equation 4.23 for Staggered Flow (Masoudi and Azad, 2017)

Reynolds	C	m
10-10 <sup>2</sup>	0.9	0.4
10 <sup>2</sup> - 10 <sup>3</sup>	0.51	0.5
10 <sup>3</sup> – 2 x 10 <sup>5</sup>	0.40	0.6
2 x 10 <sup>5</sup> – 2 x 10 <sup>6</sup>	0.022	0.84

#### 4.1.5.9. Heat Transfer Rate

The mathematical formulation of heat transfer rate is evaluated with respect to the assumption of battery cells are considered as staggered tube. Also, external source of the cooling battery temperature is fan in this thesis. In this section, effects of fan acting on battery temperature is formulated. The geometric packing of a tube bank under effects of air is shown in Figure 4.5.

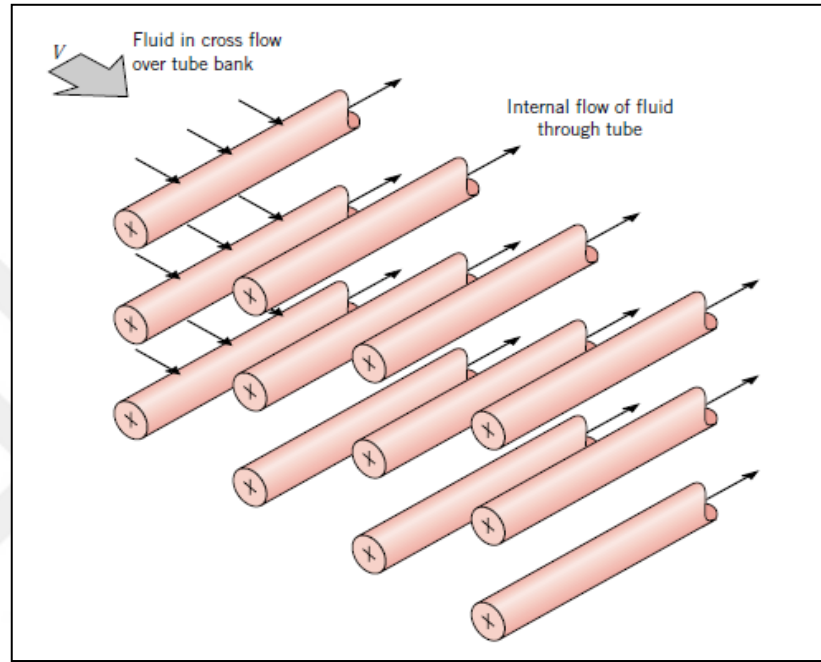


**Figure 4.5.** The Geometric Arrangement of Tube Bank in Cross Flow

While examining the effects of fan on temperature, there are two conditions that the maximum velocity of fan can be either occurred in transverse plane or the diagonal plane (Bergman et al., 2011). The following equation is used to determine where the maximum velocity occurs.

$$S_D = [S_L^2 + (\frac{S_T}{2})^2]^{\frac{1}{2}} < \frac{S_T + D}{2} \quad (4.24)$$

where,  $S_D$  is staggered tube distance in m,  $S_T$  is battery transverse pitch in m,  $S_L$  is battery longitudinal pitch in m,  $D$  is diameter of tube bank (battery pack) in m. Maximum velocity within the tube changes with equation 4.24 as follows (Bergman et al., 2011):

$$V_{max} = \frac{S_T}{S_T - D} * V_{fan} \quad (4.25)$$

$$V_{max} = \frac{S_T}{2*(S_D-D)} * V_{fan} \quad (4.26)$$

where,  $V_{fan}$  is linear speed of fan in m/s. If equation 4.24 is satisfied, maximum velocity occurs in diagonal plane and equation 4.26 is valid. On the other hand, if equation 4.24 is not satisfied, then maximum velocity occurs in transverse plane and maximum velocity is found from equation 4.25.

In the next step, convective heat transfer coefficient should be found. This parameter is used to calculate how much temperature is absorbed in tube. The formulation of this parameter is given:

$$h = \frac{Nu*\lambda}{D} \quad (4.27)$$

where,  $h$  is convective heat transfer coefficient  $W/m^2.K$ ,  $Nu$  is Nusselt Number,  $\lambda$  is thermal conductivity in  $W/K.m$ ,  $D$  is diameter of tube bank (battery pack) in m.

Since the motion of fluid in staggered tube is not aligned, the formulation of Newton's law of cooling is not simple. Figure 4.6 shows the motion of fluid within the tube.

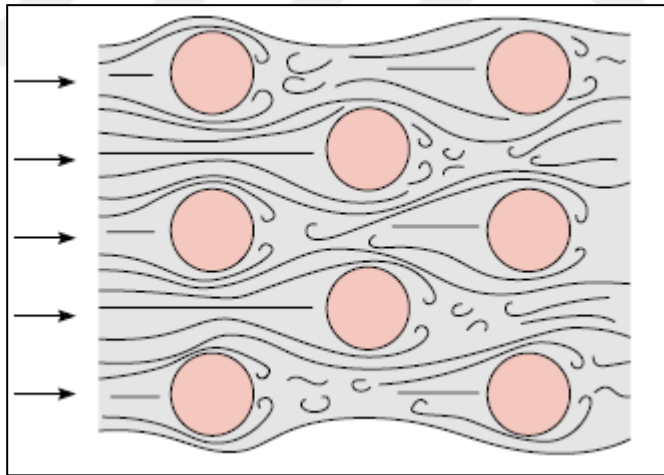


**Figure 4.6.** Flow Condition in Staggered Tube.

After finding heat transfer coefficient, the outlet temperature which leaves from tube should be evaluated. The mathematical formulation of outlet temperature is given by (Bergman et al., 2011):

$$T_o = T_s - (T_s - T_i) * \exp\left(\frac{-D\pi N h}{\rho V_{fan} N T S T C}\right) \quad (4.28)$$



where,  $N$  is the total number of tubes (total number of cells in battery pack),  $N_T$  is number of tubes (cells) in transverse pitch,  $S_T$  is length of transverse pitch in m,  $D$  is diameter of tube bank in m,  $h$  is convective heat transfer coefficient in  $W/m^2.K$ ,  $\rho$  is fluid density in  $kg/m^3$ ,  $V_{fan}$  is linear velocity of fan in m/s,  $C$  is specific heat in Joule/Kelvin,  $T_s$  is surface temperature in Kelvin,  $T_i$  is the temperatures enters into bank in Kelvin. The evaluated outlet temperature is used to calculate temperature difference ( $\Delta T$ ) from Newton's law of thermodynamic.  $\Delta T$  is calculated from log-mean temperature difference which is given by (Bergman et al., 2011):

$$\Delta T = \frac{(T_s - T_i) - (T_s - T_o)}{\ln\left(\frac{T_s - T_i}{T_s - T_o}\right)} \quad (4.29)$$

Finding temperature difference is cornerstone of determining the heat transfer rate in tube. The last formulation of obtaining heat transfer rate is given by:

$$\dot{Q}_h = N\pi h D \Delta T L \quad (4.30)$$

where,  $L$  is length of tube bank in m (in this case length of cell). This parameter shows the rate of heat transfer caused by cooling system.

#### 4.1.5.10. Temperature Change

One of the most significant part in temperature modelling is to get mathematical model of temperature change. In order to observe the effects of cooling system on battery temperature, the heat generated by battery should be found. The total amount of heat generated by battery is actually caused by internal resistance of battery. For this reason, the mathematical model of generated heat in entire battery pack is given by:

$$\dot{Q}_{gen} = N I_{bat}^2 R_{bat} \quad (4.31)$$

where,  $N$  is total cell in battery pack,  $I$  is the current flowing through cells,  $R$  is internal resistance of battery cell.

Finally, change of battery temperature can be computed from (Masoudi and Azad, 2017):

$$\dot{T} = \frac{\dot{Q}_{gen} - \dot{Q}_h}{m_{batt} c_{batt}} \quad (4.32)$$

where,  $m_{batt}$  is weight of battery in kg and  $C_{batt}$  is thermal capacity of battery module in Joule/Kelvin.

## 4.2. Simulink Model of Hybrid Vehicle

In order to increase the reliability of model, all mathematical expressions embedded into Simulink blocks. It also allows us to observe simulations of each components. The mathematical models of each component are derived in section 4.1.

In this thesis, Toyota Prius 2018 Base Model is used as a hybrid vehicle. Thus, all parameters in equations are taken with respect to this car. In this chapter, it is examined that how mathematical model of each components are converted into Simulink blocks.

### 4.2.1. Simulink Model of Vehicle Dynamic

The coefficients of vehicle model is taken by considering specifications of Toyota Prius. Table 4.2 shows the real values of these coefficients.

**Table 4.2.** Vehicle Coefficients (Toyota Prius 2018 Base Model Specifications, 2018)

Vehicle Parameters	Value	Unit
$C_d$	0.24	-
A	2.58	$m^2$
$C_{roll}$	0.015	-
m	1390	kg
g	9.81	$m/s^2$
$\rho$	1.204	$kg/m^3$
T	295.15	K
$\dot{\eta}$	0.54	-

All these coefficients are used, from equation 4.2 to equation 4.8, to find total power loss of vehicle. Equation 4.1 is used to calculate total demanded power to find vehicle speed from equation 4.6. The Simulink model of vehicle dynamic is shown in Figure 4.7.

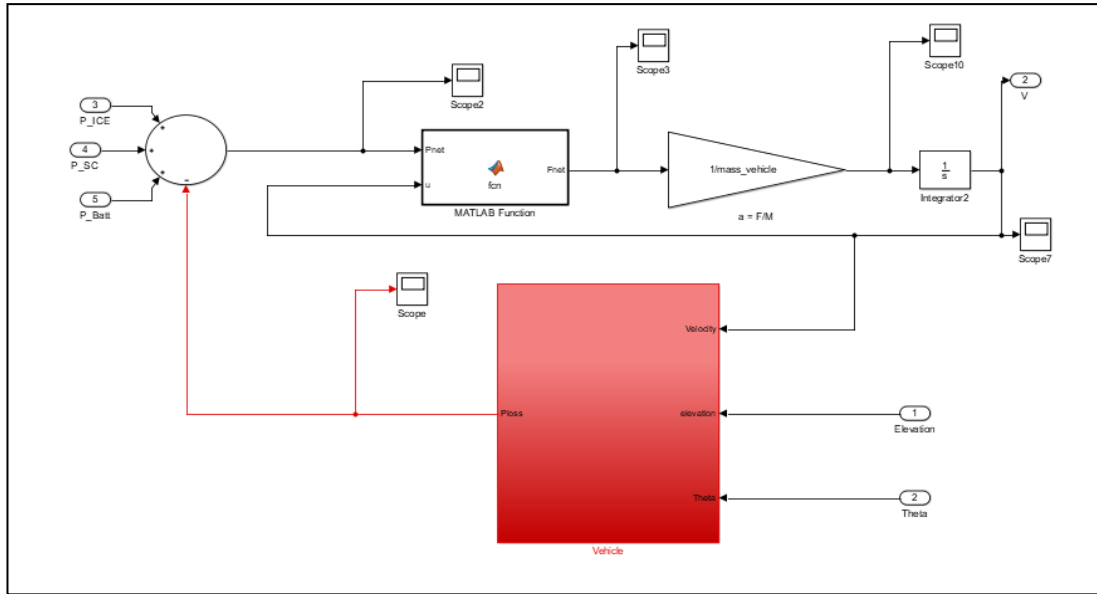


**Figure 4.7.** Simulink Model of Vehicle Dynamic

In this figure, it can be seen that the total demanded power is calculated by subtracting total losses from sum of three different power sources determined by MPC, including internal combustion engine, supercapacitor and battery. The power, which is found, is called net power. Once  $P_{net}$  is found, the velocity can be obtained by taking the integral of acceleration, which is given in equation 4.6. Finding velocity is an important criteria since it should be tracked by controller. In each time step, velocity is calculated again that is connected with feed-back loop. The values of elevation and theta can be thought as a data coming from GPS. In this thesis, these values are coming from workspace of MATLAB<sup>®</sup>.

#### 4.2.2. Simulink Model of Internal Combustion Engine (ICE)

Mathematical model of ICE, can be easily implemented in Simulink block. Table 4.3 shows the coefficients of ICE used in mathematical model.

**Table 4.3.** ICE Coefficients

ICE Parameters	Value	Unit
$\eta_{electric}$	0.6	-
$\eta_{mechanical}$	0.9	-
$C_f$	$47.3 \times 10^6$	J/kg
$P_{max}^{ICE}$	71	kW

Calorific value ( $C_f$ ), is taken by considering the source of fuel is gasoline. Efficiency parameters are logical arbitrary numbers. Also, maximum power of ICE is 71kW. Next step is to send these coefficients into Simulink blocks. Figure 4.8 shows Simulink model of ICE:

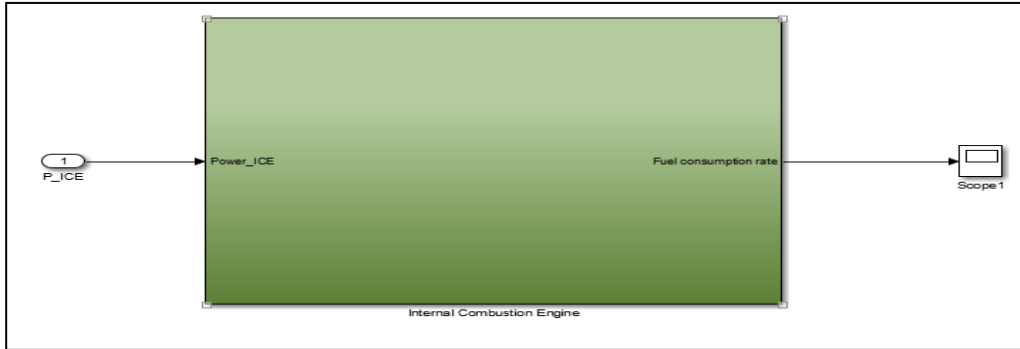


**Figure 4.8.** Simulink Model of ICE

The only input of this block is power of ICE determined by MPC. In addition, this block has only one output, which is fuel consumption that is tried to be minimized by MPC.

#### 4.2.3. Simulink Model of Battery

In battery model, there are two important parameters, including SOC and C-rate. Related coefficients are given in Table 4.4.

**Table 4.4.** Battery Coefficients (Toyota Prius Technical Specifications Including Battery Details, 2012)

Battery Parameters	Value	Unit
$\eta_{dis}$	0.85	-
$\eta_{char}$	0.85	-
$Q_k^{max}$	1.3	kWh
$p_{max}^{Batt}$	53	kW
$V_{oc}$	202	V
$C_{battery}$	6.5	Ah

Maximum power of Nickel-metal hydride battery in Toyota Prius is 53 kW and maximum energy is 1.3 kWh. In this battery module, there are 168 cells and each are

1.2 V. Total open circuit voltage is equal to multiplication of these two values which is approximately 202 V. In addition, the battery capacity is equal to 6.5 Ah. Charging and discharging efficiencies are again logical arbitrary numbers. All these data are sent into the Simulink block. Figure 4.9 shows the Simulink model of battery:

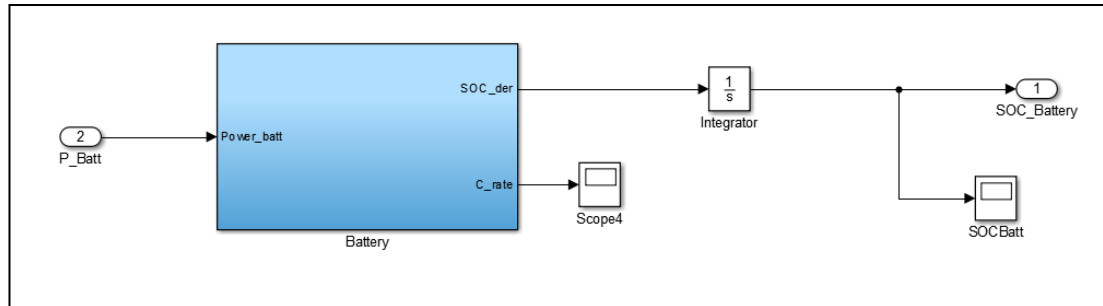


**Figure 4.9.** The Simulink Model of Battery

Input of the block is battery power determined by MPC. There are two outputs of this block, including SOC and C-rate. Since the output of SOC port is rate of change, integral of this value is taken to see current value of SOC. In addition, this value is controlled by MPC.

#### 4.2.4. Simulink Model of Supercapacitor

Usage of supercapacitor in ESS with battery is a new technology. Toyota Prius has not used this technology yet. For this reason, supercapacitor selection can be made arbitrary. Figure 4.10 illustrates some of the supercapacitor specifications (Burke and Zhao, 2015).

Device	V rate	C (F)	R (mOhm) (3)	RC sec	Wh/kg (1)	W/kg (95%) (2)	W/kg Match. Imped.	Wgt. (kg)	Vol. lit.
Maxwell	2.7	2885	.375	1.1	4.2	994	8836	.55	.414
Maxwell	2.7	605	.90	.55	2.35	1139	9597	.20	.211
Vinatech	2.7	336	3.5	1.2	4.5	1085	9656	.054	.057
Vinatech	3.0	342	6.6	2.25	5.6	710	6321	.054	.057
Ioxus	2.7	3000	.45	1.4	4.0	828	7364	.55	.49
Ioxus	2.7	2000	.54	1.1	4.0	923	8210	.37	.346
Skeleton Technol.	3.4	3200	.47	1.5	9.0	1730	15400	.40	.284
Skeleton Technol.	3.4	850	.8	.68	6.9	2796	24879	.145	.097
Yunasko*	2.7	510	.9	.46	5.0	2919	25962	.078	.055
Yunasko*	2.75	480	.25	.12	4.45	10241	91115	.060	.044
Yunasko*	2.75	1275	.11	.13	4.55	8791	78125	.22	.15
Yunasko*	2.7	7200	1.4	10	26	1230	10947	.119	.065
Yunasko*	2.7	5200	1.5	7.8	30	3395	30200	.068	.038
Ness	2.7	1800	.55	1.0	3.6	975	8674	.38	.277
Ness	2.7	3640	.30	1.1	4.2	928	8010	.65	.514
Ness (cyl.)	2.7	3160	.4	1.3	4.4	982	8728	.522	.379
LS Cable	2.8	3200	.25	.80	3.7	1400	12400	.63	.47

**Figure 4.10.** Summary of Supercapacitor Device Characteristics

From this figure, Maxwell supercapacitor is determined to use, because of high power density capacity. To find the maximum power which can be delivered by supercapacitor and energy density, more information is needed. Table 4.5 shows weight and energy density of different types of supercapacitors (Burke and Zhao, 2015).

**Table 4.5.** Specifications of Different Types of Supercapacitors

Energy Storage System	Weight of the supercapacitor [kg]	Energy capacity
Yunasko hybrid	12	300Wh
JM Energy hybrid	11	100 Wh
Yunasko C/C	22	100 Wh
Maxwell C/C	28	100 Wh
Skeleton 2014 C/C 3200 F	13	115 Wh

As it can be seen from Figure 4.10, Maxwell Supercapacitor has 994 W/kg power density. Since the weight of supercapacitor is 28 kg from Table 4.4, maximum power density can be found as 27 kW. Also, this supercapacitor has 100 Wh energy density. Efficiency of supercapacitor is chosen same as battery values. Figure 4.11, shows the Simulink model of supercapacitor:

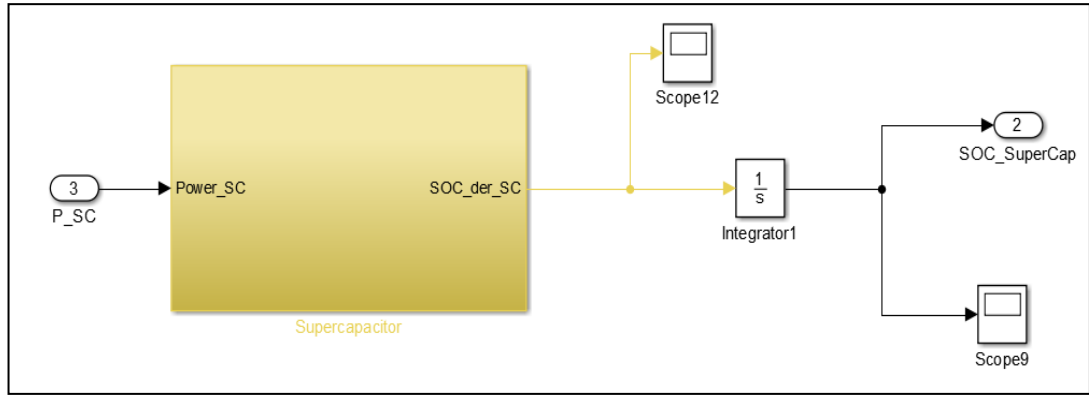


**Figure 4.11.** Simulink Model of Supercapacitor

Supercapacitor model has only one input which is power determined by MPC. Output of this Simulink block is SOC. This value is again controlled by MPC same as battery.

#### 4.2.5. Simulink Model of Battery Temperature

In this part, temperature of battery is calculated by adjusting the speed of fan. To calculate temperature from expressions given in section 4.1.5, required coefficients should be given. In Table 4.5, all required coefficients are given:

**Table 4.6** Coefficients of Battery Thermal Model

Battery Temperature Parameters	Value	Unit
D	0.06	m
L	0.285	m
N	168	-
$N_T$	6	-
$S_T$	0.09	m
$S_L$	0.09	m
$m_{batt}$	29.12	kg
$C_{batt}$	521	J/kg/°C
$R_{bat}$	0.015	ohm

Battery longitudinal and transverse pitch ( $S_L$  and  $S_T$ ) values are taken as  $3 \times R$  since battery has symmetrically placed cells (Jilte and Kumar, 2018; Pesaran and Keyser,

2001). The remaining values are taken from real battery of Toyota Prius (Toyota Prius Technical Specifications Including Battery Details, 2012). In Figure 4.12, Simulink model of battery temperature is illustrated.

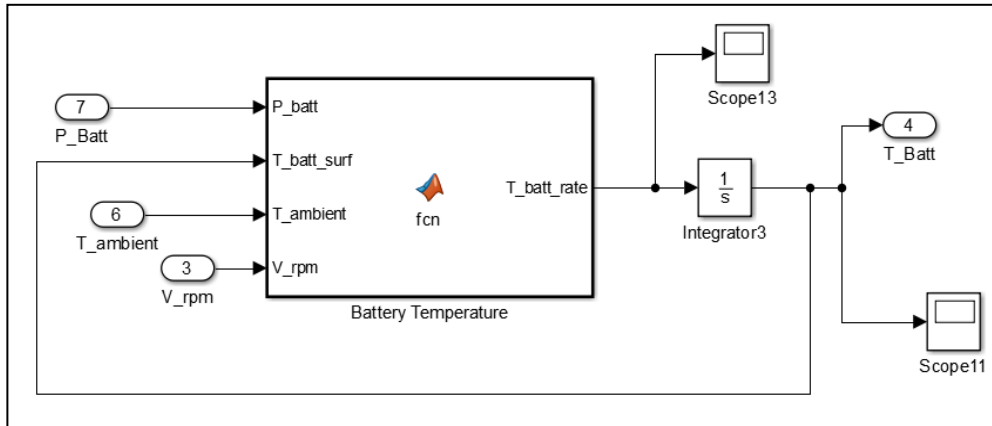


**Figure 4.12.** Simulink Model of Battery Temperature

There are four inputs and one output of this model. Fan speed and battery power are determined by MPC. Initial values of air ambient temperature and battery surface temperature are set to be 22°C and 30°C respectively. In each time step, model will calculate battery temperature thanks to MPC and send these data as an input of battery model with feedback loop. Complete MATLAB<sup>®</sup> code for Battery Temperature block is given in Appendix 1.

### 4.3. Mathematical Model of MPC

The basic principle of MPC is to minimize objective function by using internal system model to anticipate system behavior while satisfying constraints. The high-level formulation of MPC can be expressed as follows:

$$U_t(x(t)) = \min \sum_{k=0}^{N-1} q(x_{t+k}, u_{t+k}) \quad (4.33)$$

Subject to  $x_t = x(t)$  measurement

$x_{t+k+1} = Ax_{t+k} + Bu_{t+k}$  system model

$x_{t+k} \in X$  state constraints

$u_{t+k} \in U$  input constraints

$U_t = \{u_0, u_1, \dots, u_{N-1}\}$  optimization variables



As it is mentioned in section 3.1, at each sample time, MPC estimates the current state  $x_t$ . After that, it finds the optimal sequence of inputs  $u$  in prediction horizon ( $N$ ), such that the objective function  $q$  is minimized. This sequence gives us the set of  $U_t = \{u_t, u_{t+1}, \dots, u_{t+N-1}\}$ . The controller only implement the first control action  $u_t$ . For explicit explanation, the mathematical expression embedded to the block diagram and shown in Figure 4.13.

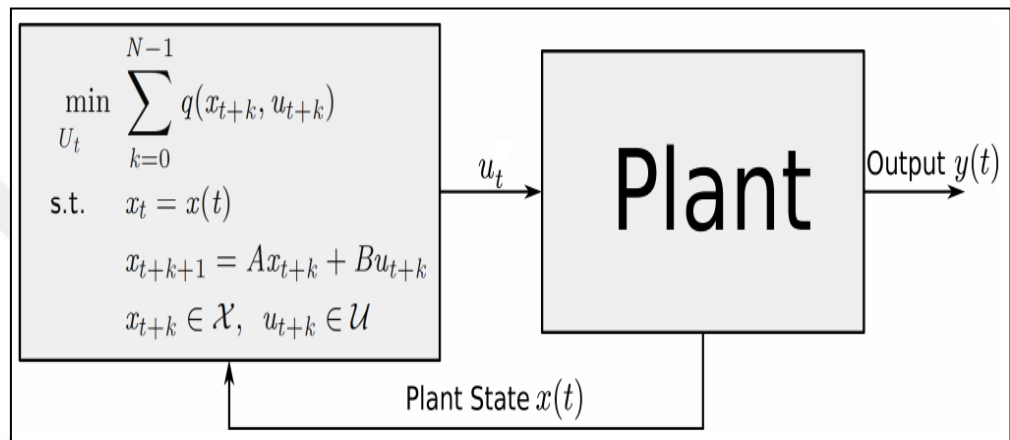


**Figure 4.13.** Structure of MPC with Mathematical Formulation

## CHAPTER 5

### MODELLING ENERGY AND THERMAL MANAGEMENT STRATEGIES AND SIMULATION RESULTS

There are two different control strategies which are developed in this thesis, including energy management and thermal management strategies by using MPC. In energy management strategy, MPC determines optimal power split between ICE, battery and supercapacitor and send these values to the plant. On the other hand, in battery thermal management strategy, MPC determines optimal fan speed to keep battery temperature in appropriate intervals. For explicit understanding, overall system's block diagram is shown in Figure 5.1.

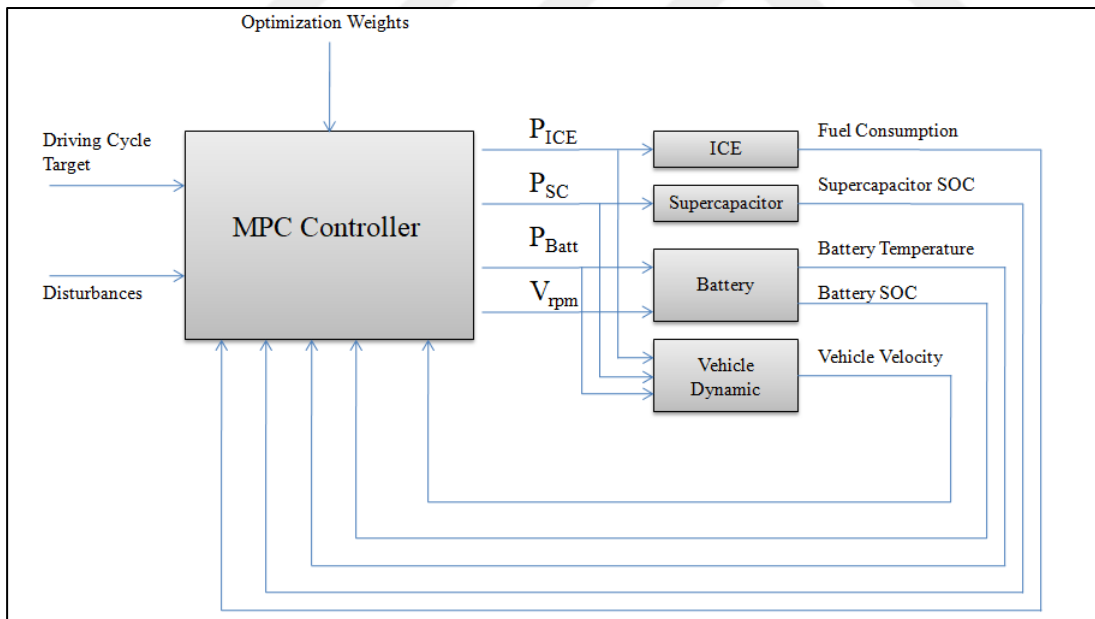


**Figure 5.1.** Block Diagram of Overall System

Internal structures and the values of coefficients inside these block diagrams are mentioned in chapter 4. In this chapter, different scenarios for EMS, TMS and combination of these two strategies are examined as follows:

**Table 5.1.** Features of Different Control Cases

Test Case	Available Component Configuration (for Optimal Power Split)			Battery Thermal Management by MPC?	Section
	ICE	Battery	Supercapacitor		
1	+	+	+		5.1.1
2	+	+			5.1.2
3		+	+		5.1.3
4	+				5.1.4
5		+		+	5.2
6	+	+	+	+	5.3

### 5.1. Energy Management Strategy

Developing useful controller is the key point of energy management strategy for hybrid car. As it is mentioned before, MPC controller is used to improve this strategy. In this part of this thesis, there are several estimated cases to get important results. For each case, making power split and designing MPC controller are the cornerstones. As a first case, hybrid car contains ICE, battery and supercapacitor to propel the vehicle. This shows us important results regarding the fuel consumption of vehicle and SOC levels of both supercapacitor and battery. In second case, the forces for propelling the car are ICE and battery. This case is actually considered the conventional hybrid car structure. By using this scenario, the effects of supercapacitor on fuel consumption rate of hybrid vehicle and battery C-rate can be examined by comparing with first case. As a third case, power sources are battery and supercapacitor, which means that the hybrid vehicle is thought as an electric vehicle. This allows us to observe advantages and disadvantages of electric vehicles

with good controller. Finally, the last case is to use conventional vehicle which has only ICE. This lets us observe the change of fuel consumption.

In each case, the test driving cycles are tracked by controller as a references. This is the proof for high reliability of MPC controller. The driving cycles are standardized speed profile that allow us to compare results of different controllers for different scenarios. Driving cycles are performed in zero slope roads (Fernandez, 2016) and for this thesis, it is also performed assuming that the car is running in zero elevation because the effects of elevation on required power is quite small. In each case, the driving cycle of the Highway Fuel Economy Test (HWFET) is tracked by controller. The duration and total distance of this driving cycle are 765 seconds and 16.45 km respectively (Different Types of Driving Cycles, 2013). In addition, in only first scenario, driving cycle of Urban Dynamometer Driving Schedule (UDDS), which represents city driving conditions, is tracked by controller. The characteristic parameters of time duration and total distance for UDDS are 1369 seconds and 12.07 km respectively. These two cycles are tried to prove the high ability of MPC controller while tracking different desired references.

### 5.1.1. Power Split for ICE, Battery and Supercapacitor

In this first case, MPC controller is developed for making power split between ICE, battery and supercapacitor. To find the optimal control strategy for a given HWFET and UDDS driving cycles, the following problem by using MPC is solved:

$$\min \sum_{k=0}^{N-1} ||W^y(y_{k+1} - r_{k+1})||^2 + ||W^u(u_{k+1} - u^{ref})||^2 + ||W^{\Delta u} * \Delta u_k||^2 \quad (5.1)$$

where

$$y = \begin{bmatrix} V \\ Temp \end{bmatrix}$$

$$u = \begin{bmatrix} P_{ICE} \\ P_{BATT} \\ P_{SC} \end{bmatrix}$$

Subject to,

$$SOC_{min} \leq SOC_{batt} \leq SOC_{max}$$

$$SOC_{min} \leq SOC_{SC} \leq SOC_{max}$$

$$V_{min} \leq V \leq V_{max}$$

$$\text{Temp}_{\min} \leq \text{Temp} \leq \text{Temp}_{\max}$$

and where  $u$  is manipulated variables,  $y$  is measured output,  $W^y$  is output weight,  $W^u$  is input weight,  $W^{\Delta u}$  is input rate weight,  $k$  is time step,  $N$  is number of time steps,  $\text{SOC}_{\text{batt}}$ ,  $\text{SOC}_{\text{SC}}$ ,  $V$ ,  $\text{Temp}$  are constraints which are battery state of charge, supercapacitor state of charge, velocity and battery temperature respectively.

The aim of MPC is to solve the optimization problem mentioned above. While solving this problem, MPC should take into account some parameters, which is shown in Figure 5.1, including manipulated variables, measured outputs, disturbances, reference and weights while satisfying constraints. This problem can be summarized that MPC controller tracks the desired driving cycle and battery temperature. In addition, it makes optimum power split between three sources and send these data to the plant while satisfying,  $\text{SOC}_{\text{batt}}$ ,  $\text{SOC}_{\text{SC}}$ ,  $V$ , and  $\text{Temp}$  intervals. The values of  $\text{SOC}_{\text{batt}}$ ,  $\text{SOC}_{\text{SC}}$ ,  $V$ , and  $\text{Temp}$  are sent to the controller with feed-back loop in each time step. Adjusting the values of these parameters is called tuning the controller. The most important part after designing overall system is to tune these variables by using MPC Toolbox in MATLAB®.

#### 5.1.1.1. Controller Synthesis for First Case

- Controller Tuning

First step of tuning the parameters of controller is to adjust default conditions of number of manipulated variables, number of measured disturbance, number of measured outputs, sample time  $T$ , prediction horizon  $N_p$  and control horizon  $N_c$ . In this case, number of manipulated variables is three, including ICE, battery and supercapacitor powers. Number of measured disturbances is three, including ambient temperature, elevation and slope of the vehicle. Ambient temperature is taken constant and it is set to be 22°C. Elevation and slope are taken as 0. These three variables are called measured disturbances, because these parameters directly affect measured outputs. Another default parameter is number of measured outputs which is four. Actually in Figure 5.1, it is illustrated that the number of measured output is five. However, since there is a direct and linear relationship between ICE and fuel consumption, controller makes error. To solve this problem, delay block should be added to the system, but this block causes deterioration in graphs. For this reason, fuel consumption is not taken as a measured output and the measured outputs are

battery state of charge, supercapacitor state of charge, velocity and battery temperature. Sample time, prediction horizon and control horizon are set to be 1, 40, 20 respectively and these values will be constant for all types of designs.

- Constraints

Second step is to adjust input and output constraints. In this case, manipulated variable (input) constraints are imposed as:

$$0 \text{ kW} \leq P_{ICE} \leq 71 \text{ kW}$$

$$-53 \text{ kW} \leq P_{batt} \leq 53 \text{ kW}$$

$$-27 \text{ kW} \leq P_{SC} \leq 27 \text{ kW}$$

The measured outputs are expressed as:

$$50\% \leq SOC_{batt} \leq 100\%$$

$$10\% \leq SOC_{SC} \leq 100\%$$

$$0 \text{ m/s} \leq V \leq 50 \text{ m/s}$$

$$10^\circ\text{C} \leq \text{Temp} \leq 40^\circ\text{C}$$

According to aim of controller, these constraints are adjusted as hard or soft constraints. For this case, all manipulated variables and measured outputs are adjusted as 0 (hard constraints). In MATLAB MPC Toolbox, these settings are valid in constraint part as minECR and maxECR and both are taken as zero in this case.

- Weights

Last step is to adjust both inputs and outputs of controller.  $P_{ICE}$ ,  $P_{batt}$  and  $P_{SC}$  weights are set to be 0.1, 0.1, 0 respectively. These values show that even if the controller does not satisfy desired constraints for supercapacitor, controller will not penalize because supercapacitor is free to be used. Rate weight values for all these parameters are 0.1.

Output weights, including  $SOC_{batt}$ ,  $SOC_{SC}$ ,  $V$ , and  $\text{Temp}$  are adjusted as 0,0,100 and 1 respectively. Since the controller must track velocity high significantly, the weight value is taken quite big.

### 5.1.1.2. Simulation Results for First Case

The most important criteria for all cases is to track driving cycle to get reliable results. Thus, two different types of driving cycle tracking are made with same controller. Figure 5.2 shows tracking performance of MPC for HWFET driving cycle.

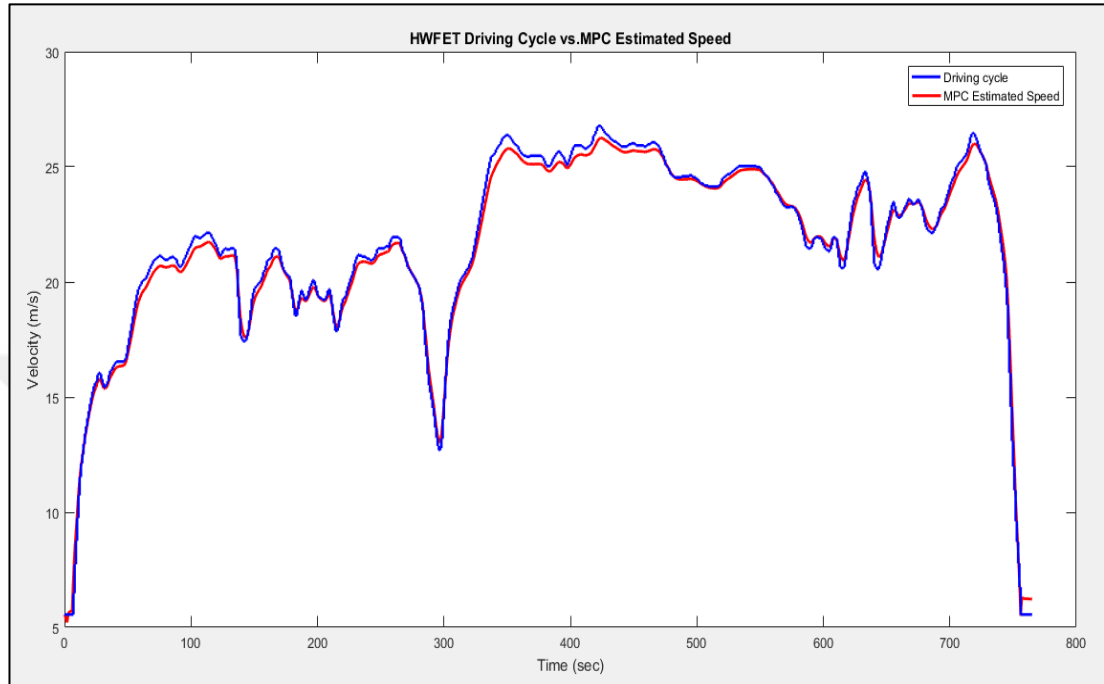


**Figure 5.2.** HWFET Driving Cycle Tracking

Figure 5.3 shows tracking performance of MPC for UDDS driving cycle.

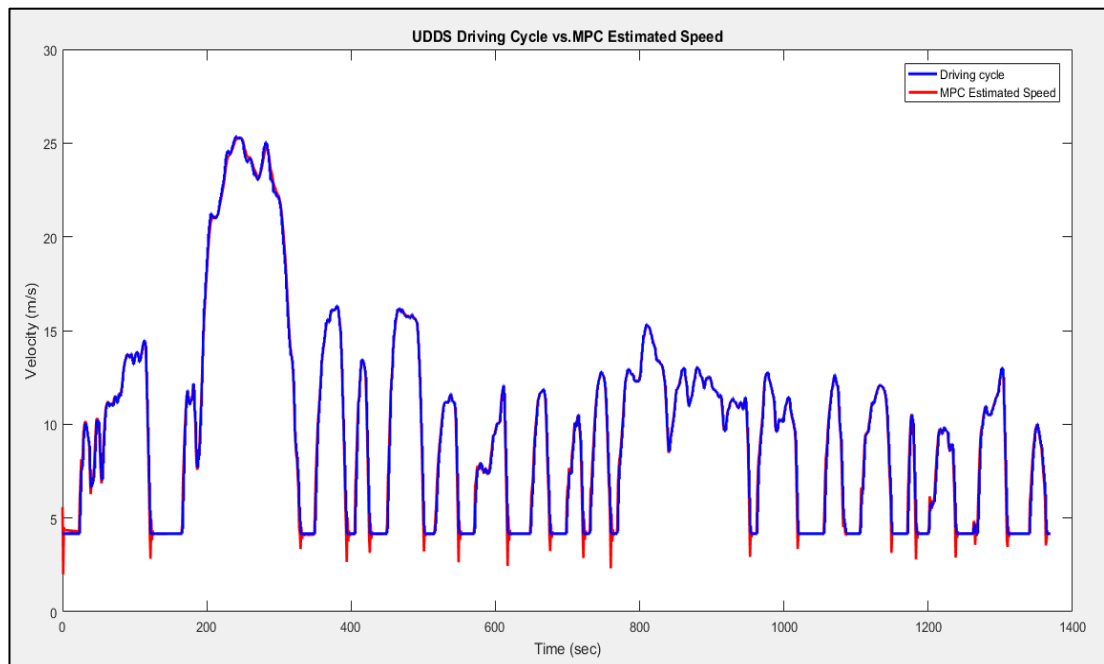


**Figure 5.3.** UDDS Driving Cycle Tracking

From Figure 5.2 and Figure 5.3, it can be concluded that, the controller can produce very good speed tracking performance. Tuning of the controller is adjusted with respect to tracking results. If this tracking is not good, the parameters of tuning should be changed. In this case, Mean Absolute Error (MAE) and Mean Absolute Percentage Error (MAPE) values of velocity tracking for HWFET are equal to 0.59 and 2.72% respectively.

Another reference is battery temperature which is less important. This reference also gives us some clue about controller performance, but good speed tracking performance is sufficient to obtain required data. Figure 5.4 shows the battery temperature reference tracking.

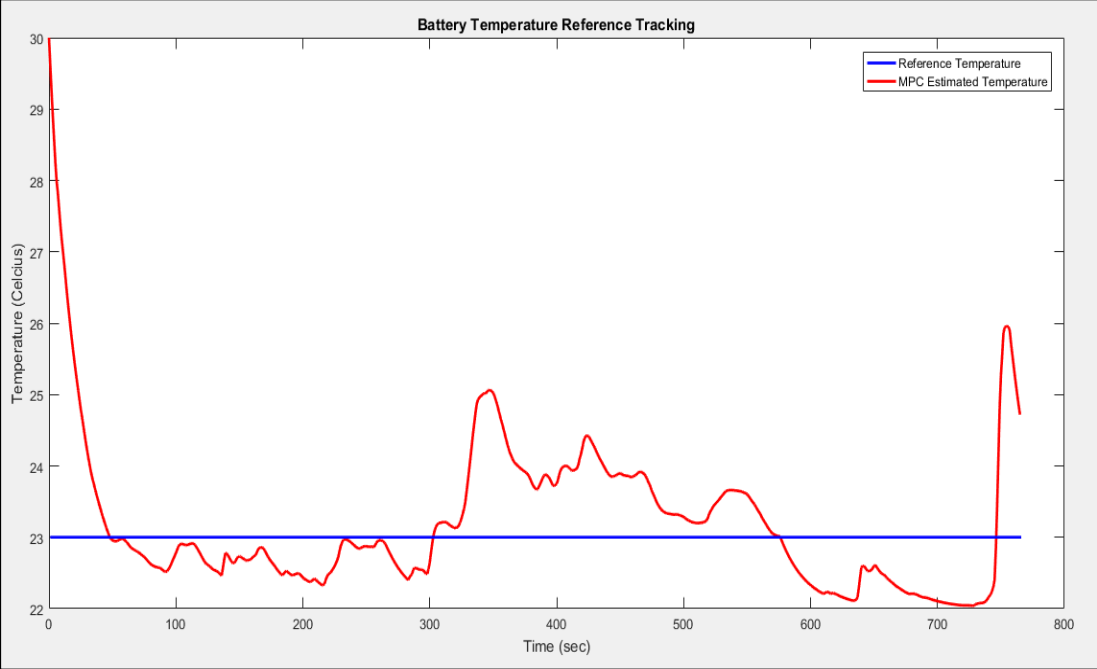


**Figure 5.4.** Battery Temperature Reference Tracking

After looking for reference tracking performances of MPC controller, power split analysis of controller should be made. In Figure 5.5, driving cycle and power split analysis are shown.



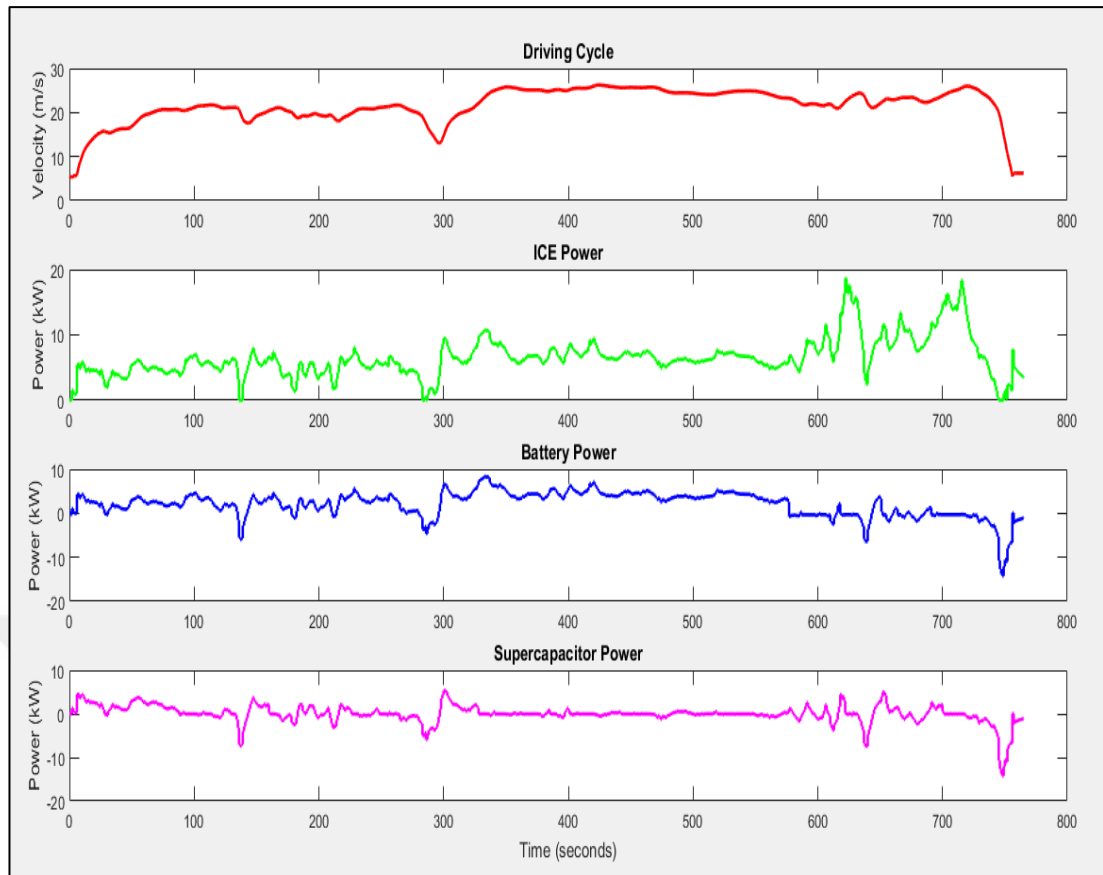


**Figure 5.5.** Power Split Analysis for Three Power Sources

As it is mentioned before, MPC controller determines manipulated variables of system. MPC controller also has plant model inside, for this reason, it can give logical values for three different power sources by making the prediction about road. Since the road slope and elevation are considered as zero, MPC makes prediction with respect to the velocity references. It can be interpreted that when the speed of the vehicle increases, demanded power also increases. On the other hand, when the speed decreases, controller can detect that power demand is small and battery and supercapacitor can be charged like in regenerative braking mode. Since the car is assumed to run on zero slope roads, controller can only understand negative slope when the speed decreases. For this reason, controller makes the decision of charging battery by predicting decrease of speed.

When the point of 300 seconds is investigated, it can be seen that the velocity of car will increase. Since, designed MPC controller can see the reference signal 40 seconds (prediction horizon) in advance, it started charging battery and supercapacitor, to decrease usage of ICE. By doing this, MPC can optimize fuel

consumption. Figure 5.6 shows the fuel consumption rate of hybrid vehicle in HWFET with designed MPC controller.

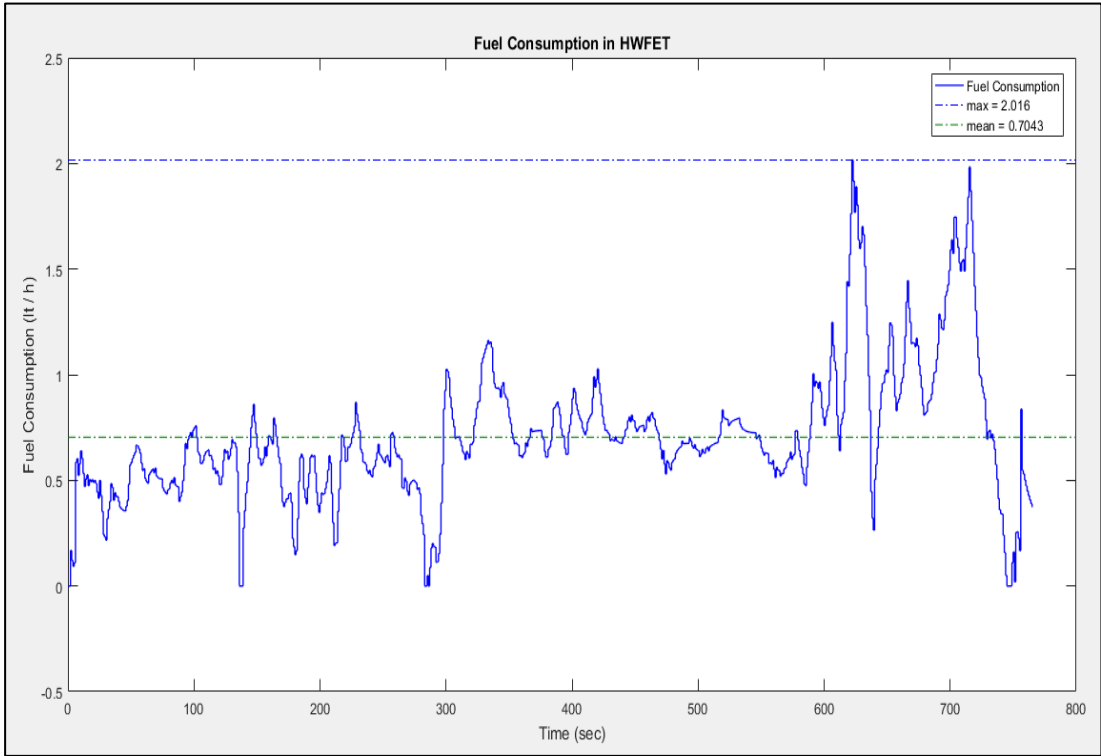


**Figure 5.6.** Fuel Consumption of Hybrid Vehicle in HWFET

By using good controller, the fuel consumption rate can be lowered down to 0.7. Another important parameters are state of charge levels for both battery and supercapacitor. These two parameters are specified as constraints and they both assumed to start from fully charged level. Controller keeps these two values in a specific interval which is given in section 5.1.1.1. This is also important to interpret about the performance of controller. Figure 5.7 illustrates the SOC level of battery power source.

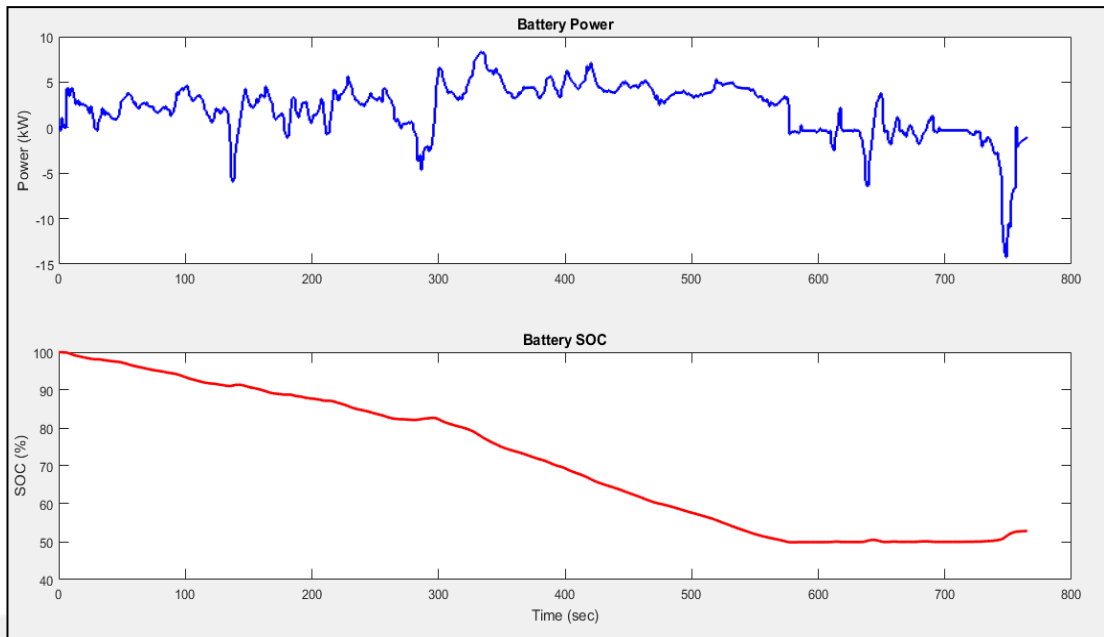


**Figure 5.7.** Battery Power and State of Charge Level

It can be indicated that, controller is able to keep SOC level of battery in specified interval. Final criteria of this scenario is to examine SOC level of supercapacitor. This is another constraint of controller. Figure 5.8 shows the ability of controller in terms of whether SOC level of supercapacitor is satisfied or not.

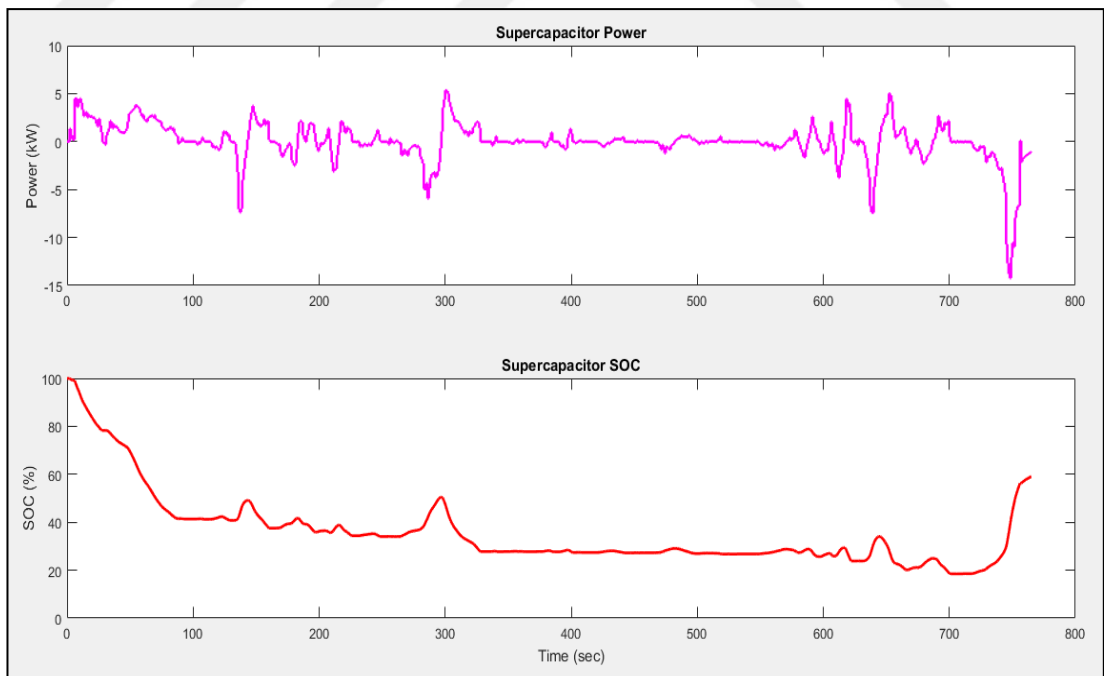


**Figure 5.8.** Supercapacitor Power and State of Charge Level

From all illustrated figures, it can be concluded that, designed controller is able to track desired references while satisfying desired constraints.

### 5.1.2. Power Split for ICE and Battery

In this second case, MPC controller is developed for making power split between ICE and battery. To find the optimal control strategy for a given HWFET driving cycle, MPC has tried to solve the same problem which is given in equation 5.1.

#### 5.1.2.1. Controller Synthesis for Second Case

- Controller Tuning

In this case, all the default conditions remain constant, because it is hard to change the controller from beginning. The main criteria in this part is to adjust supercapacitor power value as zero.

- Constraints

Second step is to adjust input and output constraints. In this case, manipulated variable (input) constraints are imposed as:

$$0 \text{ kW} \leq P_{ICE} \leq 71 \text{ kW}$$

$$-53 \text{ kW} \leq P_{batt} \leq 53 \text{ kW}$$

$$0 \text{ kW} \leq P_{SC} \leq 0 \text{ kW}$$

The measured outputs are expressed as:

$$50\% \leq SOC_{batt} \leq 100\%$$

$$10\% \leq SOC_{SC} \leq 100\%$$

$$0 \text{ m/s} \leq V \leq 50 \text{ m/s}$$

$$10^\circ\text{C} \leq \text{Temp} \leq 40^\circ\text{C}$$

The measured output constraints are again kept constant. However, in this case, SOC level of supercapacitor is considered as a soft constraint, because there is no supercapacitor. It means that the value of minECR and maxECR are taken as 1 for supercapacitor.

- Weights

The values of weights for manipulated variables are taken same as first case. Thus,  $P_{ICE}$ ,  $P_{batt}$  and  $P_{SC}$  weights are set to be 0.1, 0.1, 0 respectively. In addition, rate weight values for  $P_{ICE}$  and  $P_{batt}$  are again set to be 0.1 and  $P_{SC}$  rate weight value

adjusted as 0. Output weights, including  $SOC_{batt}$ ,  $SOC_{SC}$ ,  $V$ , and  $Temp$  are adjusted as 0,0,100 and 1 respectively. In this case, the controller must track velocity high significantly like before, so the weight value of velocity is taken quite big.

### 5.1.2.2. Simulation Results for Second Case

In this case, the main point is to look for benefits of using supercapacitor as an assistant ESS. First of all, power split performance of MPC is investigated.

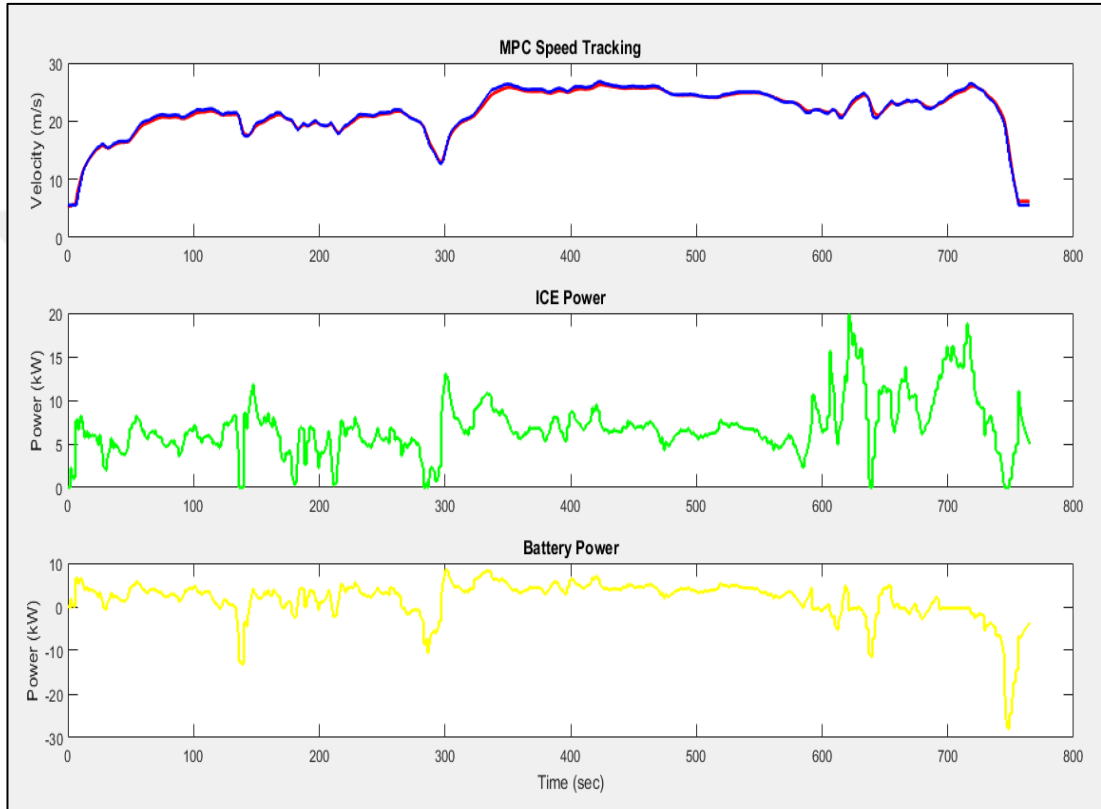


**Figure 5.9.** Power Split Analysis for ICE and Battery

Figure 5.9 shows that MPC controller has again high ability of tracking velocity reference. The values of MAPE and MAE are 2.12% and 0.46 respectively. Battery temperature tracking performance is not examined repeatedly since velocity tracking is sufficient to make a comment about controller performance. As a short comment related with power split, the interval of 100-200 seconds could be investigated. Approximately, at the point of 150 seconds, the speed of vehicle increases. For this reason, controller has decided to charge battery in order to provide demanded power from it. In Figure 5.10, the effects of supercapacitor on fuel consumption could be indicated.

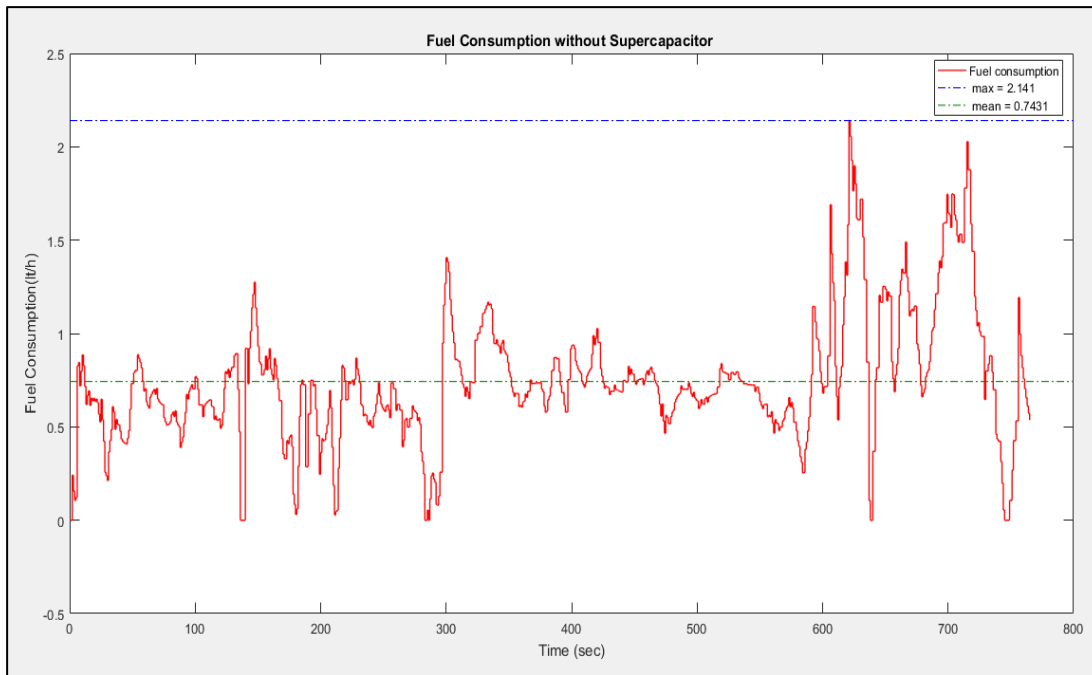


**Figure 5.10.** Fuel Consumption Rate of Hybrid Vehicle without Supercapacitor

Figure 5.10 shows that the average value of fuel consumption is 0.7431 which has increased when it is compared with first case. This result is quite important, because the aim of hybrid car is to decrease the fuel consumption rate. It proves that another method for decreasing fuel consumption rate is to use supercapacitor. Supercapacitor does not only affect fuel consumption rate.

Figure 5.11 shows another benefit of supercapacitor.

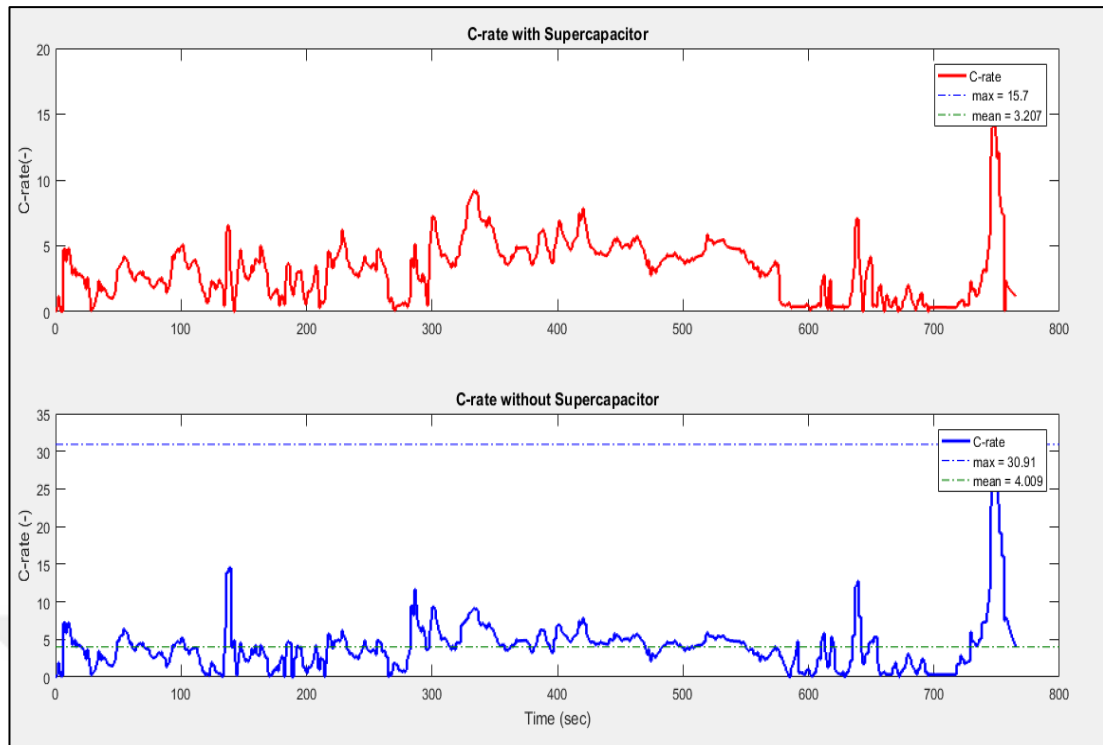


**Figure 5.11.** Battery C-rate Comparison for Two Scenarios: i) with Supercapacitor and ii) without Supercapacitor

The definition of C-rate has made and the adversely effects of this parameter on battery life has mentioned before. Figure 5.11 shows the values of C-rate for both cases. The average value of this parameter is 3.207 in Case 2, whereas it is 4.009 in Case 1. It is proved that, the life of battery could be increased by using combined supercapacitor and battery.

As it is discussed in previous case, SOC level of battery is also important parameter which could be considered. Controller has tried to keep SOC level in same interval with Case 1. Figure 5.12 shows the constraint performance of controller.

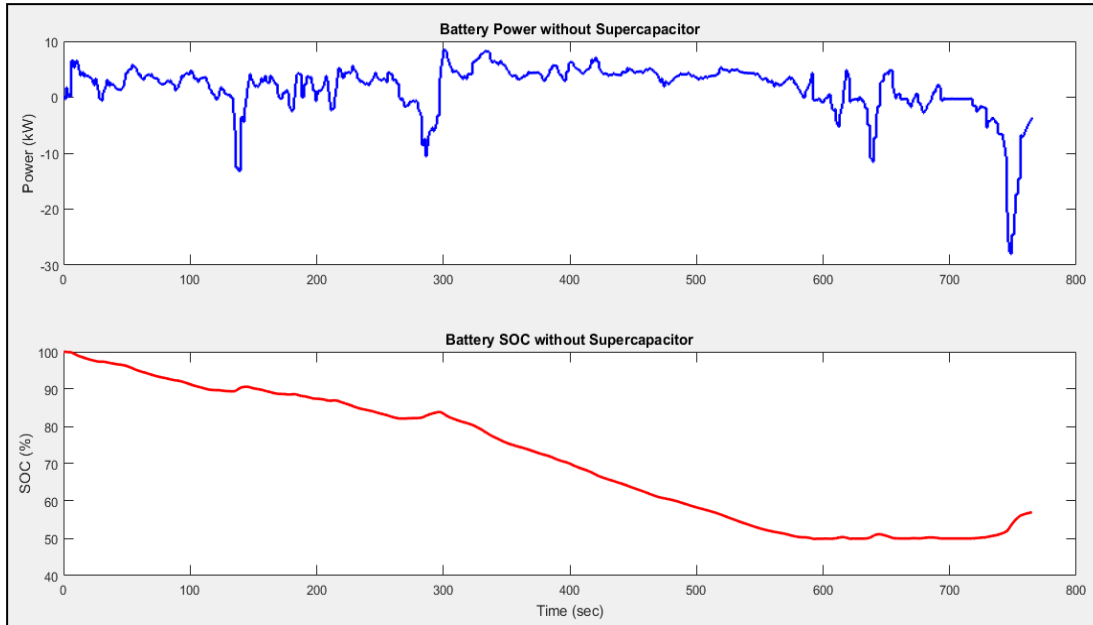


**Figure 5.12.** Battery Power and SOC Level without Supercapacitor

In this scenario, designed MPC controller has again high ability to satisfy constraints. By using this case, the merits of using supercapacitor with battery have been indicated.

### 5.1.3. Power Split for Battery and SC

In this third case, MPC controller is designed to make power split between battery and SC. It means that, hybrid car has been transformed to the electric car by eliminating ICE. To find the optimal control strategy for a given HWFET driving cycle, MPC has tried to solve the same problem which is given in equation 5.1.

#### 5.1.3.1. Controller Synthesis for Third Case

- Controller Tuning

In this third case, all the default conditions remain constant. The main criteria in this part is to adjust ICE power value as zero.

- Constraints

In this case, manipulated variable (input) constraints are imposed as:

$$0 \text{ kW} \leq P_{ICE} \leq 0 \text{ kW}$$

$$-53 \text{ kW} \leq P_{batt} \leq 53 \text{ kW}$$

$$-27 \text{ kW} \leq P_{SC} \leq 27 \text{ kW}$$



The measured outputs are expressed as:

$$50\% \leq \text{SOC}_{\text{batt}} \leq 100\%$$

$$10\% \leq \text{SOC}_{\text{SC}} \leq 100\%$$

$$0 \text{ m/s} \leq V \leq 50 \text{ m/s}$$

$$10^\circ\text{C} \leq \text{Temp} \leq 40^\circ\text{C}$$

The measured output constraints are again kept constant. All constraints except temperature are set to be hard constraints which means that ECR values of measured output are 0. ECR values of Temp is set to be 0.1, because temperature is controlled by only battery power and this criteria is not that much important in this step. While designing EMS, this term will become more significant.

- Weights

The values of weights and rate weights for  $P_{\text{ICE}}$ ,  $P_{\text{Batt}}$  and  $P_{\text{SCare}}$  taken as 0, 0.1, 0.1 respectively. The weights for measured outputs are taken exactly same with first and second cases.

### 5.1.3.2. Simulation Results for Third Case

In this part of thesis, simulation results of MPC performance without ICE has been discussed. In Figure 5.13, performance of MPC is investigated.

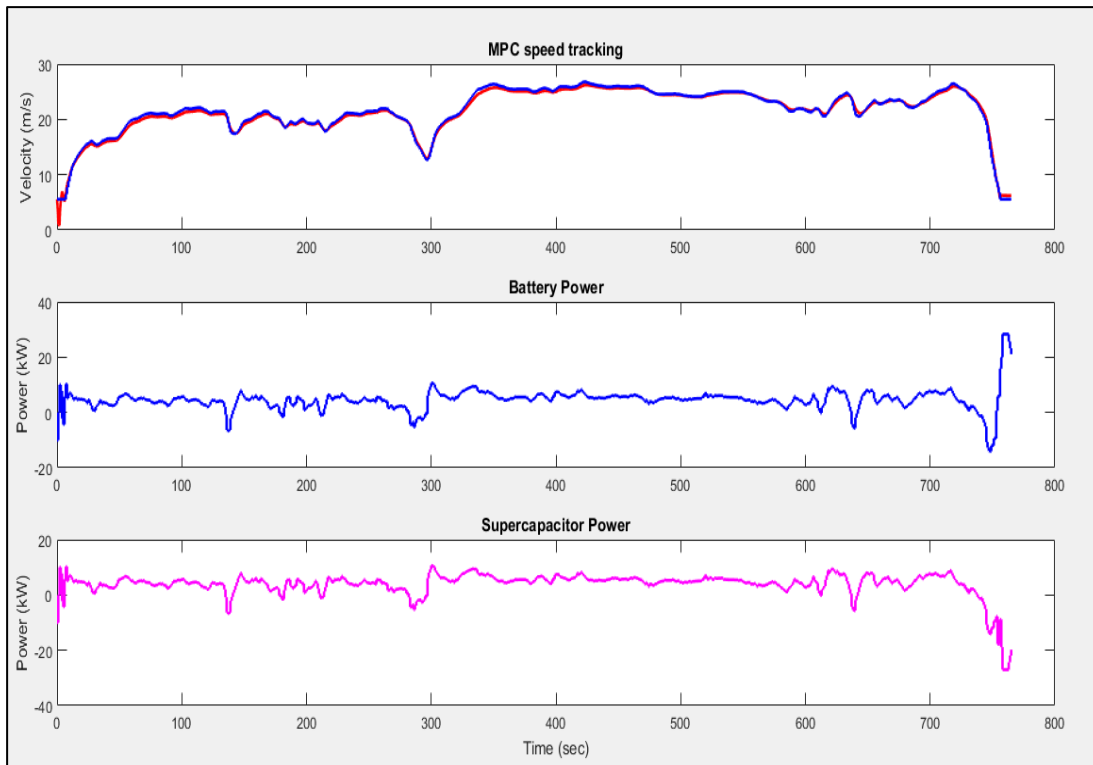


**Figure 5.13.** Power Split Analysis for Battery and SC

MPC is again quite good at tracking speed. The values of MAPE and MAE are found as 1.84% and 0.4 respectively. It can also make good prediction about behavior of speed and it charges battery and supercapacitor in logical points like 300 seconds. It is explicit that, for providing total power which the vehicle requires to run at desired velocity, vehicle only use battery and supercapacitor in this case. Thus, it is expected that battery will discharge more than other cases. This concluded as, in this case, battery C-rate value is bigger than other cases.

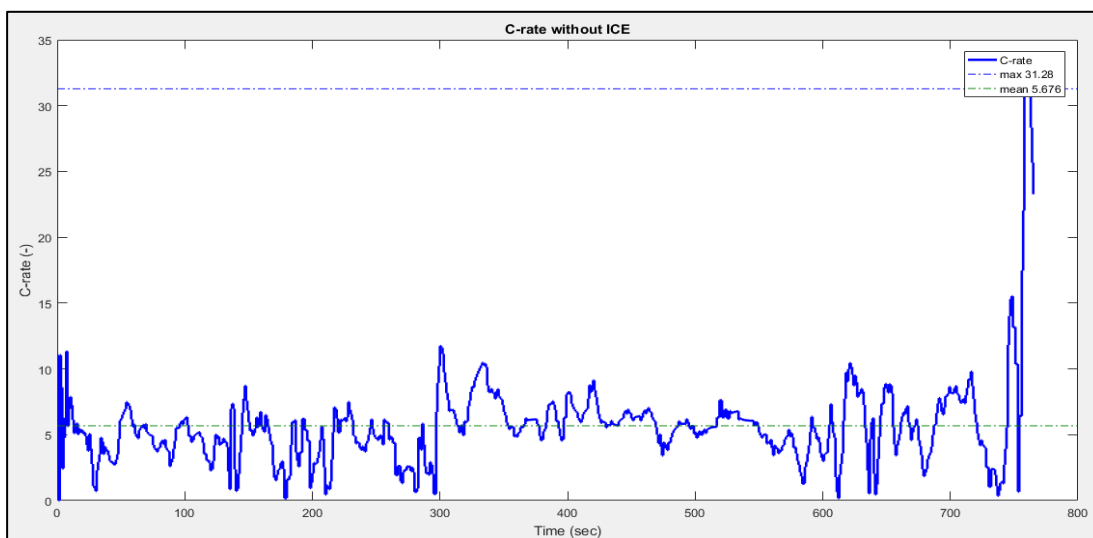


**Figure 5.14.** C-rate Graph without ICE

From Figure 5.14, C-rate of battery's value has increased. The average value of C-rate has increased up to 5.676. If the same case is carried out also without SC, C-rate value will increase more than this value. The last control is again looking for interval of constraints.

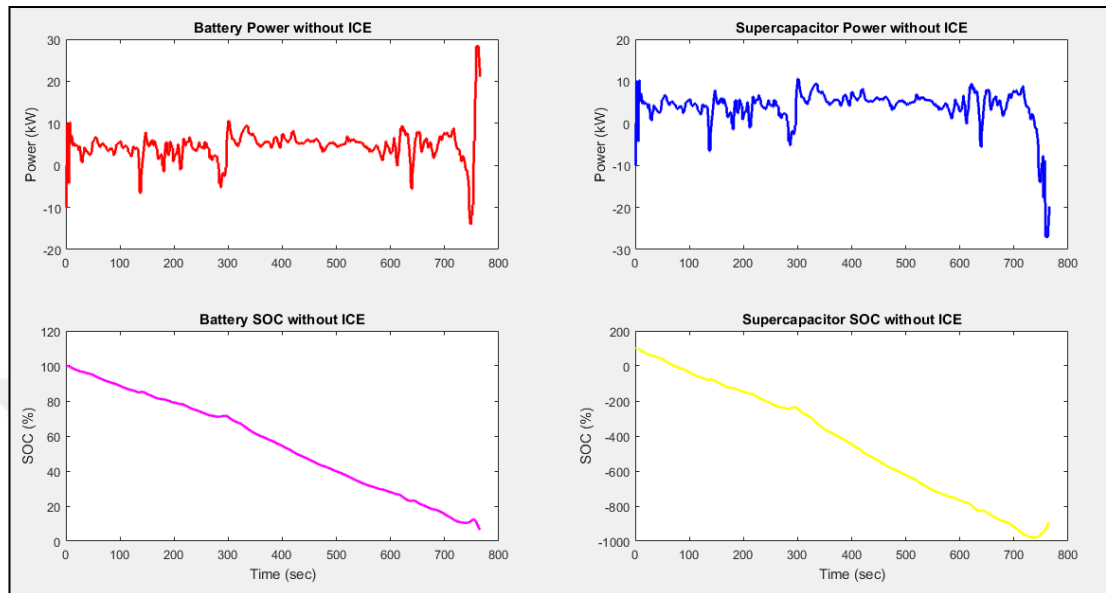


**Figure 5.15.** Power and SOC Values for Both Battery and SC

Although MPC controller has made good velocity tracking, in this case it does not satisfy constraints. The reason of this situation is that, vehicle requires big amount of power. Power could be delivered only by battery and SC. For this reason, power sources couldn't find a time for charging. When the point of approximately 300 seconds is investigated, battery and SC are charged for a very short time. However, vehicle needed to speed up, and the duration of charging has finished. To overcome with this problem, the high capacity battery should be used in this case.

#### 5.1.4. Power Split for only ICE

In this fourth case, MPC controller is developed for making power split for only ICE. Aim of this case is to observe the effects of MPC controller on fuel consumption rate of conventional vehicle. MPC again has tried to solve the same problem which is given in equation 5.1.

##### 5.1.4.1. Controller Synthesis for Fourth Case

- Controller Tuning

The main criteria in this part is to adjust battery and SC power values as zero. Other default values remain constant.

- Constraints

In this case, manipulated variable constraints are imposed as:

$$0 \text{ kW} \leq P_{ICE} \leq 71 \text{ kW}$$

$$0 \text{ kW} \leq P_{batt} \leq 0 \text{ kW}$$

$$0 \text{ kW} \leq P_{SC} \leq 0 \text{ kW}$$

The measured outputs are expressed as:

$$50\% \leq SOC_{batt} \leq 100\%$$

$$10\% \leq SOC_{SC} \leq 100\%$$

$$0 \text{ m/s} \leq V \leq 50 \text{ m/s}$$

$$10^\circ\text{C} \leq \text{Temp} \leq 40^\circ\text{C}$$

In this case, one of the most important criteria is to follow speed reference. Therefore, maximum and minimum ECR values are set to be 1 for SOC values and temperature. ECR values of velocity are set to be 0.

- Weights

The values of weights and rate weights for  $P_{ICE}$ ,  $P_{Batt}$  and  $P_{SC}$  are taken as 0.1, 0 and 0 respectively. The weights for measured outputs of SOC values and Temp value are set to be 0 whereas velocity becomes 1000.

#### **5.1.4.2. Simulation Results for Fourth Case**

In this part of thesis, simulation results of MPC performance without battery and SC has been discussed. Figure 5.16 shows performance of MPC in this case.

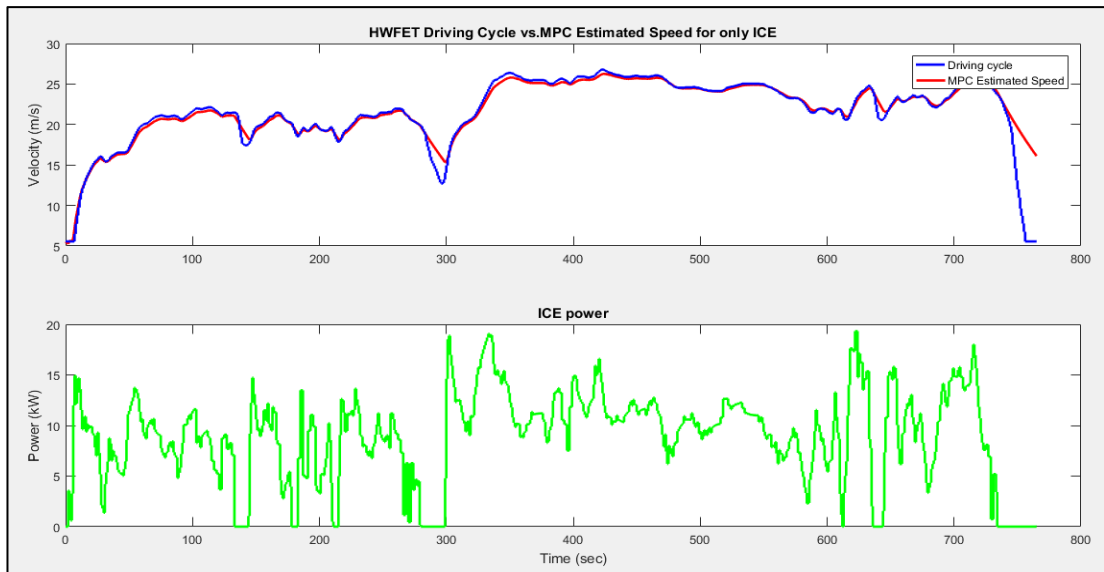


**Figure 5.16.** Power Split Analysis for Only ICE

The speed tracking performance of MPC is again good. The values of MAPE and MAE are 0.184% and 0.04 respectively. Since the system still detects battery and supercapacitor as a manipulated variable, in some parts of tracking, controller follows desired velocity with a small delay. To overcome with this problem, controller should be changed from beginning and default conditions should be changed. However, the tracking ability is still good for us to interpret about fuel consumption of conventional car.

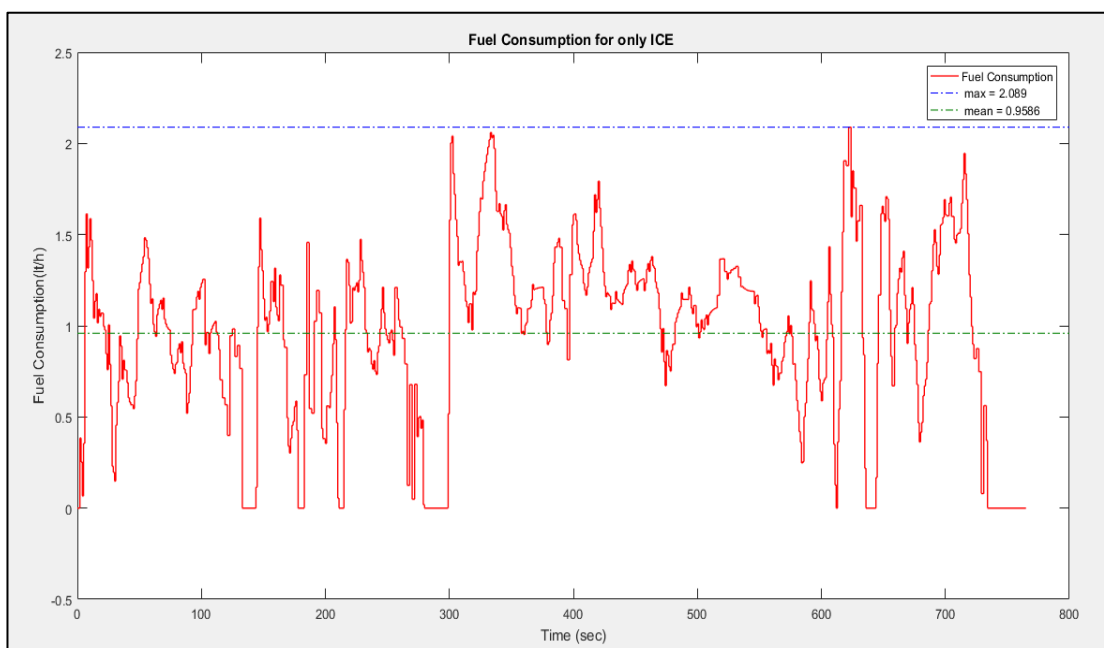


**Figure 5.17.** Fuel Consumption Analysis for Only ICE

The average fuel consumption rate is 0.9586, which is still too low. This figure indicates that, fuel consumption rate of even conventional vehicle could be minimized by using good MPC controller.

## 5.2. Battery Thermal Management Strategy

In this part of thesis, MPC controller is designed to improve thermal management strategy and this part is called fifth case from Table 5.1. Battery thermal management strategy is quite important for all types of hybrid vehicles to prolong the life of battery. The aim of this strategy is to control the battery temperature of hybrid vehicle by using fan. Although this strategy has less input and output, it is much more complex than energy management strategy, because the model of thermal part is quite nonlinear.

MPC controller is designed to solve same problem which is pointed out in equation 5.1. In this equation, the terms of measured output ( $y$ ), manipulated variable ( $u$ ) and constraint are given below:

$$y = [Temp]$$

$$u = [V_{rpm}]$$

Subject to,

$$Temp_{min} \leq Temp \leq Temp_{max}$$

### 5.2.1. Controller Synthesis for Thermal Management Strategy

- Controller Tuning

The essential point of this part is to control fan speed by MPC. Therefore, the only manipulated variable is speed of fan. MPC should determine the value of manipulated variable by considering temperature of battery. Temperature of battery is the only measured output of this system. Number of measured disturbances are two, including ambient temperature and battery power. The values of both measured disturbances are taken as 10.

- Constraints

In this case, manipulated variable constraints are imposed as:

$$20 \text{ rpm} \leq V_{rpm} \leq 800 \text{ rpm}$$

The measured outputs are expressed as:

$$10^\circ\text{C} \leq \text{Temp} \leq 40^\circ\text{C}$$

In this strategy, the only reference, that controller should track, is arbitrary temperature. This temperature is taken as  $23^\circ\text{C}$ . Since there is only one measured output, constraint is thought as hard constraint.

- Weights

The values of weights and rate weights for  $V_{rpm}$  are 0.1. The value of measured output is taken 1000.

### 5.2.2. Simulation Results for Thermal Management Strategy

In this part of thesis, simulation results of battery cooling system are discussed. Before explaining this control strategy, illustrating overall block diagram of thermal part is necessary. Figure 5.18 shows block diagram of thermal management control.

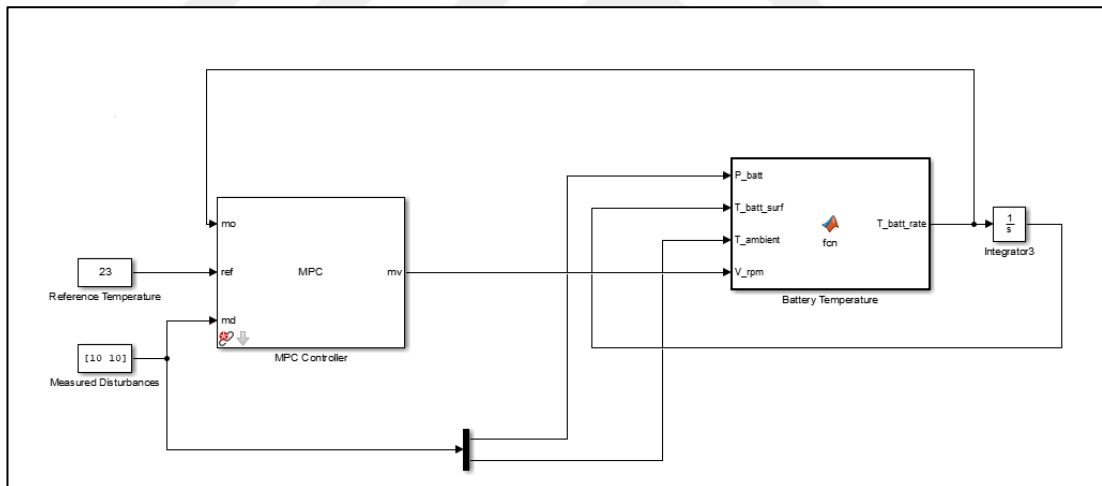


**Figure 5.18.** Block Diagram of Nonlinear Model

After all tuning parameters are embedded into the MPC controller, the system is executed. After execution, MPC estimates speed of fan in each time step. The output and manipulated variables are shown in Figure 5.19.

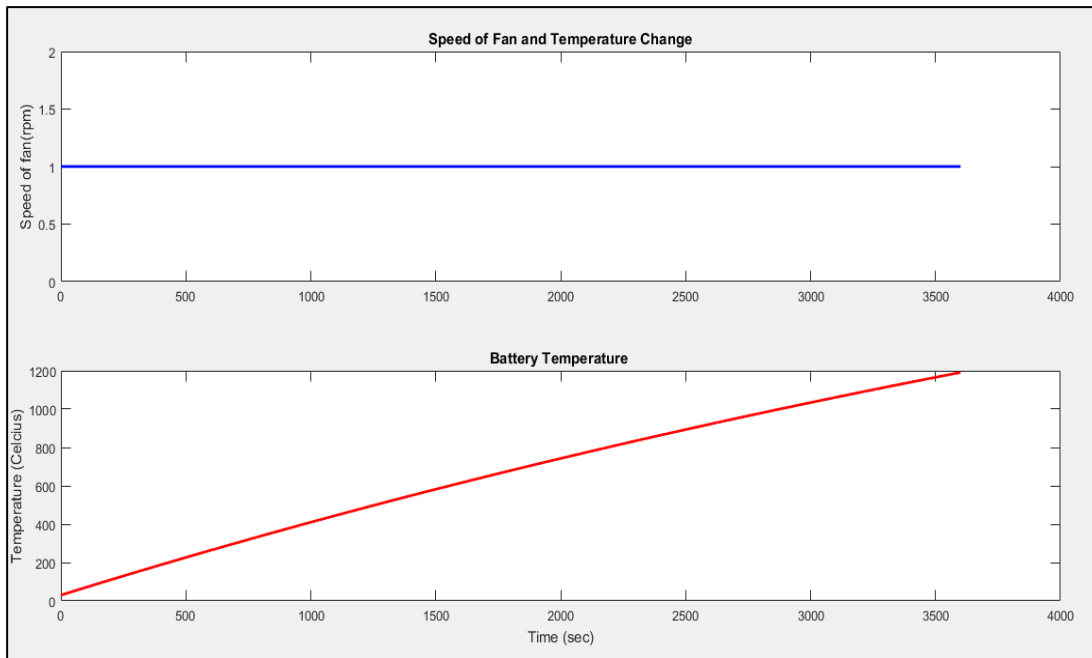


**Figure 5.19.** Speed of Fan and Temperature Change of Nonlinear Model

As it can be seen from Figure 5.19, the values of battery temperature and speed of fan are not logical. The reason for this situation is that the system has a nonlinear mathematical model. Therefore, these variables cannot converge to a specific point. This strategy needs a linear mathematical model to converge to desired points. Instead of changing the mathematical model from the beginning, a linear model should be created from a nonlinear one. One of the MATLAB Toolboxes, which is called, System Identification Toolbox, lets us convert a nonlinear model into a linear model. This toolbox creates a state space model by taking data from an unstable model. In this thesis, a first-order state space model is constructed. In this case, when the order increases, the model will become unstable. Figure 5.20 shows the comparison of a nonlinear model and a first-order state space model which is designed by the System Identification Toolbox.



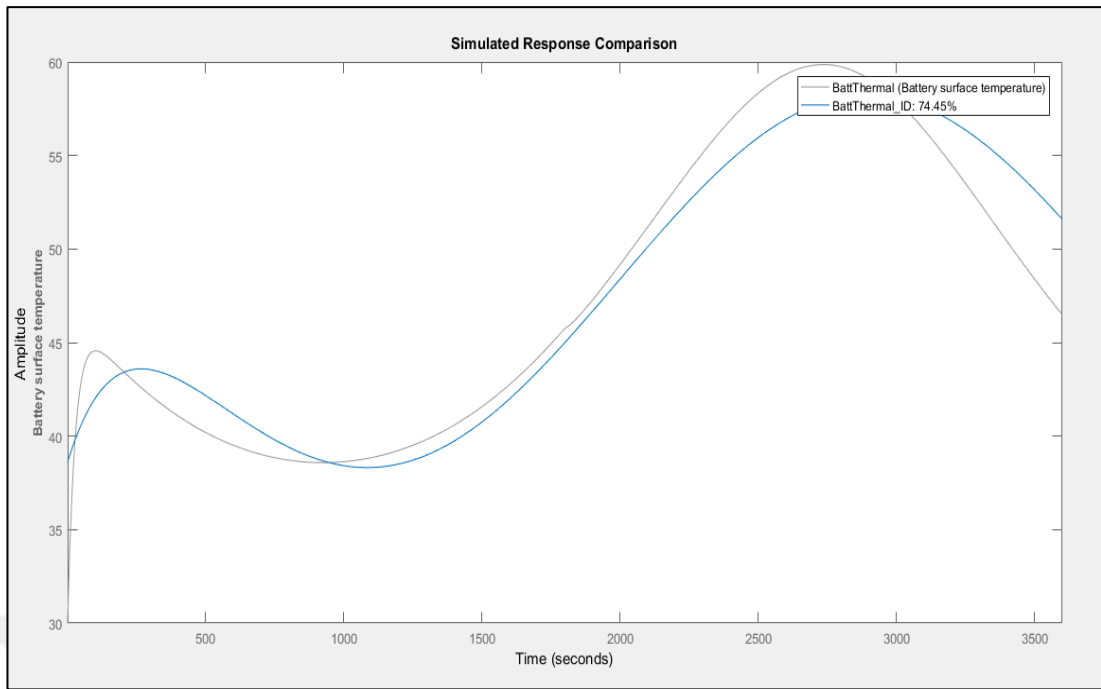


**Figure 5.20.** Comparison of Linear and Nonlinear Model

There is 74.45% identity between linear and nonlinear model. Actually, when the order of state space model increases, the identity ratio will increase. However, as it is said before, system becomes unstable again. For clear explanation, block diagram of state space temperature model is illustrated, in Figure 5.21.

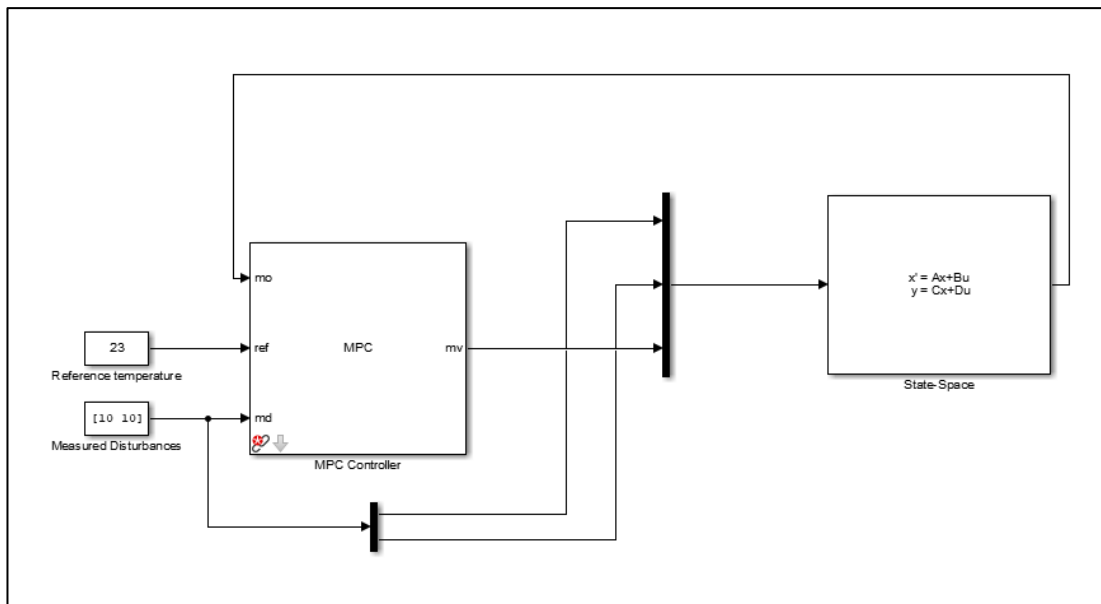


**Figure 5.21.** Block Diagram of State-Space Model

MPC controller is developed with respect to state-space model, instead of using nonlinear model. Before executing the system, stability control can be done by

looking at the eigenvalues of  $A$  in state space model. In this case, eigenvalue of this parameter is  $-0.005$  that is stable.

The results of measured output and manipulated variable of state-space thermal model are shown in Figure 5.22.

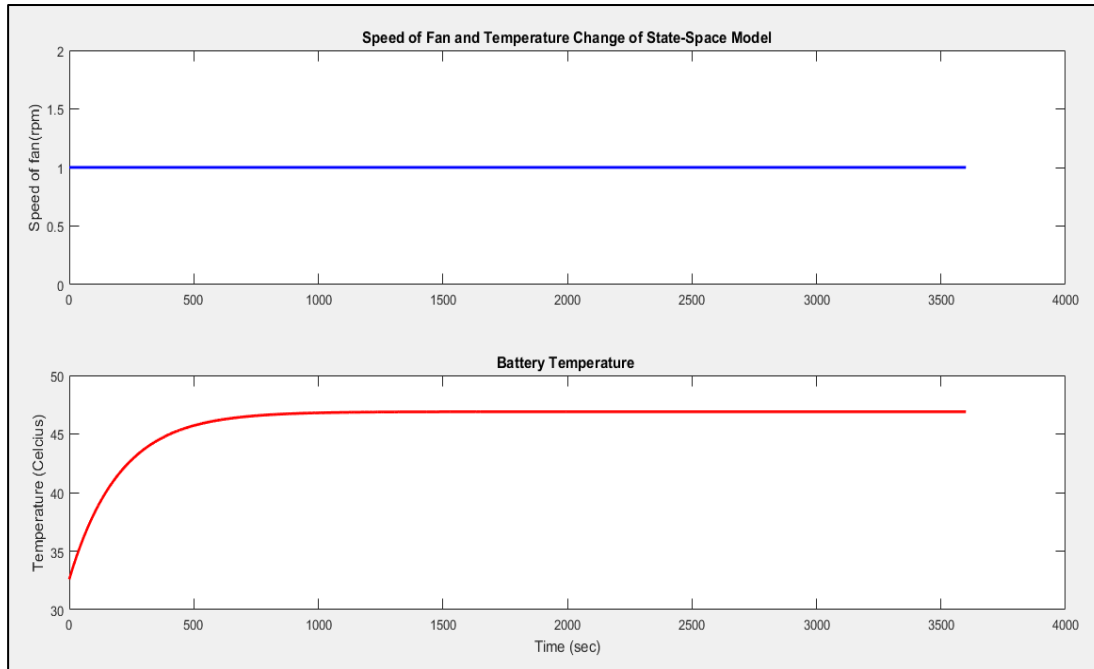


**Figure 5.22.** Speed of Fan and Temperature Change of State-Space Model

It can be interpreted that, controller has some trouble to overcome with constraints, but temperature of battery converges to one point. It means that, temperature strategy has become stable. The fan is turning with the speed of 1 rpm. This speed is not enough to decrease the battery temperature. Hence, the temperature of battery increases up to  $46^{\circ}\text{C}$  and then it has become constant.

In summary, the unstable mathematical model of battery temperature turns into stable model by using system identification. When EMS and TMS are combined each other, this process will become more important. Therefore, tuning of controller is not that much significant in this case. In this part, the main problem was obtaining stable model and it has become successful.

### **5.3. Combined Energy Management and Thermal Management Strategies**

This part of thesis is the last step of design procedure and it is called sixth case from Table 5.1. In Figure 5.1, overall system block diagram was illustrated. Now, the Simulink block diagram of combination of EMS and TMS is shown in Figure 5.23.

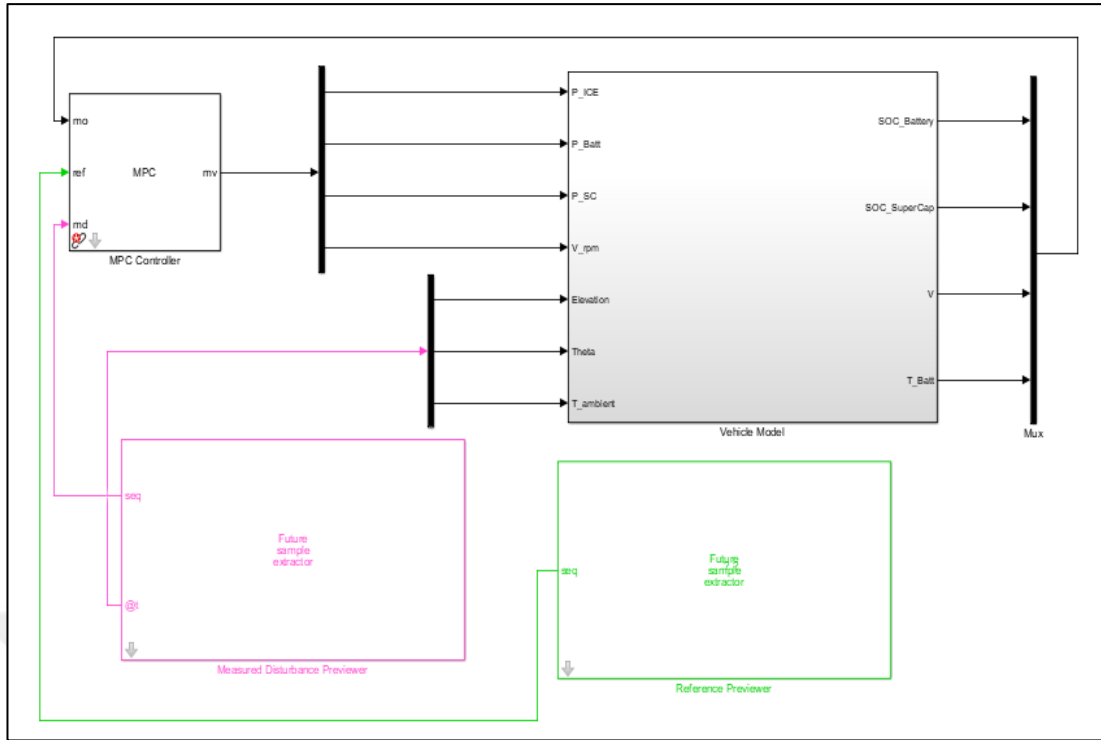


**Figure 5.23.** Simulink Block Diagram of Combined EMS and TMS

In this combined strategy, the aim is to make power split between three different sources and to control the speed of fan in order to keep battery temperature in specific interval.

MPC controller is designed to solve same problem which is given in equation 5.1. In this equation, the terms of measured output ( $y$ ), manipulated variable ( $u$ ) and constraint are given below:

$$y = \begin{bmatrix} V \\ Temp \end{bmatrix}$$

$$u = \begin{bmatrix} P_{ICE} \\ P_{batt} \\ P_{SC} \\ V_{rpm} \end{bmatrix}$$

Subject to,

$$SOC_{min} \leq SOC_{batt} \leq SOC_{max}$$

$$SOC_{min} \leq SOC_{SC} \leq SOC_{max}$$

$$V_{min} \leq V \leq V_{max}$$

$$Temp_{min} \leq Temp \leq Temp_{max}$$

In next steps of this part, detailed design procedures is mentioned.

### 5.3.1. Controller Synthesis for Combined Strategies

- Controller Tuning

The significant point of this part is to make power split and to control fan speed by MPC at the same time. Therefore, the number of manipulated variable is four including three power sources and speed of fan. MPC should determine the values of manipulated variables by considering SOC levels, velocity and battery temperature. Number of measured disturbances is three, including ambient temperature, elevation of car and slope of road. Ambient temperature is set to be 22°C, whereas other two disturbances are 0. Velocity of vehicle and temperature of battery are taken as references. Controller should strictly track these data. Velocity of vehicle is taken again from HWFET driving cycle and the value of battery temperature is taken 25°C as a references.

- Constraints

In this case, manipulated variable constraints are imposed as:

$$0 \text{ kW} \leq P_{ICE} \leq 71 \text{ kW}$$

$$-53 \text{ kW} \leq P_{batt} \leq 53 \text{ kW}$$

$$-27 \text{ kW} \leq P_{SC} \leq 27 \text{ kW}$$

$$20 \text{ rpm} \leq V_{rpm} \leq 800 \text{ rpm}$$

The measured outputs are expressed as:

$$50\% \leq \text{SOC}_{batt} \leq 100\%$$

$$10\% \leq \text{SOC}_{SC} \leq 100\%$$

$$0 \text{ m/s} \leq V \leq 50 \text{ m/s}$$

$$10^\circ\text{C} \leq \text{Temp} \leq 40^\circ\text{C}$$

In this case, controller aims to track velocity and battery temperature. Therefore, maximum and minimum ECR values are set to be 1 for both SOC value, because it is not necessary to strictly track these values. Velocity has higher priority to be tracked by controller. Thus, ECR values for velocity and temperature are 0 and 0.1 respectively.

- Weights

The values of weights for  $P_{ICE}$ ,  $P_{Batt}$ ,  $P_{SC}$  and  $V_{rmp}$  are taken as 0.1, 0.1, 0 and 0.1 respectively. Rate weights values are taken as 0.1 for all manipulated variables. The weights for measured outputs of  $SOC_{batt}$ ,  $SOC_{SC}$ ,  $V$  and  $Temp$  values are set to be 0, 0, 100 and 1 respectively.

### 5.3.2. Simulation Results for Combined EMS and TMS

After tuning controller parameters, system is executed. In first trial, plant model includes vehicle model and nonlinear battery temperature model. The reliability of controller is checked from speed tracking performance. Although EMS and TMS are combined and controlled by same controller, the results of these two control strategies are discussed separately. In Figure 5.24, speed tracking ability of controller is shown.

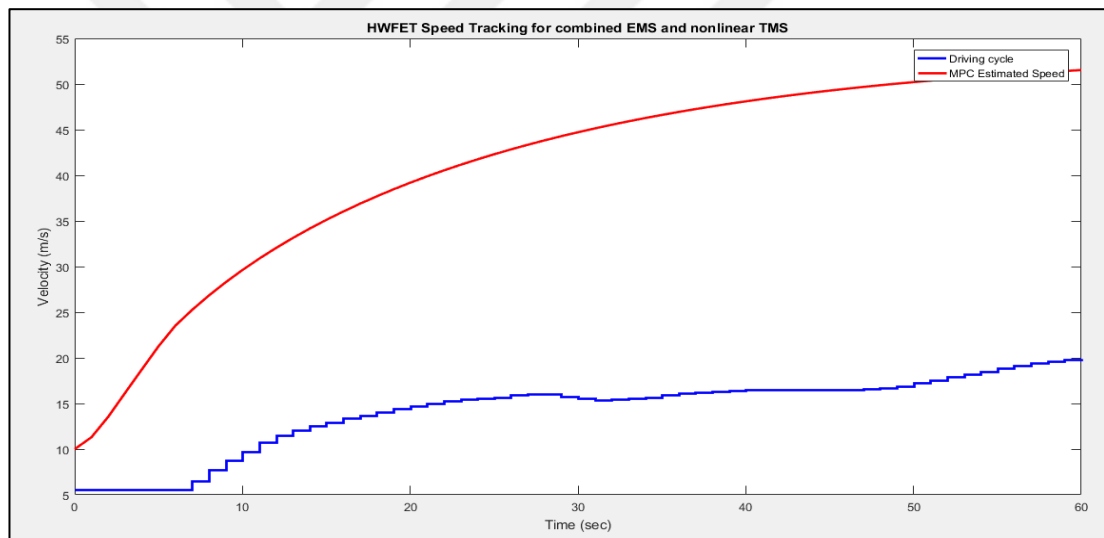


**Figure 5.24.** Speed Tracking for Combined EMS and Nonlinear TMS

It is enough to look for a short period of time to understand whether the output of system converges or not. Figure 5.24 proves that nonlinear model cannot be used to perform this task in initial situation. Therefore, same state-space model which is designed by using system identification toolbox is embedded into the overall model.

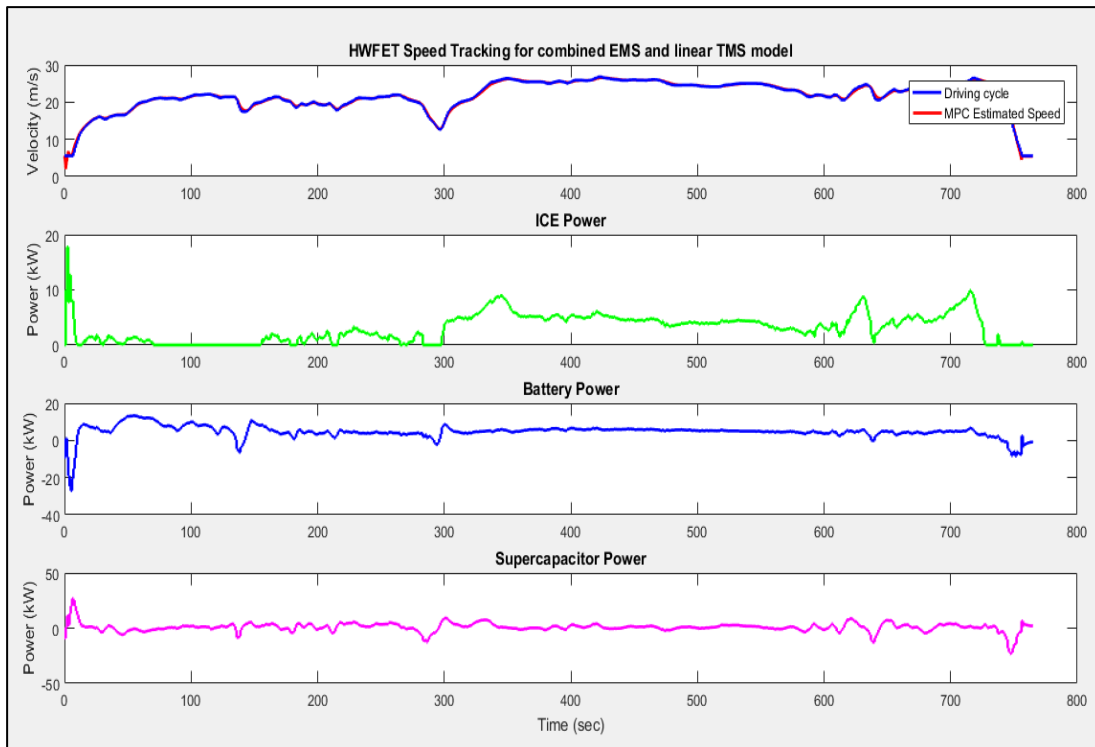


**Figure 5.25.** Speed Tracking and Power Split for Combined EMS and Linear TMS

Figure 5.25 proves that the speed tracking ability of MPC controller has increased by using linear temperature model. In this case, the values of MAPE and MAE are found as 0.92% and 0.2 respectively. The effects of good MPC controller on fuel consumption rate is also satisfactory. Figure 5.26 illustrates the effects of MPC controller on fuel consumption rate.

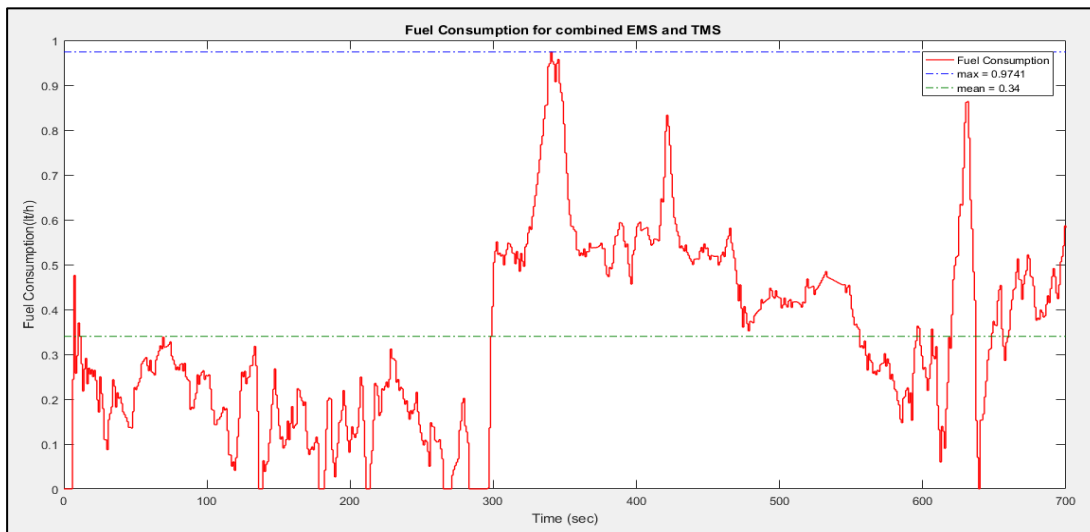


**Figure 5.25.** Fuel Consumption Rate for Combined EMS and TMS

This figure can be interpreted that fuel consumption rate of vehicle could be decreased by using combination of two types of control strategies. The average fuel consumption rate is brought down to 0.34 lt/h.

Last step of designing procedure is to show speed of fan and temperature change. As it is mentioned before, at the beginning of this process, nonlinear temperature model has tried to control by MPC. Then, linear model is developed and this model is achieved to control by MPC. In this step, there is a tricky point which is carried out. First of all, the overall model is executed with state-space model and MPC controller has adjusted required variables with respect to this model. After that, nonlinear model is converted into state-space model with same MPC controller. Since MPC still detects state-space model, even the nonlinear model is executed, MPC can control the output of overall system without giving an error. The comparison of fan control and temperature change of battery is given in Figure 5.26.

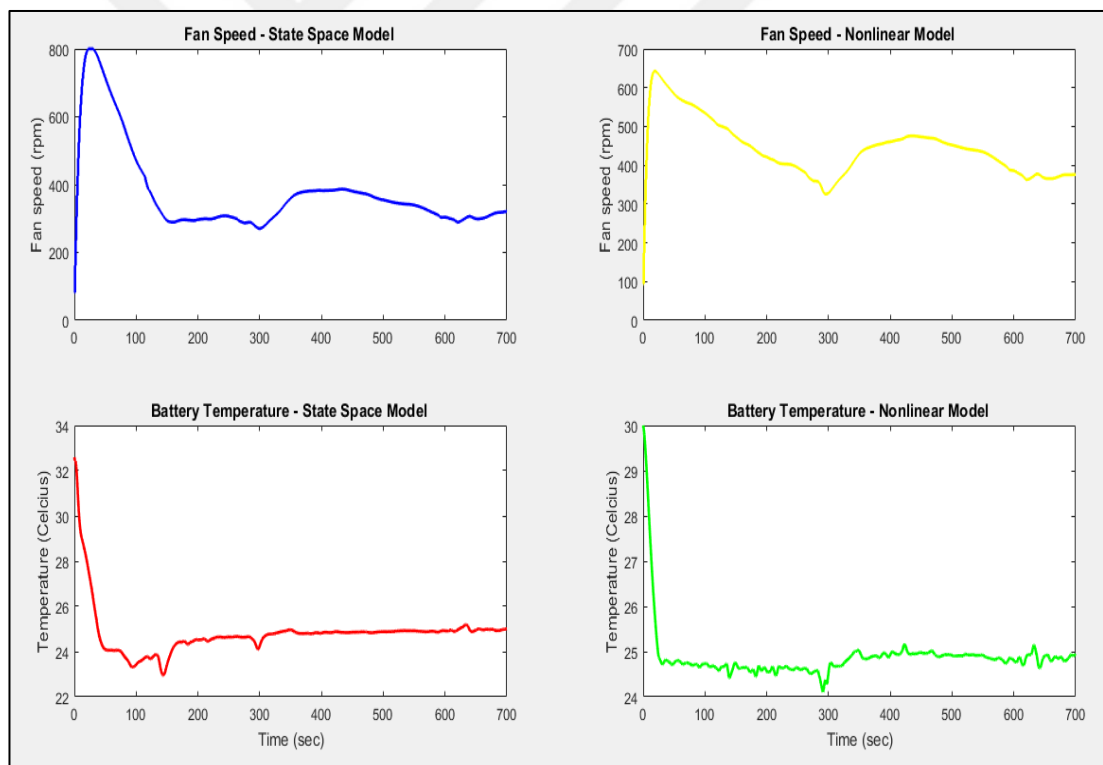


**Figure 5.26.** Comparison of Fan Control and Temperature Change for State-Space and Nonlinear Model

As it discussed before, the aim of this strategy is to keep battery temperature by changing the velocity of fan. Desired temperature of battery was adjusted as 25 °C. In both cases, MPC controller has become quite successful to keep temperature in this value. The initial condition of battery surface temperature is taken as 30°C. Since

this value is far away from our desired temperature, controller executes the fan with maximum speed. Then, controller has achieved to cool down the battery temperature and it has come down to specified value. When the power removed from battery increases, controller speeds up the fan in order not to exceed desired temperature. Since there is 74.45% identity between two models, the initial conditions of battery temperature and maximum velocity of fan are different from each other.

**5.4. Discussion of Results**

In this part of thesis, the summary of different types of control strategies are discussed. Table 5.2 shows C-rate changes in different cases.

**Table 5.2.** Different Estimated C-rate Values for Case 1, Case 2 and Case 3

	<b>C-rate max</b>	<b>C-rate mean</b>
Case 1	15.7	3.207
Case 2	30.91	4.009
Case 3	31.28	5.676

Comparison of Case 1 and Case 2 indicates the benefits of additional ESS. In first case, since supercapacitor is used with battery, stress on battery is achieved to be lowered. Therefore, the average value of C-rate can be decreased from 4.009 to 3.207 by using supercapacitor. This proves that the life of battery is achieved to prolong thanks to additional ESS and good MPC control strategy.

We were expecting that, without using ICE, stress on battery and supercapacitor increases. When we look at the Table 5.2, it shows that C-rate value is maximum in Case 3. This is the important issue which should be considered to prolong the life of battery in plug in electric vehicles. It is explicit that if we had not used additional ESS, the value of C-rate would have been bigger.



**Table 5.3.** Different estimated fuel consumption rate values for Case 1, Case 2, Case 4 and Case 6

	<b>Mean Fuel Consumption (lt/h)</b>	<b>Mean Fuel Consumption (lt/100km)</b>
Case 1	0.7043	0.9064
Case 2	0.7431	0.9563
Case 4	0.9586	1.2337
Case 6	0.34	0.4375

Now, the fuel consumption rates in different cases are discussed. As it is expected that the maximum average of fuel consumption rate is observed in Case 4. Although this value is maximum when it is compared with other cases, it is quite low when compared with real world applications.

When case 1 and case 2 are compared, positive effects of additional ESS on fuel consumption rate can be seen. These values are again too low thanks to good MPC controller. This result actually demonstrates that additional ESS contributes both the life of battery and fuel consumption rate.

The lowest value of fuel consumption is obtained when EMS and TMS are used and controlled by MPC like in Case 6. By combining both management strategies, MPC estimated the best results about fuel consumption rate and reference tracking performance.

## **CHAPTER 6**

### **CONCLUSIONS AND FUTURE RESEARCH**

#### **6.1. Conclusion**

Conventional vehicles play one of the important roles in affecting the environment in a bad way. They emit some harmful gas like carbon dioxide and nitrogen gas. The idea of having greener and cleaner environment led scientists to find new sources. They have improved the idea of using only electricity as a propulsion power of vehicle. However, in this case, they have faced with low mileage problems. This problem has widened the usage of hybrid vehicles.

Using hybrid vehicles can contribute to decrease the emission of harmful gas. However, the best results can be obtained when the vehicle is supported by good controller. The hybrid vehicles have several complex components and taking the model of each component is quite challenging. Designed controller should deal with each component and satisfy different desired purposes at the same time. Therefore, in most literature studies, model predictive controller is chosen to perform these tasks. In previous studies, researchers have focused on energy management strategy for hybrid vehicles to decrease fuel consumption. Also, they have investigated this strategy with additional energy storage system which is supercapacitor. However in most case, researchers have investigated these two tasks separately. We have combined these two objectives and we have added one more task which is TMS.

Three main purposes of this thesis have been achieved successfully; the first one was to develop EMS to make optimum power split and to get low fuel consumption rate. The second one was to use additional ESS which is supercapacitor for decreasing the stress of battery. The last objective is to keep the battery temperature in desired interval by designing TMS. All three objectives have been carried out by using MPC.

In order to achieve objectives, six different cases have been carried out and each case, we have achieved to track driving cycle. Given a look at Case 2 and Case 4, the average fuel consumption rate is 0.9563 lt/100km and 1.2337 lt/100km respectively.

This results indicate that optimum power split can be made and fuel consumption rate can be decreased by controller. When Case 1 and Case 2 are investigated, we have achieved that by using supercapacitor, fuel consumption rate can be reduced by 5.221%. In addition, by using additional ESS, C-rate can be reduced by 24.49%. Lastly, by using the combination of EMS and TMS, fuel consumption can be reduced by 51.72%. The summary of these results could be pointed out that fuel consumption rate can be minimized and life of battery can be extended by using high performance MPC controller.

## **6.2. Future Work**

Optimal system configuration and sizing can be determined by combining “design optimization” and “operational optimization” under the MPC framework. In this study, we only interested in operational optimization part. By using different types of components, the results can be changed and improved.

Another future work is that more advanced vehicle models can be used in the MPC controller to better represent dynamics, by addressing tuning and converge challenges.

## REFERENCES

- Altaf, F., Egardt, B., & Mårdh, L. J. (2017). Load management of modular battery using model predictive control: Thermal and state-of-charge balancing. *IEEE Transactions on Control Systems Technology*, 25(1), 47-62.
- Bemporad, A., & Morari, M. (1999). Robust model predictive control: A survey. In *Robustness in identification and control* (pp. 207-226). Springer, London.
- Bergman, T. L., Incropera, F. P., DeWitt, D. P., & Lavine, A. S. (2011). *Fundamentals of heat and mass transfer*. John Wiley & Sons.
- Borhan, H. A., & Vahidi, A. (2010, June). Model predictive control of a power-split hybrid electric vehicle with combined battery and ultracapacitor energy storage. In *American Control Conference (ACC), 2010* (pp. 5031-5036). IEEE.
- Borrelli, F., Bemporad, A., Fodor, M., & Hrovat, D. (2006). An MPC/hybrid system approach to traction control. *IEEE Transactions on Control Systems Technology*, 14(3), 541-552.
- Brahma, A., Guezennec, Y., & Rizzoni, G. (2000, September). Optimal energy management in series hybrid electric vehicles. In *American Control Conference, 2000. Proceedings of the 2000* (Vol. 1, No. 6, pp. 60-64). IEEE.
- Burke, A., & Zhao, H. (2015, April). Applications of supercapacitors in electric and hybrid vehicles. In *5th European Symposium on Supercapacitor and Hybrid Solutions (ESSCAP), Brasov, Romania*.
- Camacho, E. F., & Alba, C. B. (2013). *Model predictive control*. Springer Science & Business Media.
- Choi, S. S., & Lim, H. S. (2002). Factors that affect cycle-life and possible degradation mechanisms of a Li-ion cell based on LiCoO<sub>2</sub>. *Journal of Power Sources*, 111(1), 130-136.
- Clarke, D. W., Mohtadi, C., & Tuffs, P. S. (1987). Generalized predictive control—Part I. The basic algorithm. *Automatica*, 23(2), 137-148.
- Clarke, D. W., & Scattolini, R. (1991, July). Constrained receding horizon predictive control. In *IEE Proceedings D-Control Theory and Applications* (Vol. 138, No. 4, pp. 347-354). IET.
- Cutler, C. R. and B. L. Ramaker, “Dynamic Matrix Control – a computer control algorithm. AIChE National Mgt, Houston, Texas (1979)
- Di Cairano, S., Tseng, H. E., Bernardini, D., & Bemporad, A. (2010). Steering

vehicle control by switched model predictive control. *IFAC Proceedings Volumes*, 43(7), 1-6.

Different Types of Driving Cycles,

<http://www.car-engineer.com/the-different-driving-cycles/> (Access Date: May 2013)

Di Cairano, S., Yanakiev, D., Bemporad, A., Kolmanovsky, I. V., & Hrovat, D. (2012). Model predictive idle speed control: Design, analysis, and experimental evaluation. *IEEE Transactions on Control Systems Technology*, 20(1), 84-97.

FERNÁNDEZ, D. C. Model Building and Energy Efficient Control of a Series-Parallel Plug-in Hybrid Electric Vehicle, 2016.

Garcia, C. E., Prett, D. M., & Morari, M. (1989). Model predictive control: theory and practice—a survey. *Automatica*, 25(3), 335-348.

Grimm, G., Messina, M. J., Tuna, S. E., & Teel, A. R. (2005). Model predictive control: for want of a local control Lyapunov function, all is not lost. *IEEE Transactions on Automatic Control*, 50(5), 546-558.

Grüne, L., Pannek, J., Seehafer, M., & Worthmann, K. (2010). Analysis of unconstrained nonlinear MPC schemes with time varying control horizon. *SIAM Journal on Control and Optimization*, 48(8), 4938-4962.

Hasselby, F. (2013). Dynamic Modelling of Battery Cooling Systems for Automotive Applications.

Hrovat, D., Di Cairano, S., Tseng, H. E., & Kolmanovsky, I. V. (2012, October). The development of model predictive control in automotive industry: A survey. In *Control Applications (CCA), 2012 IEEE International Conference on* (pp. 295-302). IEEE.

Ismail, N. H. F., Toha, S. F., Azubir, N. A. M., Ishak, N. H. M., Hassan, M. K., & Ibrahim, B. S. K. (2013). Simplified heat generation model for lithium ion battery used in electric vehicle. In *IOP Conference Series: Materials Science and Engineering* (Vol. 53, No. 1, p. 012014). IOP Publishing.

Jilte, R. D., & Kumar, R. (2018). Numerical investigation on cooling performance of Li-ion battery thermal management system at high galvanostatic discharge. *Engineering science and technology, an international journal*, 21(5), 957-969.

Jinrui, N., Zhifu, W., & Qinglian, R. (2006, September). Simulation and Analysis of Performance of a Pure Electric Vehicle with a Super-capacitor. In *Vehicle Power and Propulsion Conference, 2006. VPPC'06. IEEE* (pp. 1-6). IEEE.

- Karabasoglu, O., Kimball, P., Styler, A., Nourbakhsh, I., & Michalek, J. (2018). Global Control Optimization of Electric Vehicles with Supercapacitor-Battery Systems. *Submitted to Journal of Power Sources*.
- Kouvaritakis, B., Rossiter, J. A., & Chang, A. O. T. (1992, July). Stable generalised predictive control: an algorithm with guaranteed stability. In *IEE Proceedings D-Control Theory and Applications* (Vol. 139, No. 4, pp. 349-362). IET.
- Lajunen, A. (2010, September). Evaluation of the benefits of using dual-source energy storage in hybrid electric vehicles. In *Vehicle Power and Propulsion Conference (VPPC), 2010 IEEE*(pp. 1-6). IEEE.
- LI, J., & ZHU, Z. (2014). Battery Thermal Management Systems of Electric Vehicles.
- Lu, Z., Song, J., Yuan, H., & Shen, L. (2013, July). MPC-based torque distribution strategy for energy management of power-split hybrid electric vehicles. In *Control Conference (CCC), 2013 32nd Chinese* (pp. 7650-7655). IEEE.
- Masoudi, Y., & Azad, N. L. (2017, May). MPC-based battery thermal management controller for Plug-in hybrid electric vehicles. In *American Control Conference (ACC), 2017* (pp. 4365-4370). IEEE.
- Miller, J. M. (2007, October). Energy storage technology markets and application's: ultracapacitors in combination with lithium-ion. In *Power Electronics, 2007. ICPE'07. 7th International Conference on* (pp. 16-22). IEEE.
- Miller, J. M., McCleer, P. J., & Everett, M. (2005, May). Comparative assessment of ultra-capacitors and advanced battery energy storage systems in PowerSplit electronic-CVT vehicle powertrains. In *Electric Machines and Drives, 2005 IEEE International Conference on* (pp. 1513-1520). IEEE.
- Ortner, P., & Del Re, L. (2007). Predictive control of a diesel engine air path. *IEEE transactions on control systems technology*, 15(3), 449-456.
- Pesaran, A. A., & Keyser, M. (2001, January). Thermal characteristics of selected EV and HEV batteries. In *Proceedings of the Annual Battery Conference: Advances and Applications, Long Beach, CA, Jan* (pp. 9-12).
- Peterka, V. (1984). Predictor-based self-tuning control. *Automatica*, 20(1), 39-50.
- Poramapojana, P., & Chen, B. (2012, July). Minimizing HEV fuel consumption using model predictive control. In *Mechatronics and Embedded Systems and Applications (MESA), 2012 IEEE/ASME International Conference on* (pp. 148-153). IEEE.
- Prabhu, S., & George, K. (2014, June). Performance improvement in MPC with time-varying horizon via switching. In *Control & Automation (ICCA), 11th IEEE International Conference on* (pp. 168-173). IEEE.

- Richalet, J. A., A. Rault, J. L. Papon (1978), “Model Predictive Heuristic Control: application to an industrial process”, *Automatica*, 14, 413-428
- Rossiter, J. A. (2003). *Model-based predictive control: a practical approach*. CRC press.
- Sadoun, R., Rizoug, N., Bartholomeüs, P., Barbedette, B., & Le Moigne, P. (2011, September). Optimal sizing of hybrid supply for electric vehicle using Li-ion battery and supercapacitor. In *Vehicle Power and Propulsion Conference (VPPC), 2011 IEEE*(pp. 1-8). IEEE.
- Sciarretta, A., & Guzzella, L. (2007). Control of hybrid electric vehicles. *IEEE Control systems*, 27(2), 60-70.
- Toyota Prius Technical Specifications Including Battery Details  
[https://media.toyota.co.uk/wpcontent/files\\_mf/1329489972120216MTOYOTAPRIUSTECHNICALSPECIFICATIONS.pdf](https://media.toyota.co.uk/wpcontent/files_mf/1329489972120216MTOYOTAPRIUSTECHNICALSPECIFICATIONS.pdf) (Access Date : 2012)
- Toyota Prius 2018 Base Model Specifications,  
<https://www.guideautoweb.com/en/makes/toyota/prius/2018/specifications/base/>  
(Access Date: 2018)
- Vermillion, C., Sun, J., & Butts, K. (2011). Predictive control allocation for a thermal management system based on an inner loop reference model—design, analysis, and experimental results. *IEEE transactions on control systems technology*, 19(4), 772-781.
- Wang, W., Jia, S., Xiang, C., Huang, K., & Zhao, Y. (2014, December). Model predictive control-based controller design for a power-split hybrid electric vehicle. In *Modelling, Identification & Control (ICMIC), 2014 Proceedings of the 6th International Conference on* (pp. 219-224). IEEE.
- Wikipedia, the free encyclopedia, “Honda Civic Hybrid”,  
[https://en.wikipedia.org/wiki/Honda\\_Civic\\_Hybrid](https://en.wikipedia.org/wiki/Honda_Civic_Hybrid) (Access Date: 2015)





## APPENDIX 1 – Battery Temperature Code

MATLAB<sup>®</sup> code for battery temperature block in Simulink is given below:

```
function T_batt_rate = fcn(P_batt,T_batt_surf,T_ambient,V_rpm)
%Constant parameters for battery and fan
D = 0.06; % diameter of battery cell [m]
L = 0.285; % length of the battery [m]
N = 168; % number of cells in entire pack [-]
N_T = 6; % number of cell in each module [-]
N_L = 28; % number of battery module [-]
S_T = 0.09; % battery transverse pitch taken 3*R [m]
S_L = 0.09; % battery longitudinal pitch taken 3*R [m]
N_Voltage=1.2; %cell voltage [V]
m_module=1.04; %module weight [kg]
m_batt=m_module*N_L; %battery weight [kg]
Cp_batt=521; %Heat capacity of battery [J/kg/celcius]
D_fan = 0.2; % diameter of fan [m]

%Air Properties for different ambient temperature
if (T_ambient>=0) && (T_ambient<5)
rho_i = 1.292; % air density [kg/m^3]
Sh_i = 1006; % specific heat [J/kg-K]
Kv_i = 1.338e-5; % kinematic viscosity [m^2/s]
Tc_i = 0.02364; % thermal conductivity [W/m-K]
Pr_i = 0.7362; % Prandtl number [-]
elseif (T_ambient>=5) && (T_ambient<10)
rho_i = 1.269;
Sh_i = 1006;
Kv_i = 1.382e-5;
Tc_i = 0.02401;
Pr_i = 0.7350;
elseif (T_ambient>=10) && (T_ambient<15)
rho_i = 1.246;
Sh_i = 1006;
Kv_i = 1.426e-5;
Tc_i = 0.02439;
Pr_i = 0.7336;
elseif (T_ambient>=15) && (T_ambient<20)
rho_i = 1.225;
Sh_i = 1007;
Kv_i = 1.470e-5;
Tc_i = 0.02476;
Pr_i = 0.7323;
elseif (T_ambient>=20) && (T_ambient<25)
rho_i = 1.204;
Sh_i = 1007;
Kv_i = 1.516e-5;
Tc_i = 0.02514;
Pr_i = 0.7309;
elseif (T_ambient>=25) && (T_ambient<30)
rho_i = 1.184;
Sh_i = 1007;
Kv_i = 1.562e-5;
Tc_i = 0.02551;
Pr_i = 0.7296;
elseif (T_ambient>=30) && (T_ambient<35)
rho_i = 1.164;
Sh_i = 1007;
```

```

Kv_i = 1.608e-5;
Tc_i = 0.02588;
Pr_i = 0.7282;
    elseif (T_ambient>=35) && (T_ambient<40)
rho_i = 1.145;
Sh_i = 1007;
Kv_i = 1.655e-5;
Tc_i = 0.02625;
Pr_i = 0.7268;
    elseif (T_ambient>=40) && (T_ambient<45)
rho_i = 1.127;
Sh_i = 1007;
Kv_i = 1.702e-5;
Tc_i = 0.02662;
Pr_i = 0.7255;
    elseif (T_ambient>=45) && (T_ambient<50)
rho_i = 1.109;
Sh_i = 1007;
Kv_i = 1.750e-5;
Tc_i = 0.02699;
Pr_i = 0.7241;
    elseif (T_ambient>=50) && (T_ambient<60)
rho_i = 1.092;
Sh_i = 1007;
Kv_i = 1.798e-5;
Tc_i = 0.02735;
Pr_i = 0.7228;
    elseif (T_ambient>=60) && (T_ambient<70)
rho_i = 1.059;
Sh_i = 1007;
Kv_i = 1.896e-5;
Tc_i = 0.02808;
Pr_i = 0.7202;
    elseif (T_ambient>=70) && (T_ambient<80)
rho_i = 1.028;
Sh_i = 1007;
Kv_i = 1.995e-5;
Tc_i = 0.02881;
Pr_i = 0.7177;
else
rho_i = 0.9994;
Sh_i = 1008;
Kv_i = 2.097e-5;
Tc_i = 0.02953;
Pr_i = 0.7154;
end

%Prandtl number selection for battery surface
if (T_batt_surf>=0) && (T_batt_surf<5)
Pr_l = 0.7362; % Prandtl number [-]
    elseif (T_batt_surf>=5) && (T_batt_surf<10)
Pr_l = 0.7350;
    elseif (T_batt_surf>=10) && (T_batt_surf<15)
Pr_l = 0.7336;
    elseif (T_batt_surf>=15) && (T_batt_surf<20)
Pr_l = 0.7323;
    elseif (T_batt_surf>=20) && (T_batt_surf<25)
Pr_l = 0.7309;
    elseif (T_batt_surf>=25) && (T_batt_surf<30)
Pr_l = 0.7296;
    elseif (T_batt_surf>=30) && (T_batt_surf<35)

```

```

Pr_l = 0.7282;
    elseif (T_batt_surf>=35) && (T_batt_surf<40)
Pr_l = 0.7268;
    elseif (T_batt_surf>=40) && (T_batt_surf<45)
Pr_l = 0.7255;
    elseif (T_batt_surf>=45) && (T_batt_surf<50)
Pr_l = 0.7241;
    elseif (T_batt_surf>=50) && (T_batt_surf<60)
Pr_l = 0.7228;
    elseif (T_batt_surf>=60) && (T_batt_surf<70)
Pr_l = 0.7208;
    elseif (T_batt_surf>=70) && (T_batt_surf<80)
Pr_l = 0.7202;
    else
Pr_l = 0.7177;
    end

%Determining maximum velocity of fan
V_ang = (1/60)*(V_rpm*2*pi); % fan angular velocity [rad/s]
V_line = (D_fan/2)*V_ang; % fan linear velocity [m/s]
D1 = (S_L^2 + (0.5*S_T)^2)^0.5; % staggered tube distance [m]
D2 = 0.5*(S_T + D); % comparison distance [m]
if D1 > D2
    V_max = (S_T*V_line)/(S_T-D); % max air velocity [m/s]
else
    V_max = (S_T*V_line)/(2*(D1-D));
end

%Reynolds Number
Re = (V_max*D)/Kv_i; % Reynolds number [-]

%Nusselt Number
%Determine C1 and m constants
if (Re>=10) && (Re<10e2);
    C = 0.90;
    m = 0.40;
elseif (Re>=10e2) && (Re<10e3);
    C = 0.51;
    m = 0.50;
elseif (Re>=10e3) && (Re<2*10e5);
    C = 0.40;
    m = 0.60;
else
    C = 0.022;
    m = 0.84;
end
Nus = C*(Re^m)*(Pr_i^0.36)*(Pr_i/Pr_l)^0.25; % Nusselt number [-]

%Heat Transfer Coefficient for convective heat
h = (Nus*Tc_i)/D; % heat transfer coefficient [W/m^2-K]

%Air Outlet Temperature
To=T_batt_surf(T_batt_surf-T_ambient)*exp((- D*pi*N_T*N_L*h)/(rho_i*V_line*N_T*S_T*Sh_i)); %outlet temperature [C]

%Log-Mean Temperature Difference
T_log = ((T_batt_surf-T_ambient)-(T_batt_surf-To))/log((T_batt_surf-T_ambient)/(T_batt_surf-To)); % log-mean temperature [C]

%Heat Transfer Rate
q_p = N*pi*h*D*T_log*L; % heat transfer rate [W]

```

```
%Generated heat by battery
I = (P_batt*1000)/(N*N_Voltage); % current in battery cells
R = 0.015; % internal resistance of battery cell [ohm]
q = N*I^2*R; % heat generated in whole battery pack [W]

%The rate of battery temperature
T_batt_rate=((q-q_p)/(m_batt*Cp_batt)); %Rate of temperature change
```





## APPENDIX 2 – A Sample MATLAB/Simulink MPC Toolbox Interface for Only Test Case 6

Adjustment of MPC parameters and Toolbox interface is mentioned step by step. After entering the MPC block, the default conditions of MPC controller is adjusted as shown in Figure App.2.1.

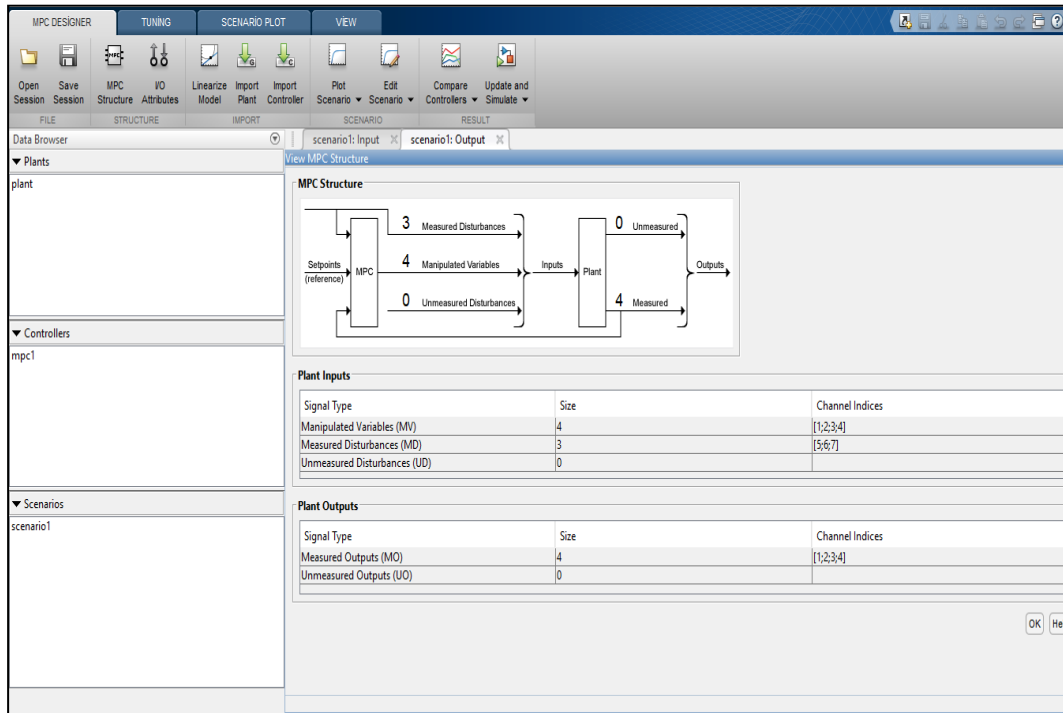


**Figure A2.1.** Adjustment of MPC default conditions

Next step is to make input and output configuration from I/O Attributes tab. Figure App. 2.2 shows the interface of this configuration. This tab allows us to enter the name of parameters and nominal values.

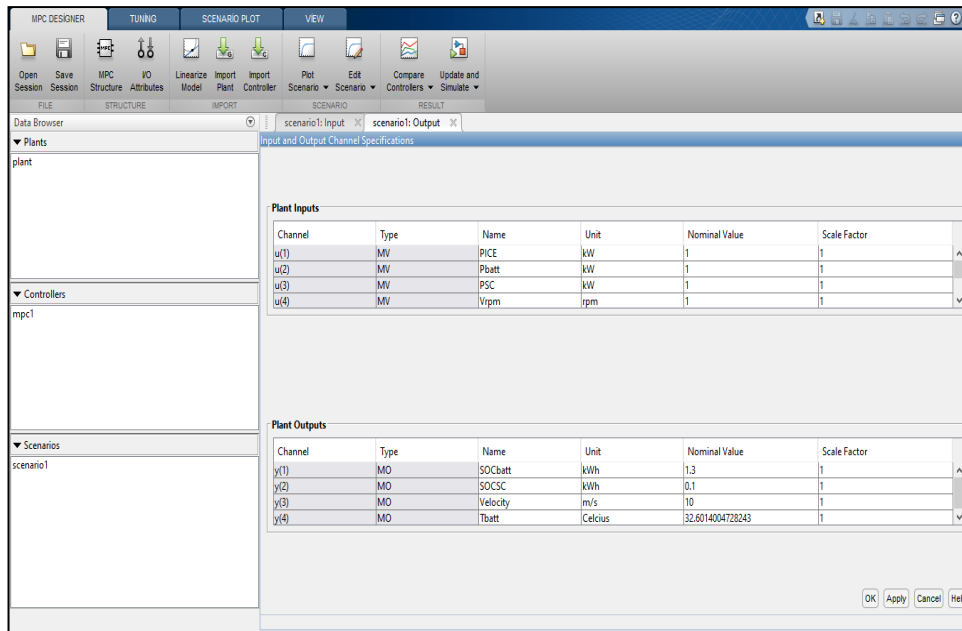


**Figure A2.2.** Input and output configuration of MPC

Then the values of sample time, prediction horizon, control horizon and constraints should be adjusted. Figure App. 2.3 shows the adjustment of these parameters.

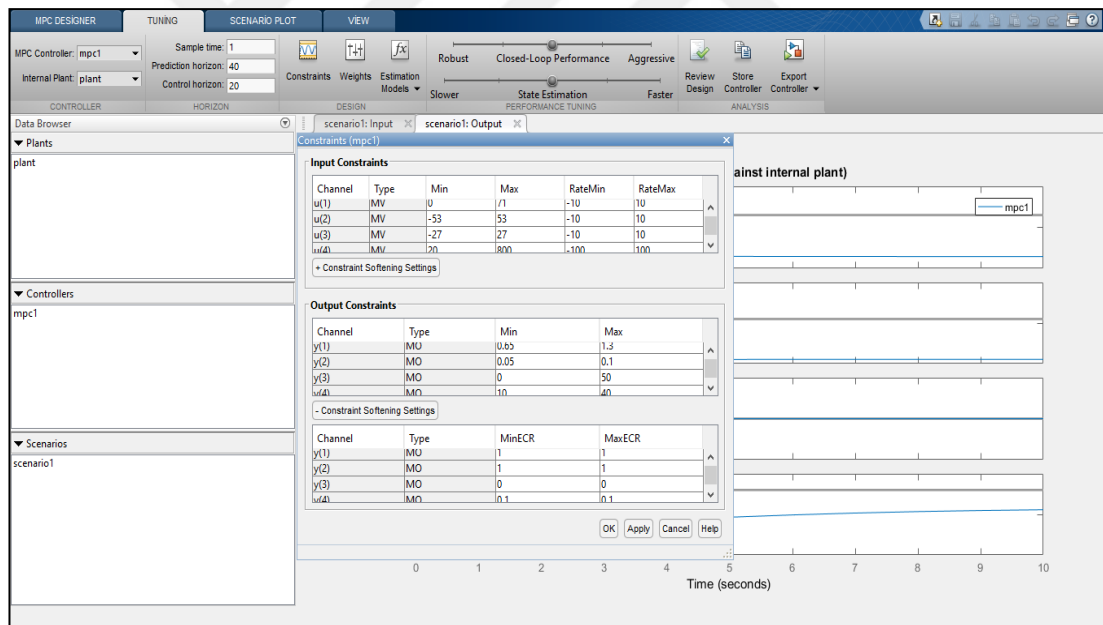


**Figure A2.3.** Sample time, prediction horizon, control horizon and constraints adjustment interface

The last step is to adjust weights parameters. Figure App. 2.4 shows the adjustment weights.

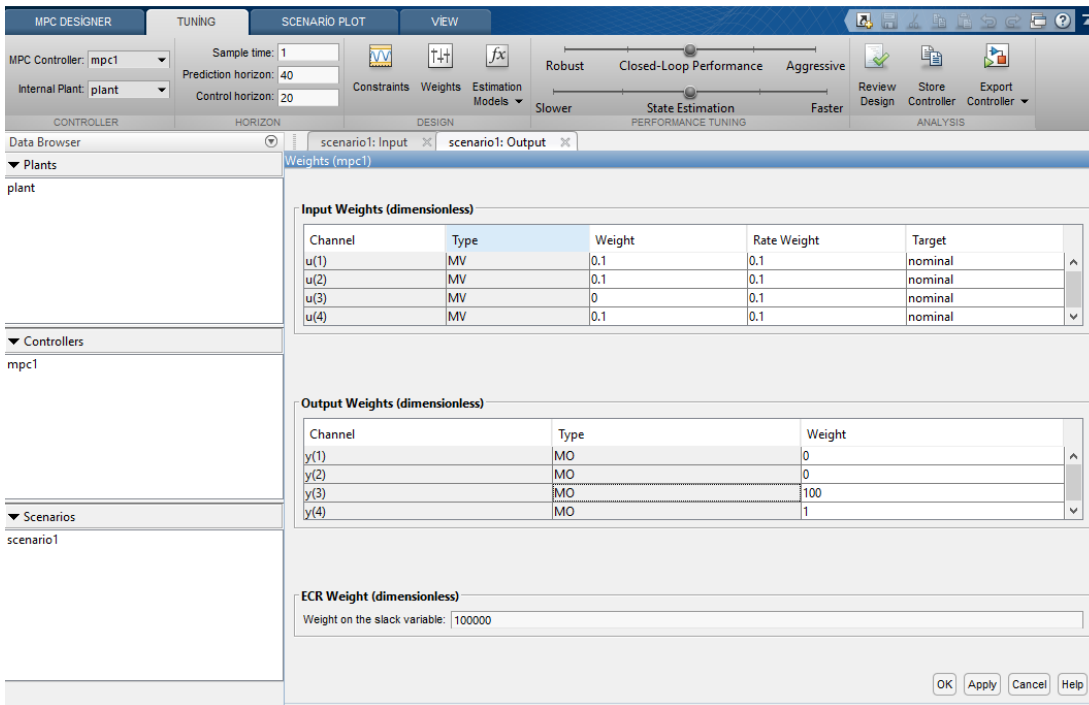


Figure A2.4. Weights adjustment interface

After all tunings, the output response of MPC controller is illustrated in App. 2.5.

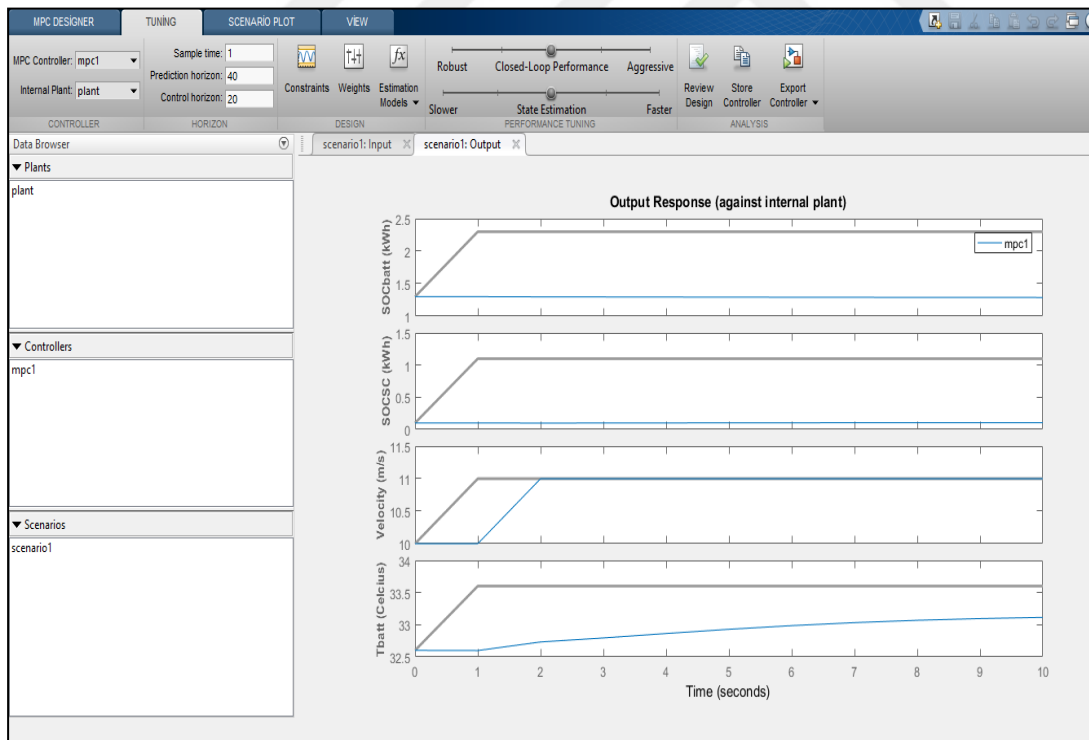


Figure A2.5. Output response of MPC controller